NATURAL FRACTURE SYSTEMS IN THE WOODFORD SHALE, ARBUCKLE MOUNTAINS, OKLAHOMA

By

ONUR ATAMAN

Bachelor of Science in Geological Engineering

Cukurova University

Adana

2006

Submitted to the Faculty of the
Graduate College of the
Oklahoma State University
in partial fulfillment of
the requirements for
the Degree of
MASTER OF SCIENCE
December.2008

NATURAL FRACTURE SYSTEMS IN THE

WOODFORD SHALE, ARBUCKLE MOUNTAINS,

OKLAHOMA

Thesis Approved:

Dr. Ibrahim Cemen

Thesis Adviser

Dr. James Puckette

Dr. Darwin Boardman

Dr. A. Gordon Emslie

Dean of the Graduate College

ACKNOWLEDGEMENTS

First and foremost, I would like to thank to my thesis advisor Dr. Ibrahim Cemen for his work ethic and dedication to this project, the countless hours spent with me in the field, and motivational and affable conversations during the field trips. Without him I would never be able to finish this thesis. Special appreciation is also extended to other committee members, Dr. Jim Puckette and Dr. Darwin Boardman for their ideas, invaluable support, useful feedback, comments and encouragement throughout my graduate career.

I would like to thank New Field Exploration Company for funding this project and giving me the chance to comprehend how hard dealing with the Woodford Shale fracture systems. I would also like to give the American Association of Petroleum Geologists Foundation my gratitude for the Hugh D. Miser Memorial Grant that helped with the funding of this project.

From Oklahoma State University, I would like to offer my sincere thanks all my colleagues and friends, especially Emre Diniz, Niranjan Aryal, Vukenkeng Che Alota, Cody Winchester, Huanyu Zhao, Braydn Johnson, Brad Holland and Jennifer Gamrod for their friendship and invaluable encouragement during the preparation of this thesis.

Especially, I would like to express deep gratitude to my undergrad teacher, Prof. Dr. Cavit Demirkol. I will be forever grateful to him that my journey to USA has begun with a conversation during my last undergrad semester in Turkey. Without his

encouragement, I would never be able to get through the difficulties that I had during throughout my graduate career.

I would like to express my deepest gratitude to my family; my parents, Sevil and Mehmet Ataman, my brother Basar, my grandmother Unal Sevindik and my aunt Jale Sevindik. Thank you for always being there for me in the good or the bad times during my life, and make me feel your support.

Last but not least, I would like to thank my lovely wife Ipek for her endless love and support during our relationship. She spent countless hours and sleepiness nights with me even she was back in Turkey. The distance between us was imperceptible with your dedication to our relationship. You never let me feel loneliness. Thank you!

TABLE OF CONTENTS

LIST OF FIGURES

CHAPTER I

INTRODUCTION

Natural fractures are present in almost every rock outcrop. However, their origin and the factors that control their intensity are not well understood. In addition to lithological factors, proximity to local structures such as folds and faults are important factors that play significant role on intensity and distribution of natural fractures.

Lithologic factors, which control brittleness and the mechanical properties of a rock body, are very comprehensive and broadly discussed by many workers (Corbett, 1985; Corbet et. al., 1987; Gross et. al. 1995; Hatcher, 1995; Hanks, 1995; Laderia, 1981; Lambert, 1993; Narr, 1991; Nelson, 1985; Underwood et. al., 2003). The primary lithologic factors are composition, bed thickness, clay type and porosity. A sedimentary rock unit composed of more brittle constituents such as dolomite and quartz has higher fracture densities (Nelson, 1985). The bed thickness is another significant factor that has a direct influence on abundance and development of fractures. Thick beds tend to have fewer fractures because the thicker beds have ability to compensate more stress (Harris et. al, 1960). Other two factors; clay content (Brace, 1961; Corbett et al., 1987) and porosity (Price, 1966) also have effect on fracture density. The strength of rocks decreases with increasing porosity and clay content.

Structural position and the tectonic history of the rocks also have crucial effects on the development and distribution of natural fractures. Fracture density increases with proximity of rock bodies to folds and faults and fractures accumulate in the vicinity of a fold or/and fault. Nino et al. (2005) showed an increment of the number of fractures near folds and fault zones. They also determined that fracture density is variable along the azimuth of folded structures because of shear strain variation.

The main purpose of this study is to determine the effect of structural and lithological factors on natural fracture development and distribution within the Upper Devonian/Lower Mississippian Woodford Shale in the Arbuckle Mountains. This study is based on field measurements of fractures in selected outcrops. Field work comprised a) measuring strike and dip of fractures; b) analyzing the mechanical stratigraphy within the inventory squares and along the scanlines, and c) collecting rock samples from specific units. Fracture data are analyzed to characterize natural fracture systems and to understand the controls of structural and tectonic events on fracture development. Inventory squares and scanlines provide the data to create graphical charts to visualize the effects of bed thicknesses and facies changes on natural fracture distributions. Additionally, thin sections and X-Ray diffraction analysis help to understand the effects of composition and clay content on development of natural fractures.

Study Area

The Woodford shale is well-exposed at several locations in the Arbuckle Mountains in Oklahoma. This study focused on a total of 7 outcrops of which six are located in the Arbuckle Mountains in the southern Oklahoma (Fig.1). The other outcrop is located in the frontal fault zone of the Ouachita Mountains. The first three outcrops are in close proximity to Interstate Highway 35; and include (1) Lake Classen Spillway outcrop in Murray County (T1S, R1E, NW/4 Section 26, T2S, R2E); (2) I-35 North Limb outcrop in Murray County (NE/4 Section 30, T.1S. R2E) and (3) I-35 south Limb outcrop in Carter County (NW1/4, SE1/4, Sec. 25, T.2S, R.2E) . The Lake Classen Spillway and I-35 North limb outcrops are exposed on the overturned northern limb of the Arbuckle Anticline and I-35 South Limb outcrop is exposed on the southern limb of the Arbuckle anticline. The last outcrop in the western part of the study area is the Mc Alister, McAllister Cemetery Pit outcrop (N/2 SW1/4, Sec.36, T.5S, R7E), is located in the Criner Hills near Overbrook, Oklahoma. One outcrop in the frontal fold belt of the western Ouachita Mountain area; It is called the Scratch Hill/East Atoka Road Cut outcrop (N34°22'321; W096°06'34,4) in Atoka county. Two outcrops were examined in the eastern Arbuckle Mountain (1) Wapanucka Shale Pit outcrop in Johnston county (34°18'59.61"N; 96°26'47.43"W) and (2) Clarita Shale Pit outcrop (34°28'6.52"N; 96°28'40.06"W) in Coal county.

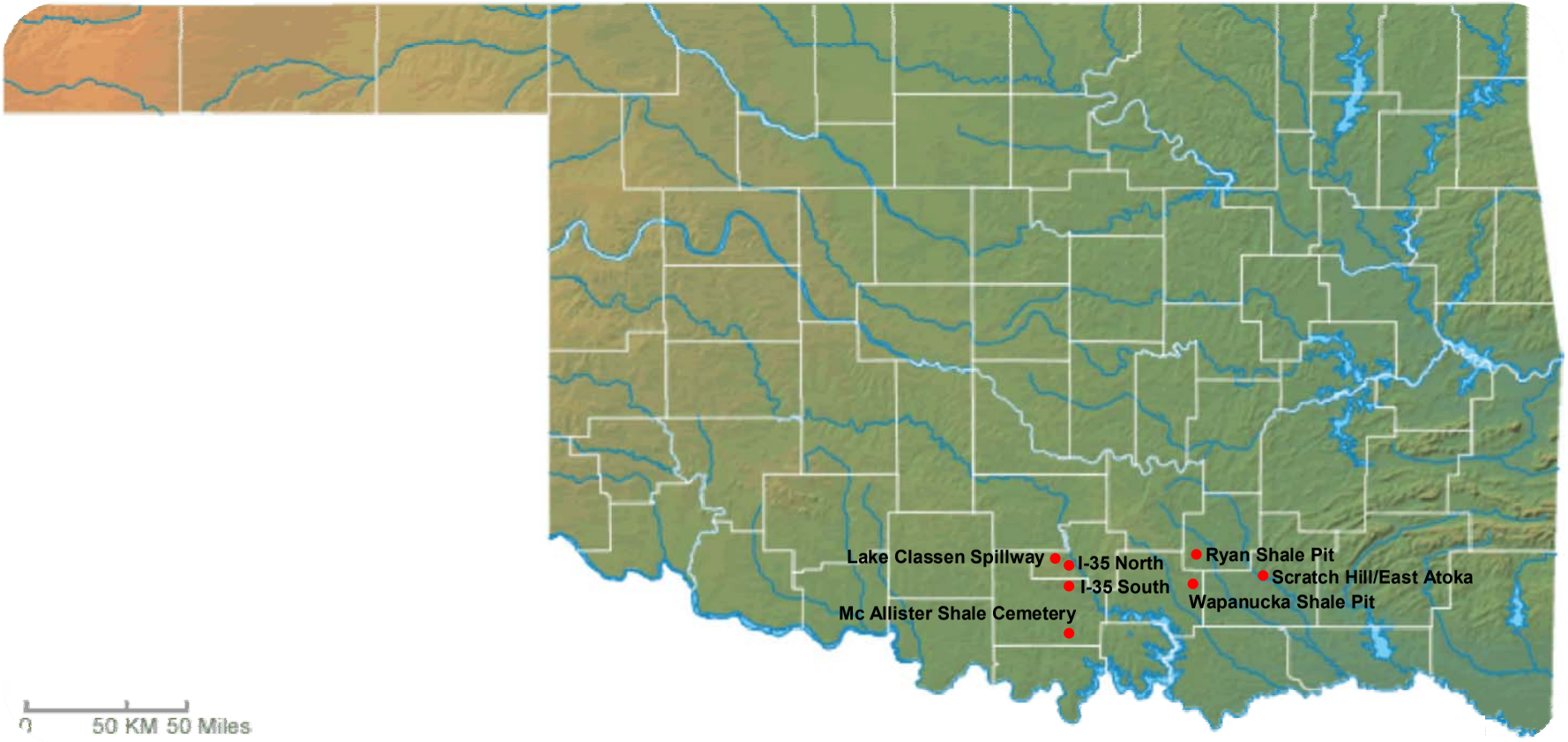

Figure 1. Location of the seven outcrops of the Woodford Shale studied during this investigation

Methodology

Fracture analysis was conducted systematically by examining seven Woodford outcrops. The geological map of the study area by Fay (1989) was used to recognize the major structures and formation boundaries in the Arbuckle Mountains. The "NASA World Wind" software was used to construct topographic maps. The geological map of Fay (1989) and the topographic maps were combined using computer software. Fracture orientations and dips were measured using a Brunton compass. Fracture sets, relationships between each sets and characteristics were examined and recorded the all outcrops. The exact locations of the outcrops were recorded by a Garmin GPS unit. These locations were plotted on the digitized geological map.

Fracture measurements were plotted on rose diagrams and equal area stereonets using Geologic Utilities function in the RockWorks software. Point densities were contoured on a equal area (Lambert) projection in order to better portray the fracture patterns. On each outcrop, fracture density analyses were conducted in 50cm x 50cm inventory squares located at the different stratigraphic positions. Bed thicknesses, lithology, the number of fractures on each bed, fracture spacings and fracture fillings were recorded. Rock samples were taken from specific fissile and non-fissile units for thin section analysis and X-ray diffraction. The thin sections were prepared by Mineralogy Inc., in Tulsa. X-ray diffraction analyses were conducted to examine the mineral composition and determine the clay type within each bed.

Significance of Studying Fractures in Woodford Shale

The Woodford Shale is recognized as one of most important unconventional gas reservoirs of the mid-continent region. Energy companies are producing natural gas from the Woodford Shale in the Arkoma Basin. These companies report that natural fractures are important in unconventional reservoirs because reservoir permeability is directly controlled by either open natural fracture systems or fractures induced during or completion. Therefore, a good understanding of the geometry of natural fractures is very crucial to increase the gas production from unconventional gas reservoirs.

Hydrocarbon accumulations are found within the fractures as free gas or absorbed by beds. Flow rate and the amount of hydrocarbons found within the fractures depend on fracture density and fracture properties such as: height, length, fracture array and cement. Therefore reservoir permeability and reservoir capacity is controlled by fractures.

Fracture orientations and connectivity also play crucial role in order to determine primary migration paths and pervasiveness of hydrocarbon accumulations. Hydrocarbon migration paths are predicted from the orientation of natural fracture systems and thereby future well locations can be determined. Orientation of fracture systems also gives important information about principal stress directions, which is needed in order to determine the orientation of horizontal wells and conduct hydraulic fracture treatments.

Furthermore, fracture filling cement should be determined in order to choose the type of fracturing fluid. Therefore, a fundemental understanding of the characteristics of natural fractures is very important to facilitate the gas production from unconventional gas reservoirs.

CHAPTER II

REVIEW OF LITERATURE

Natural Fractures in Rock

Fractures are any mechanical discontinuity surfaces in rocks such as faults or joints. They are usually planar and the material has lost its cohesion (Twiss and Moores, 1992). Pollard and Aydin (1988) point out that joints are also fractures however joints have no appreciable parallel displacement and have only movement normal to the fracture plane.

The relative motion that occurs across the fracture surface during fracture development is required for recognizing the deformation mode of a fracture. There are three types of fractures and each type has a different kind of motion (Fig.2). Mode I fractures are joints formed by the opening of the fracture in which the relative motion is perpendicular to the fracture surfaces. Mode II and III fractures are shear fractures. The difference between them is the relative motion, which is a sliding motion perpendicular to the edge of the fracture for Mode II whereas, it is a sliding motion parallel to the fracture edge for Mode III. A fracture that has a motion both parallel and perpendicular to the fracture surfaces is called a mixed mode or oblique extension fracture.

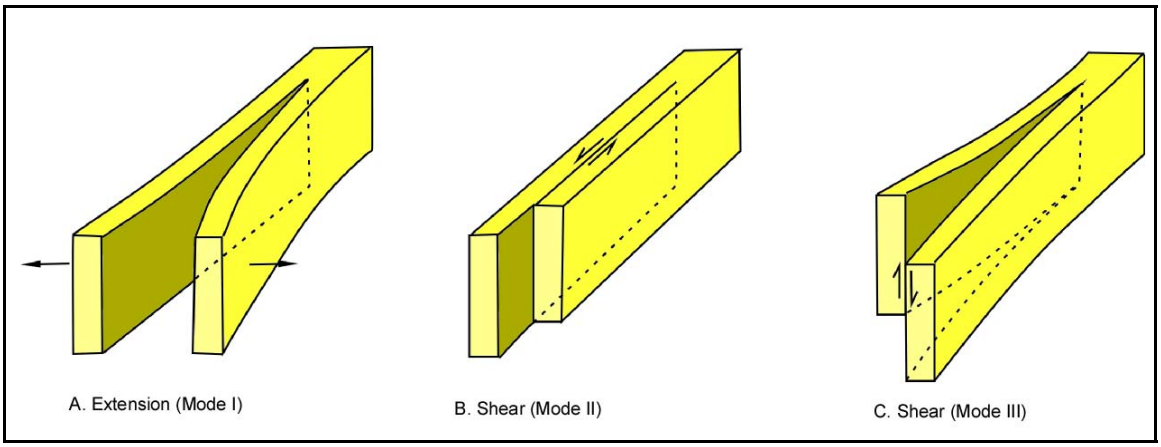

Figure 2. Three modes of fracture formation. A. Extension or mode I fracture. The relative displacement is perpendicular to the fracture. B. Shear fractures, mode II. Relative displacement is a sliding parallel motion to the fracture and perpendicular to the edge of fracture. C. Shear fracture, mode III. Relative displacement is a sliding parallel motion to the fracture and to the edge of the fracture

Fractures are planar or irregular surfaces that may be characterized as systematic or nonsystematic (Fig 3) (Twiss and Moores, 1992). Systematic fractures are characterized by parallel or subparallel orientation and regular spacing. If adjacent fractures have a similar geometry and orientation on a rock, they are referred to as a fracture set. Fractures those are curved and irregular in geometry and do not share a common orientation are referred to as nonsystematic fractures. Nonsystematic fractures can form at the same time with systematic fractures however if they die out within the intersection of the systematic fractures, this indicates nonsystematic fractures formed later (Twiss and Moores, 1992).

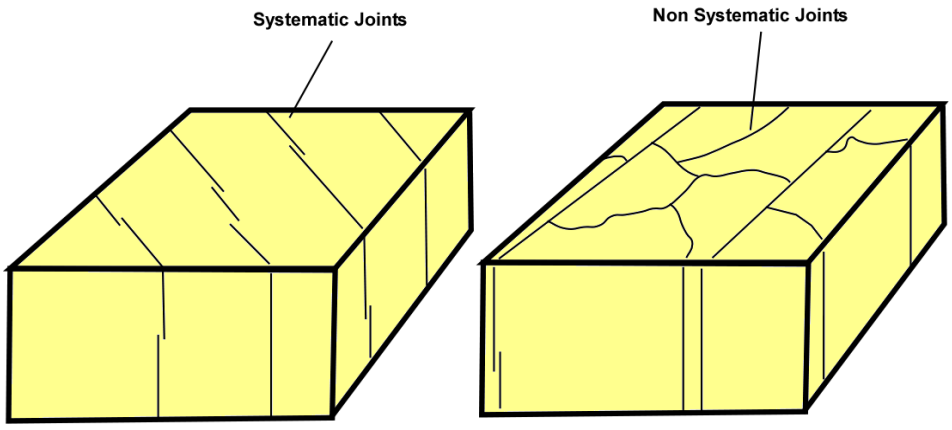

Figure 3. Diagrammatic views of the fracture sets and fracture systems. A. Geometry of a systematic joint set. B. Typical pattern of nonsystematic joints and termination against systematic joints (Modified from Twiss and Moores, 1992*).*

Shear Fractures

A shear fracture is a surface that occurs when the shear stress parallel to the surface is sufficiently large (Pluijm and Marshak, 2004). In brittle rocks, shear fractures would form along surfaces which shear stress is the greatest (Dennis, 1972). Shear fractures form when all three principal stresses are compressive. They form at some acute angle to the maximum compressive stress direction (σ_1) and at a wide angle to the minimum compressive stress direction (σ_3) within a rock sample. Usually, two shear fractures occur at the same time within a specimen so that the angle between shear fractures and the maximum compressive stress (σ_1) would be the same. The angle between shear fractures depends on: (1) the mechanical properties of the rock, (2) the magnitude of the minimum compressive stress direction (σ_3) and (3) the magnitude of the intermediate principal stress (σ_2). When σ_2 approaches σ_1 the angle between σ_1 and the fracture plane decreases (Nelson, 2001).

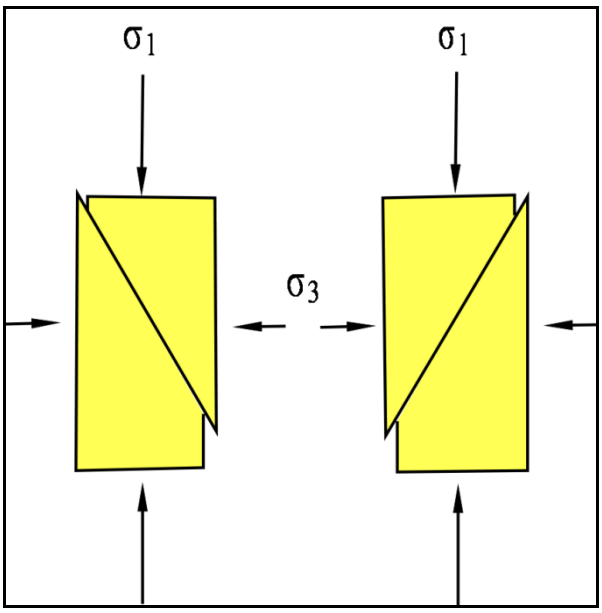

Figure 4. Shear fractures develop during laboratory experiments (Modified from Twiss and Moores, 1992*).*

Significance of Fracture Orientations

Gross (1993) concludes that fracture patterns exposed on horizontal surfaces and vertical outcrops may be used to infer paleostress orientations, therefore this may reveal the tectonic history of the region. Regional and local fracture sets are differentiated from each other by collecting dominant fracture orientations on a wide region and correlating them from one outcrop to another. In addition to this, the extent of the tectonic and regional forces can be inferred. Regional fracture orientations can be determined by measuring strike and dip of fractures over a wide area (Hatcher, 1995). However, Twiss and Moores (1992) state that interpretations of fracture sets should not only depend on

fracture orientations, but they should include other evidences such as fracture deformation types.

Furthermore, analyzing orientation of a systematic fracture set can provide crucial information to determine recent principal stress directions. This information can be used to improve oil and gas production rates by prowling input for oriented hydraulic fracture treatments or future well locations.

Fold Related Fractures

A significant amount of literature has been published describing possible fracture developments during folding (Stearns, 1964; Roznovsky, 2001; Bergbauer, 2004). The stresses and strains applied to rocks change during fold evolution. This variation of stresses and strains causes different fracture patterns. Some studies have found that former fracture sets already may have been existed in a rock body before folding because of prior tectonic events (Bergbauer, 2004). On the other hand, during folding, it is possible to observe different fracture patterns from one place to another on a fold. Stearns (1964) concludes that the position and intensity of the fracture sets developed with folding vary with fold shape and origin.

Also, fracture orientations, densities and positions are distributed unequally on bedding surfaces during folding (Fig 7). Every fold has its own stress and strain patterns and therefore the fold related fracture features will be different during fold evolution (Twiss and Moores, 1992). An orthogonal system (a, b, c) is convenient to refer to the orientation of fractures on a fold. The a axis is perpendicular to the fold axis, the c axis is perpendicular to the bedding and b axis is parallel to the fold axis. Fractures parallel to

the a and c axis are called ac fractures whereas fractures parallel to the b and c axes are called bc fractures. In set A and B, the ac fractures and the bc fractures bisect the acute angle between two other fracture sets, which are called oblique fractures. In set D, the bc fractures bisect the obtuse angle between the oblique fractures. The fractures in sets C and E are parallel to the fold axis and inclined. Fractures in C have low angle with bedding whereas those in E have high angle with bedding. Fracture sets in A and D are common in fold limbs and those in B and E tend to be associated with the convex sides of a fold (Twiss and Moores, 1992). All the ac and bc fractures are extension fractures whereas the oblique and inclined fractures are usually shear fractures.

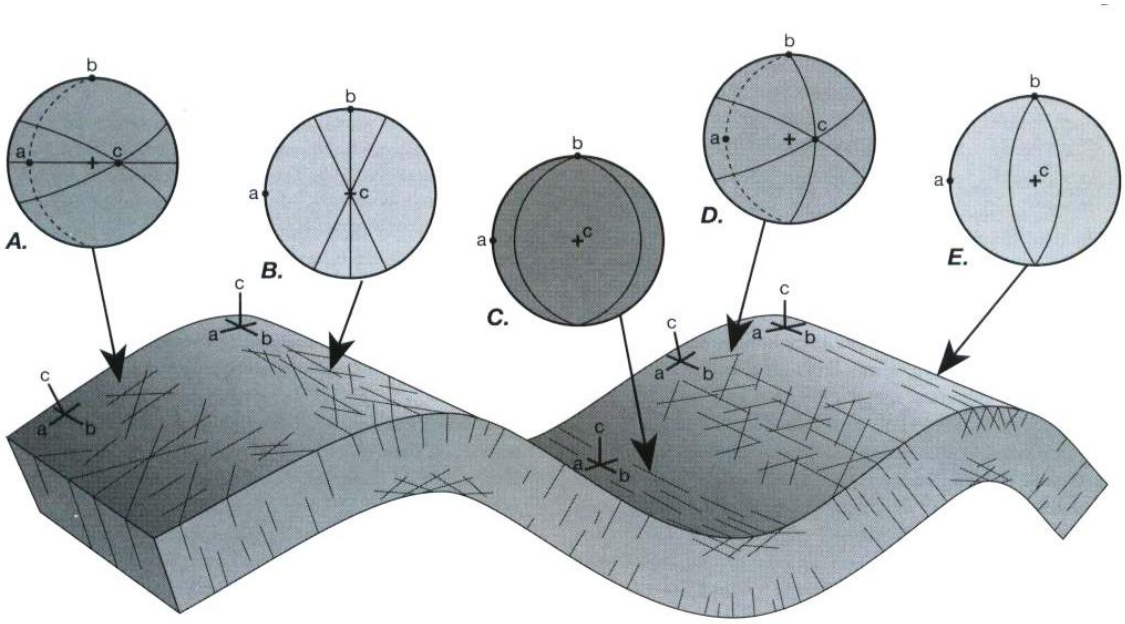

Figure 5. *Fractures associated with folds. The stereographic projections show the guide axes (a, b, c). The dotted great circles show the inclination of the beds and the solid great circles show the fracture orientations (from* Twiss and Moores, 1992*).*

Stearns (1968) proposes fold-related fracture developments in folded strata and he determines five fracture patterns that form systematically with respect to the fold axis and bedding (Fig 8). Fracture set 1 resulting from a vertical intermediate stress and a maximum principal stress parallel to the dip direction of bedding includes two shear fracture and one extension fracture. The least compressive stress is parallel to the dip direction. He concludes that the fracture set 1 could only form below the neutral surface of a convex upward plate and it is genetically related to fracture set 2, which can form above the neutral surface. Additionally, fracture set 3 has two shear fractures and one extension fracture whereas set 4 includes only two shear fractures. Above the neutral surface the shear fractures have normal offset, but in contrast, below the neutral surface, shear fractures are thrusts. Proposed fracture sets occur under different circumstances. Set 1 forms early during folding, set 2 forms when the extension normal to the fold becomes large and set 3 and 4 reflect locally developed bending or buckling. He also concludes that attitudes of fracture sets can change spatially and that they may have different orientations and densities at the nose of a plunging anticline or at the limbs of the same anticline.

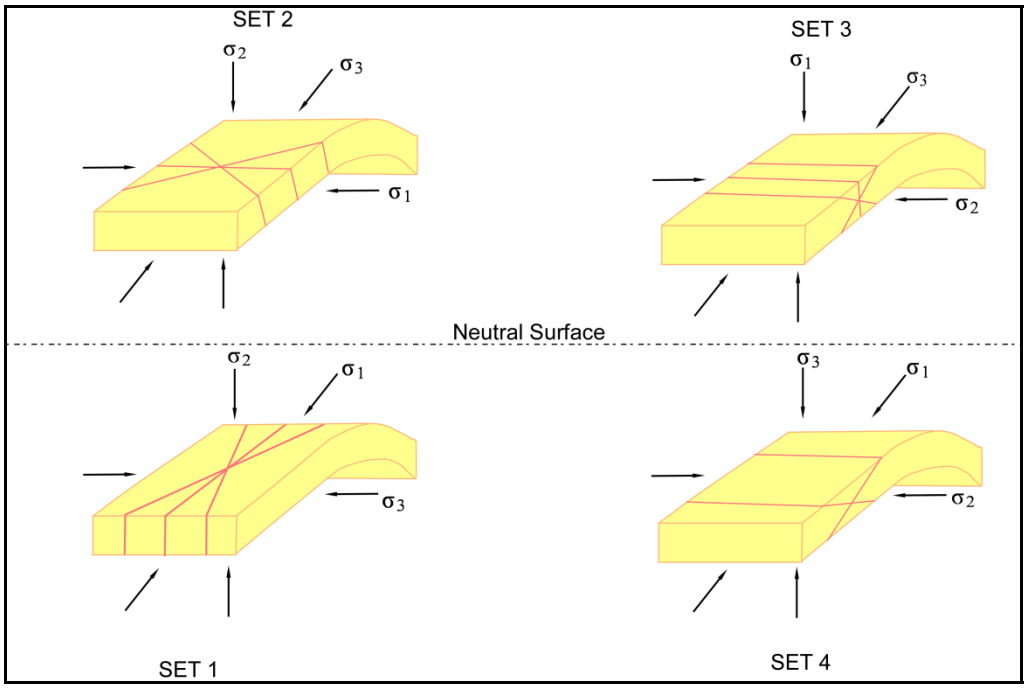

Figure 6. Conceptual model of Stearns (1968); multiple fracture sets are assumed to from symmetrically of fold axis (picture modified from Stearns, 1968).

However, Bergbauer and Pollard (2004) oppose that the existing models not only contradict the laboratory observations, but also fail to account for field observations of folded and fractured sedimentary rocks. They suggest that the specific evidence for extensional and shear displacements across fractures, the spatial distributions of fractures and the sequence of fracture formation should be used in formulating interpretations of fracture development.

Spacing and Density of Fractures

The average spacing between fractures in a systematic set can be determined by measuring the average perpendicular distance between fractures or the average number of the fractures found in a scanline or an inventory area. A high fracture density represents a more brittle response with more fractures, whereas a low fracture density represents a more ductile response with fewer fractures. There is an abundance literature concerning the spacing of fractures and fracture densities that contribute to understanding fracture densities (Hodgson, 1961; Price, 1966; Hobbs, 1967; Ramez et al, 1967; Nelson, 1985, 2001; Narr and Suppe, 1991).

The strength and brittleness of a rock play significant roles on fracture distribution and spacing. The major factors controlling the strength and brittleness are: (1) lithology, (2) grain size, (3) porosity, (4) bed thickness, (5) structural position and (6) the tectonic history of the region (Wiltschko et. al., 1991). The most important factor that controls the fracture spacing and distribution is the bed thickness (Harris et. al, 1960; Price 1966, Laderia and Price, 1981). Nelson (2001) concludes that if all the parameters and loading conditions are equal, thinner beds will have more fractures than thicker beds. Price (1966) concludes that fracture spacing can be different in different lithologic units with approximately same thickness. Hodgson (1961) also concludes that fractures which are distributed regularly in sedimentary rocks can be scaled with the thickness of the fractured layer. Therefore, the average spacing of fractures mainly depends on the rock type and the thickness of the beds.

Nelson (1985) shows that rocks composed primarily of more brittle constituents such as dolomite, quartz and feldspar have a higher number of fractures. Also, the clay

content is an important factor is that smectite content correlates with the strength of the rock (Brace, 1961; Corbett, 1987). The higher clay content values yield to pressure solution at a stress lower than that of brittle rock failure. Rock strength also increases with decreasing porosity (Price 1966; Corbett, 1987). Ramez and Mosalamy (1969) show that when grain size decreases compressive strength of a rock increases.

Hobbs (1967) explains mathematical calculations regarding the fracture spacing. He concludes that the fracture would form at the weakest point in the rock. He also proposes that the tensile stress will be released in the vicinity of the fracture; however it will remain within the rock. Thus, later fractures will form at finite distances from the first fracture. In contrast, Narr and Suppe (1991) realize that spacings between fractures do not match with Hobbs` model. They conclude that the presence of flaws, such as fossils, concretions, bedding plane irregularities and other inhomogeneties in rocks will reduce the strength of the rocks. In this model, new fractures will form at flaw instead of at regular distances from the first fracture.

CHAPTER III

GEOLOGIC SETTING

A solid understanding of the lithological properties of the Woodford Shale, the structural styles of the Southern Oklahoma Aulacogen and Ouachita Mountains is important to interpret fracture systems within the study area. Fortunately, southern Oklahoma has been a playground for geologists and the tectonic history of southern Oklahoma has been studied by many workers (Ham, 1973; Dewey and Burke, 1974; Walper, 1977; Wickham 1978; Webster, 1980; Hardie, 1990; Bixler, 1993; Saxon, 1994, 1998). Although there are many controversial idea, concerning the origin of these provinces, the general steps of the deformation stages are widely accepted. In addition to the tectonic history of the regions, and the interest in gas reservoirs, conventional reservoirs and in the Woodford Shale, the number of published papers have increased dramatically in the last decade.

In this chapter, the general properties of the Woodford Shale and the tectonic setting of southern Oklahoma will be examined. Structural styles of the outcrop locations: (1) the Arbuckle Mountains and (2) the Criner Hills, (3) Ouachita Mountains will be summarized.

Woodford Shale

The Woodford Shale is among the more important black shales formed from sediments deposited during the late Devonian. It consists of organic rich, dark gray to black shale with light gray chert beds and phosphatic horizons. Organic rich beds are generally darker colored than silica rich beds. The upper stratigraphic member of the Woodford Shale is lighter colored, cherty and more phosphatic than the lower and middle members. These characteristics correlate with TOC levels (Hester, 1990). The cherty beds are thicker and more solid when compared to organic rich beds.

Woodford sediments were deposited in the Permian Basin of western Texas and southeastern New Mexico, and in the Anadarko Basin of western Oklahoma (Amsden, 1975). Its equivalent "Chattanooga Shale" is found in Nebraska, Kansas and eastern Oklahoma, Arkansas and Tennessee (Amsden, 1980). The basal Woodford is typically sand-rich and called of the Misener Sandstone in Oklahoma where it unconformably overlies Silurian to early Devonian Hunton Group carbonates and older units. The Woodford is overlain by the Mississippian Sycamore Formation which consists of fine grained, silty limestone with interbedded thin dark shales (Fig 16). The Woodford Shale basically represents a transition from early Paleozoic carbonates to Paleozoic clastics (Cardott and Lambert, 1985).

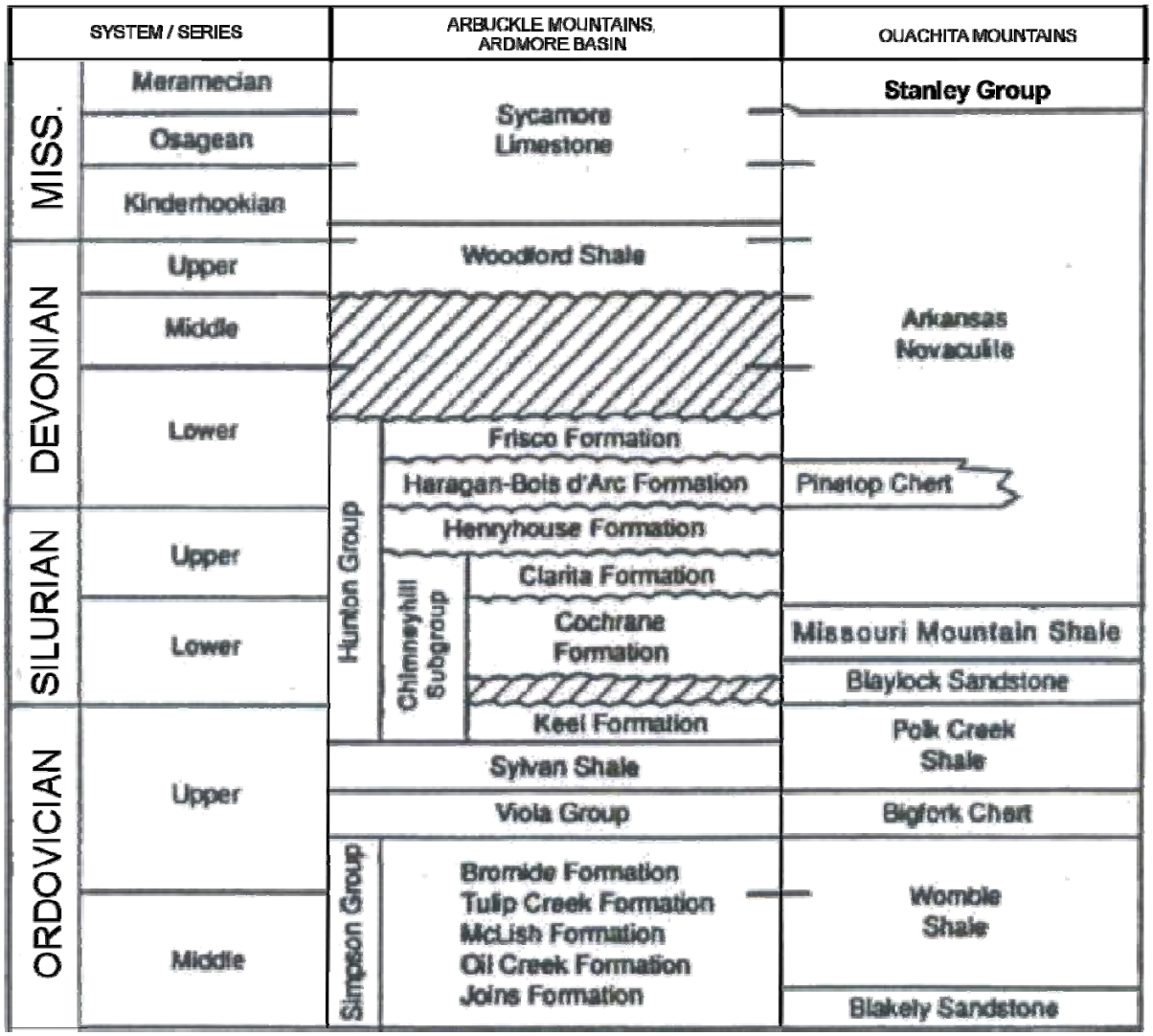

Figure 7. Stratigraphic relationship between the Woodford Shale and Devonian, Silurian and Ordovician units in Southern Oklahoma.

Hass and Huddle (1965) determined Late Devonian age for the most of the Woodford and Early Mississippian for the uppermost part. Woodford deposition occurred slowly in a low oxygen environment (Sullivan, 1985). The Woodford Shale and its equivalents are distributed over much of North America, implying a deep water origin

(Lambert, 1993). All these deposition conditions provide adequate opportunity for carbon presentation and for the Woodford to be a rich source rock for oil and gas.

The Woodford Shale is "hot" shale that can be easily identified on well logs. It has a higher radioactivity when compared to other formations. For example, Hunton shows gamma ray deflection in the range of 10 to 60 API units, where the Woodford Shale has value in the range of 90 to 200+ API units. The Woodford Shale is divided into three informal shale members using wireline well logs. The lower shale member has a gamma ray deflection approximately more than 300 API units in the Southern Oklahoma Aulacogen, the middle member have 300+ API units and the upper shale member produces a response that is more than 200 API units in northwestern Oklahoma. The middle member of the Woodford Shale has the greatest aerial extent and thickness (Lambert, 1993). The radioactivity of each shale member decreases to the north. The middle member of the Woodford has more than 320 API units in Oklahoma, decreasing between 240 and 320 in Southern Kansas and 100 in northern Kansas. Similarly other shale members decrease towards northern Kansas (Lambert, 1993). Furthermore, the color of the shale members progressively change in subsurface samples in that, shales in southern Oklahoma darker color than shale of Kansas (Lee, 1956). Decreasing gamma ray readings and the trend of the color indicate that organic content of the shale decreases to the north (Lambert, 1993). In addition, Hester (1990) proposes that the middle member of the Woodford has a higher TOC with 5.5 wt%, whereas the lower and the upper "members" have 3.2 and 2.7 wt%, respectively.

The lower member of the Woodford Shale contains highly oxidized type IV. Walper (1985) believes that this type of kerogen has no capacity to generate

hydrocarbons. The middle member contains type I and type II kerogen of marine origin, and type III kerogen, which is of terrestrial origin (Lambert, 1993). The upper member has mostly type III and IV kerogen. It is for these reasons; the lower member contains mostly Woodford Shale may not be a petroleum source rock, whereas the middle member of the Woodford has the greatest potential to generate hydrocarbons.

Southern Oklahoma Aulacogen

Tectonic forces intensely affected the southern Oklahoma region from the late Precambrian to Late Pennsylvanian. The very first tectonic activity was the rifting stage in the late Precambrian that separated North America from the proto-Afro-South American plate (Walper, 1977; Wickham 1978). This rifting occurred as a series of triple junctions in which upwelling mantle plumes thinned the crust and formed oceanic spreading centers along the Ouachita Mountain system (Fig.9) (Dewey and Burke, 1974). Two arms of each triple junction experienced spreading. These arms were connected to each other to form the continental boundary. The third arm did not spread and it extended landward. The third arm received an accumulation igneous rocks initially and later thick sedimentary package. Thiselongate fault-bounded trough was termed as an aulacogen by Schatski (1946). The Southern Oklahoma Aulacogen represent the failed arm of a triple junction.

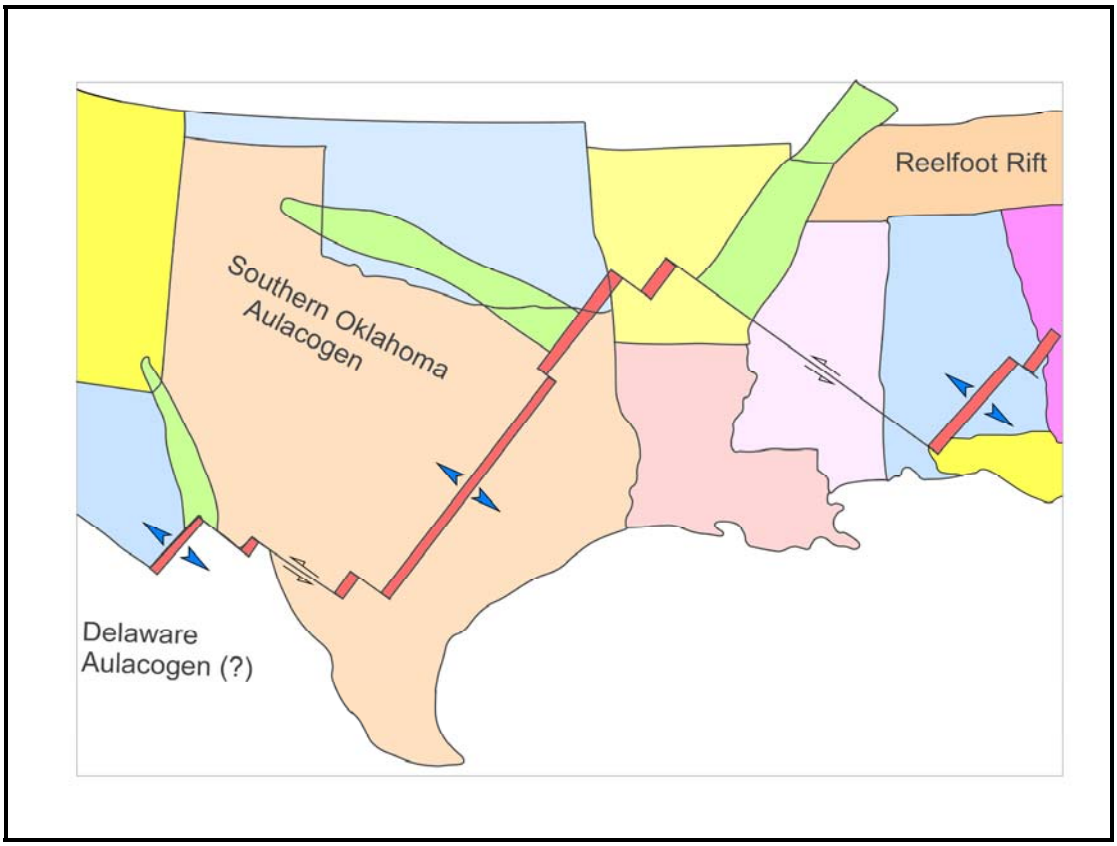

Figure 8. A plate tectonic model of southern North America in the Cambrian (Figure modified from Suneson, 1996).

The Southern Oklahoma Aulacogen was accompanied with the development of normal faults and generated igneous rocks in the rifting stage (Hoffman and others, 1974). Marine transgression covered these igneous rocks, and shallow marine sediments deposited represented by Cambrian Reagan sandstone. The rift cooled and began subsiding further with sediment accumulations. The thickness of the sediments was more within the aulacogen than on the surrounding craton. Marine sediments from Late Cambrian to Mississippian were deposited within the aulacogen (Fig. 11), (Ham, 1973). Later, the subsiding stage accompanied with little folding and faulting (Webster, 1980).

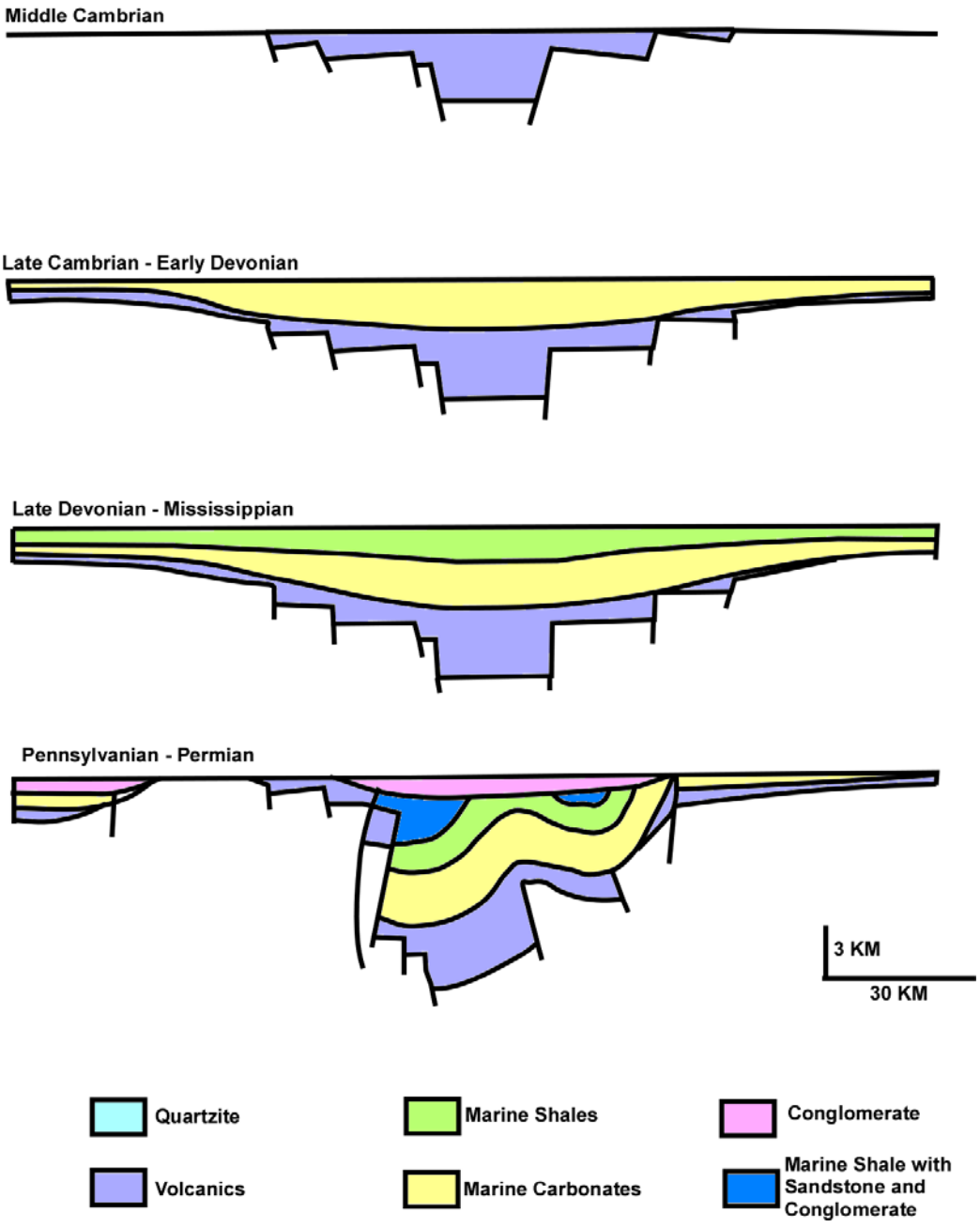

Figure 9. Structural development of the Southern Oklahoma Aulacogen. Rifting, Subsidence and Deformation stages (modified from Bixler, 1993)

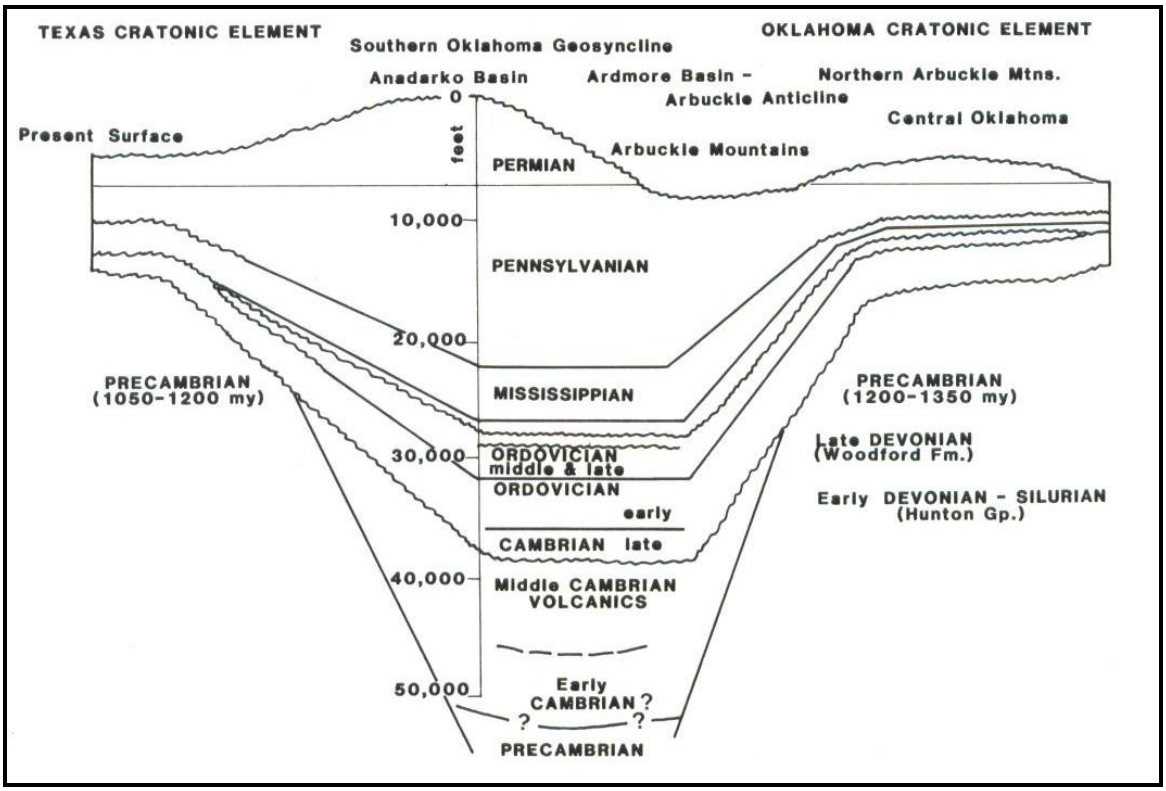

Figure 11. Diagrammatic cross section demonstrating the thickening of sediment in the Southern Oklahoma Aulacogen (from Ham 1973)

The deformation stage was the last stage in the evolution of the Southern Oklahoma Aulocogen. The area underwent crustal shortening along basement faults from Late Mississippian to Early Permian. Several thick invtervals of synorogenic sediments were deposited along the basins of southern margin during crustal shortening.

Orogenic activity in the SOA began with the Wichita Orogeny along the Wichita Mountains and Criner Hills in Late Mississippian and ended with Arbuckle Orogeny in Virgilian (Hardie, 1990). The Wichita Uplift formed the Anadarko Basin; the Wichita Mountains and Criner Hills intensely deformed during Morrowan. The Wichita Orogeny

continued during Early Atokan and folded the Amarillo-Wichita-Criner trend (Hardie, 1990). The Criner Hills uplifted 10.000 to 15.000 feet structurally higher than the Ardmore Basin (Tomlinson, 1952).

The Arbuckle Orogeny, which occurred from Late Missourian to Early Permian, represented a later pulse of deformation, and reactivated the Wichita uplift, Hunton Anticline, Tishomingo Anticline and Criner Hills systems (Fig. 12). Compression of the area between Tishomingo-Hunton and Criner Hills formed northwest-southeast trending Ardmore Basin and the Arbuckle Anticline (Hardie, 1990). Uplift of the Arbuckle Anticline resulted with the deposition of the Virgilian Collings Ranch and Vanoss Conglomerates. The Collings Ranch Conglomerate was folded and faulted during the final stages of the deformation along the Arbuckle Anticline (Ham, 1967). The late Pennsylvanian Arbuckle Orogeny was the last mountain building pulse in the Southern Oklahoma Aulacogen.

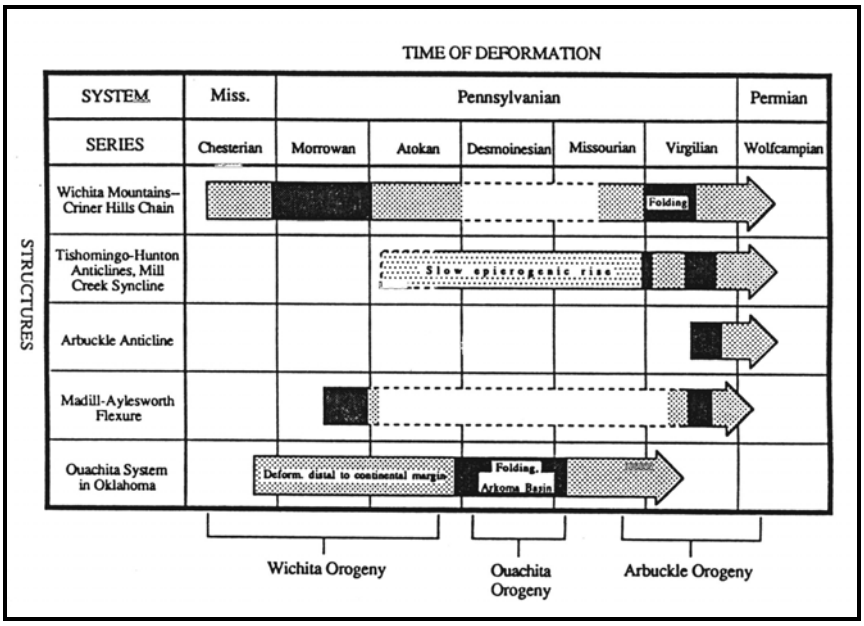

Figure 12. Chart of the sequential orogenic deformation of the Southern Oklahoma showing relationships of the Wichita, Ouachita and Arbuckle orogenies. Shaded areas show significant pulses of deformations (from Hardie, 1990)

Extensional tectonics began shortly after maximum uplift and formed normal faults parallel to, and reactivating, major thrusts that cut many structures (Saxon, 1998). This relaxation is associated with normal movement on the Meers Fault in the Wichitas. The Criner Hills and the Arbuckle also cut by normal faults as well (Saxon, 1998). Saxon (1994) indicated that a late-stage extensional system formed shortly after maximum uplift of the Arbuckle Anticline was obtained. He also concluded that the extension occurred as a relaxation of compressive stress and/or gravity instability, but it was followed by a tectonic compression. The reason of these deformations was thought to be associated with closing of the proto-Gulf of Mexico and Iapetus Ocean, the suturing of South America to North America and the formation of Pangaea.

Structural Styles of the Arbuckle Mountains

Orogenic pulses have affected the Arbuckle Mountain region many times *(Hardie, 1990; Walper, 1977 Saxon, 1998; Hart, 1974)*. Several deformational models have applied to the Arbuckle Mountain region; block uplift system along high angle normal faults, local gravity slide fault system, right lateral strike-slip fault system, left lateral strike-slip fault system and low angle reverse fault system (Saxon, 1998). In the block uplift, right lateral and left lateral systems, a high angle fault system is assumed whereas, in the low angle reverse system, fault planes flatten with increasing depth. The most commonly applied model is the left lateral strike slip fault system. The support for the left lateral movement along the Washita Valley fault is a combination of en echelon folds, faults which steepen with depths, synthetic and antithetic strike-slip faults, and horizontal slickensides along the northwest trending fractures (Wickham, 1978). Additionally, according to Pybas and Cemen (1987), the Collings Ranch Conglomerate has deposited in a pull-apart basin which has formed as result of strike slip movement. They also conclude that the Arbuckle Group trusts over the Collings Ranch Conglomerate suggesting a small convergent (transpressional) region. Cox (1988) explains the evidences for transpressive left-lateral motion along the WVF in four aspects; (1) a nearly vertical attitude of the WVF suggests a strike-slip motion produced this fault. Approximately, 150 m left-lateral offset of an anticline also suggest the movement of WVF is later than the compressional event. (2) The presence of antithetic right-lateral faults, synthetic left-lateral faults and their vertical attitudes are consistent with strike-slip motion. (3) The deposition of the Collings Ranch Conglomerate in the pull-apart basin of the WVF branches. (4) The possible 5 km offset of the Simpson Group

across the WVF. These studies suggest mostly a left lateral strike-slip and an oblique-slip combination in the Washita Valley Fault.

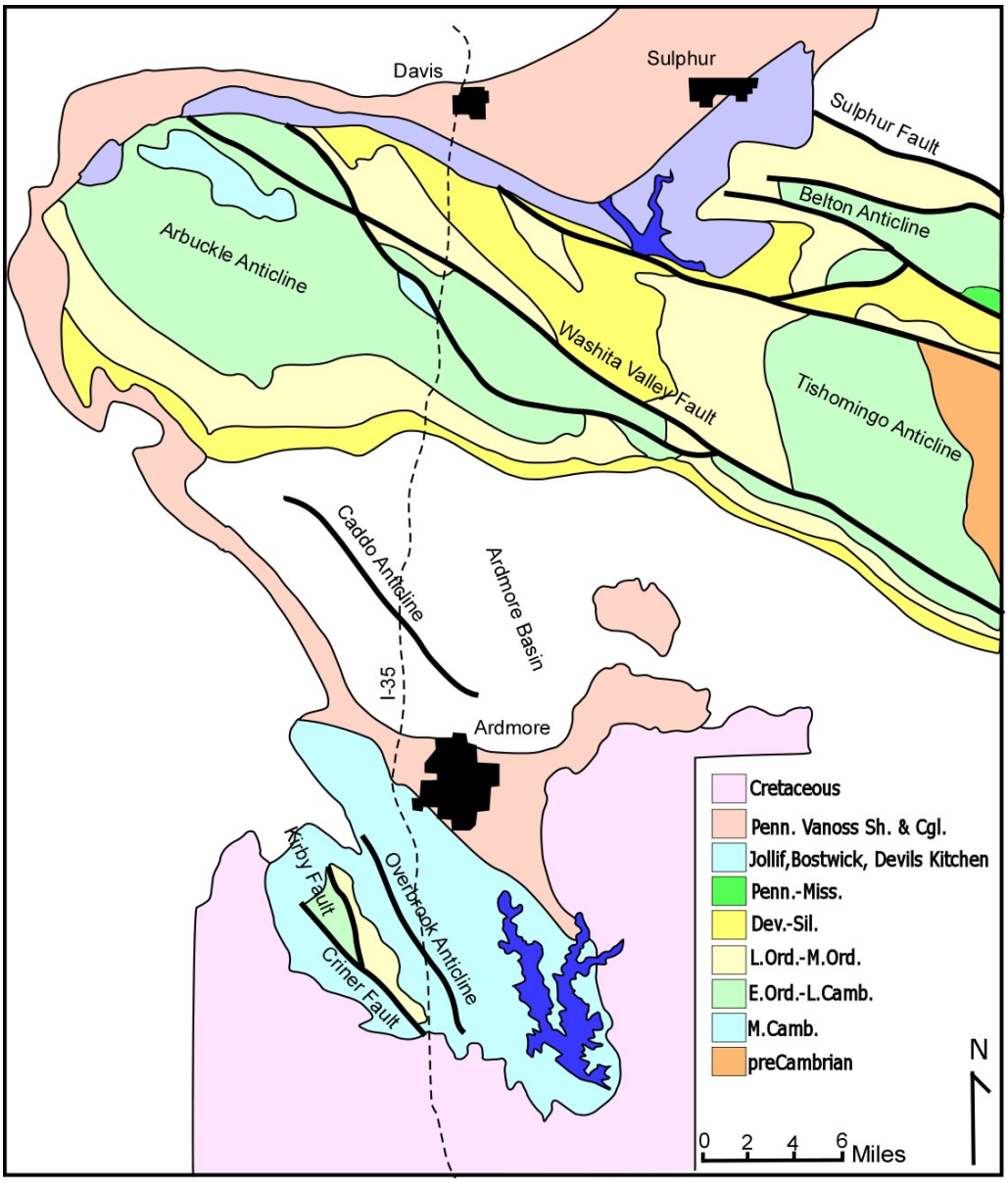

Figure 13. The Arbuckle mountain region is comprised of a series of anticlines and synclines separated by large folds. Structurally deformed rocks in the region range from Precambrian granite to Pennsylvanian conglomerate (modified from Grayson, 1985)

Ham (1951) proposes the Arbuckle Mountain region as a system of low angle reverse faults. Folded and thrust-faulted beds in the Wichita and the Arbuckle systems strongly indicate the presence of an extensive horizontal shortening in this area. Furthermore, most of the folds are asymmetric anticlines that are overturned to the north whereas the southern limbs are dipping with fewer angles (Brown and Grayson, 1985). The low-angle reverse fault model has been reviewed by Brown (1984) and he has restored the Oil Creek Sandstone to its predeformation location, and has suggested that the structural shortening along the Washita Valley Fault zone is explained by the apparent separation of the Oil Creek Sandstone with no or little lateral movement.

The Arbuckle Anticline

The Arbuckle Mountains are located in the Southern Oklahoma Aulacogen that several northwest-trending structures; the Wichita-Criner Hills trend, the Anadarko Basin and the Ardmore Basin are adjacent to the region (Fig. 13). It is located on the northeast side of the Southern Oklahoma Aulacogen. The three outcrops: (1) The Classen Lake, I-35 North and I-35 South are located on the limbs of the Arbuckle Anticline.

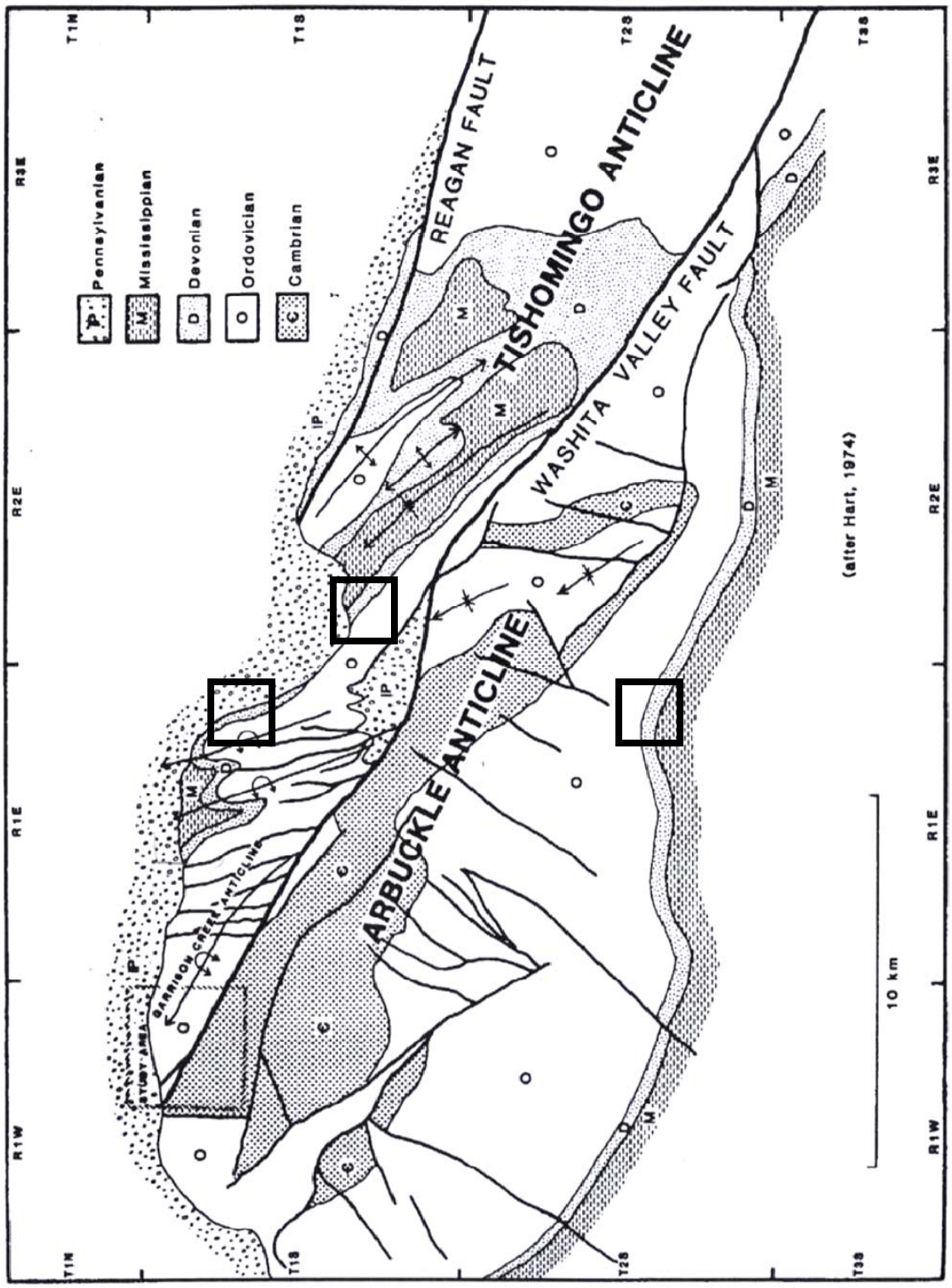

Figure 14. Structural elements of the Arbuckle Mountains (from Hart, 1974). Outcrop localities at the limbs of Arbuckle Anticline shown with squares.

The Arbuckle Anticline is a highly overturned fold to the northeast. The structure of the Arbuckle anticline is complicated due to secondary faulting of the Washita Valley Fault (Ham, 1955). There are several folds and faults in the region trending approximately northwest to southeast. The Arbuckle Mountains is the hanging wall of the Arbuckle Thrust (Saxon, 1994). He also refers to the Arbuckle Anticline as the main anticline south of the Washita Valley Fault which is dipping to the southwest direction. Thus, the Washita Valley fault is thought to be the north-eastern boundary of the Arbuckle Anticline. According to Tanner (1967), it is a vertical fault which extends from north of Doyle Field, south Eola Field, across the Arbuckle Anticline, and forms the south boundary of the Tishomingo Uplift. It displays predominantly parallel folding and low-angle thrusting with back-limb basement involved thrusts; the Joins Ranch Thrust and the Chapman Ranch Thrust (Saxon, 1998).

Saxon (1998) determines the Arbuckle thrust fault as the main fault and the Washita Valley Fault as the backlimb. The WVF imbricates to the buried Arbuckle thrust fault and merges at depth (fig.14). It loses its slip and dies out to the northwest and terminates against an un-named fault to the southeast (Saxon, 1998). It has some component of left lateral slip however, it is not the dominant slip of the movement and it not conclusively proven either (Saxon, 1998).

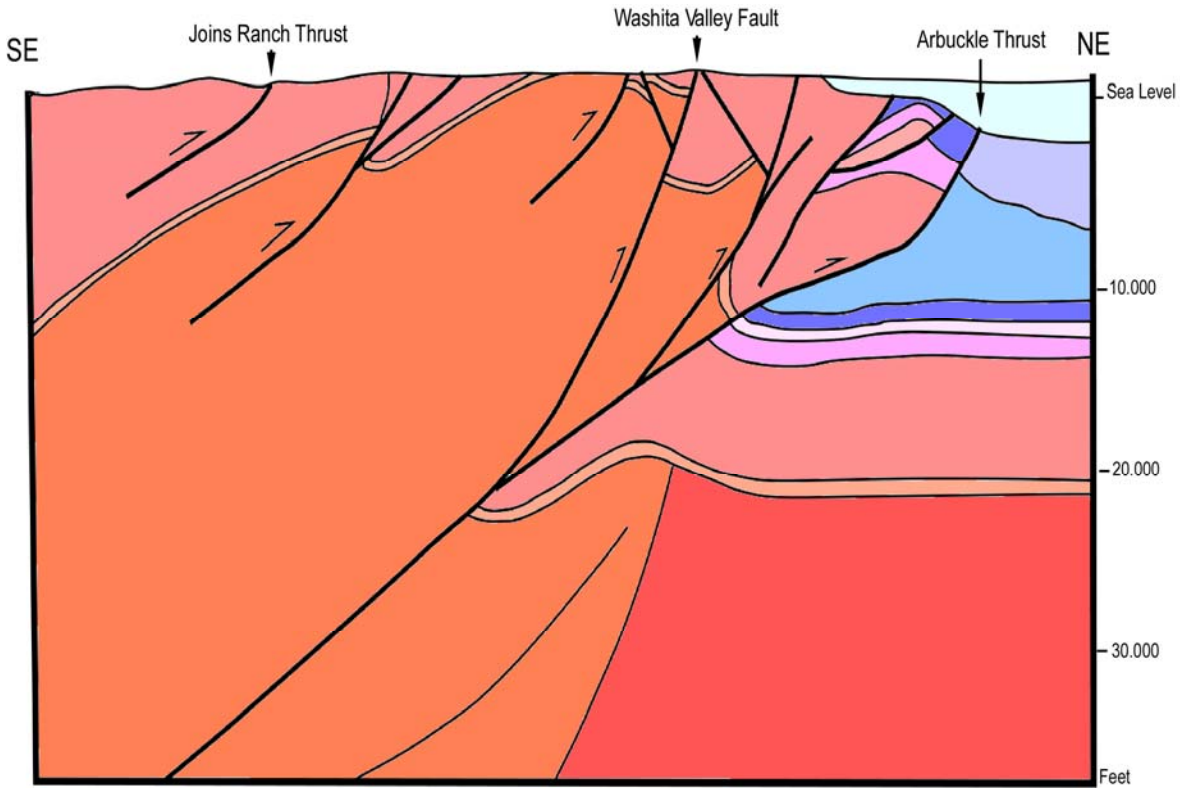

Figure 15. Cross section (A-A[1]) across the central Arbuckle Uplift

(Modified from Saxon, 1998)

The Criner Hills

The Criner Hills are located in T.5S., R.1E, at Carter County and T.6S., R.1E., at Love County, in the Southern Oklahoma Aulacogen. It is structurally complicated as the Arbuckle Anticline and is a topographic high between Ardmore Basin and Marietta Basin (Fig. 16). The McAllister Shale Pit outcrop is located in this area.

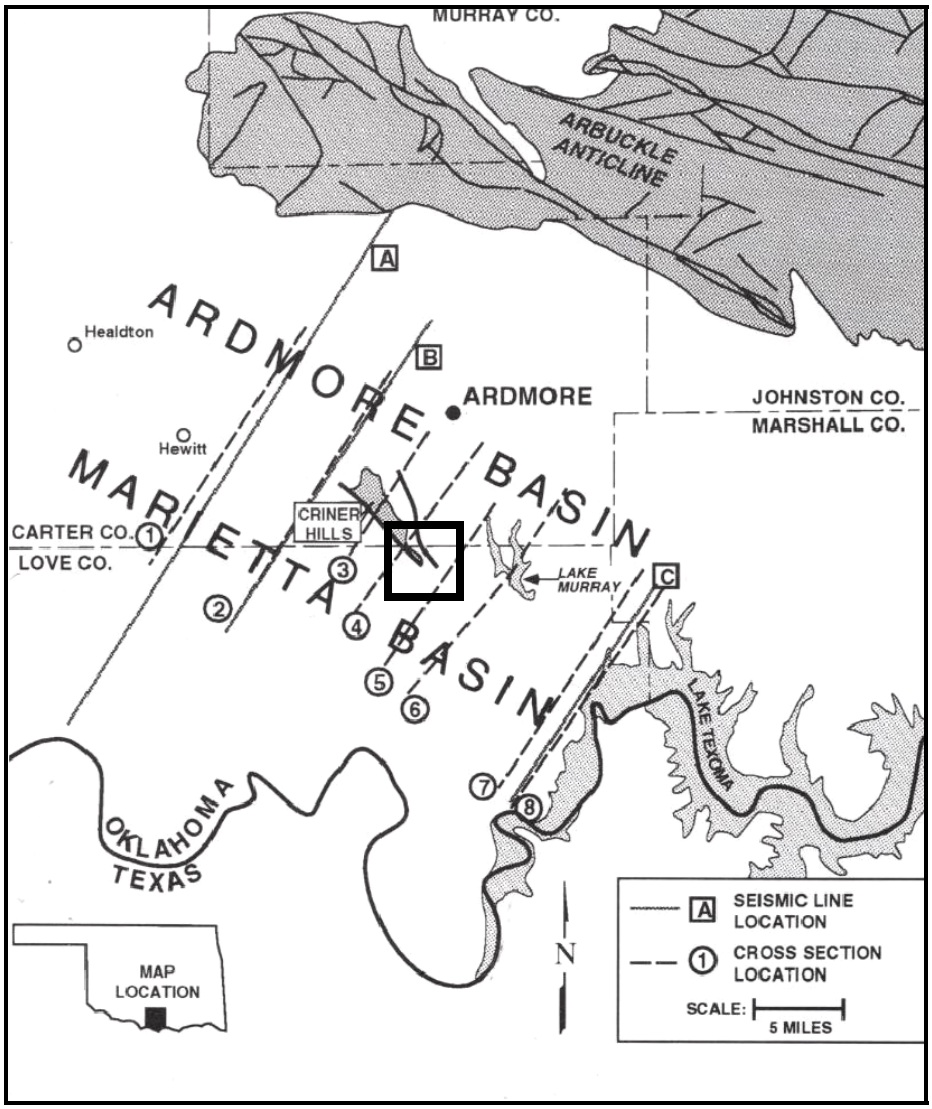

Figure 16. Generalized map of the Criner Hills and Ardmore Basin. The Criner Hills separate Ardmore Basin from Marietta Basin. The Line 4 gets by the McAllister Shale Pit outcrop.

The Criner Hills trend is an intensely folded and faulted region. The major fault is the Criner fault that is found to the southwest of the region and it has a trend to NW-SE directions and parallel to the axis of the anticline. The beds are dipping 65° SE and 49° NE at the both side of the hinge line of the anticline (Stone, 1929). The Criner Hills and the Arbuckle Mountains are contemporary uplifts that the age of folding and faulting, stratigraphy, the same direction of trend are practically the same (Stone, 1929). He also concludes that the same tectonic forces played significant and major role for two uplifts.

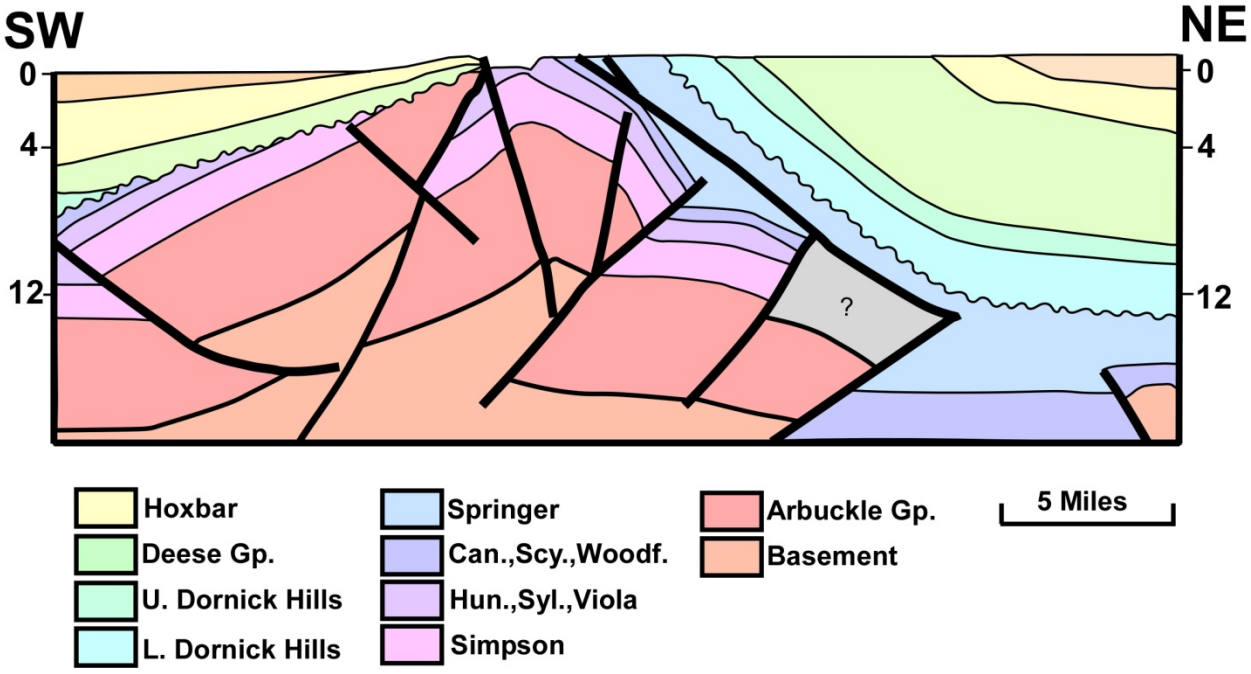

Figure 17.Cross Section 4 from the Criner Hills generalized map (modified from Cooper, 1995)

Cooper (1995) summarizes the deformation history of the Criner Hills trend. The tectonic forces have taken place from Late Mississippian through Pennsylvanian. Compressional forces have effected with substantial shortening and associated uplift. A

southwest-to-northeast deformation sequence predominates. Both high angle and low angle faulting accompanied with these compressional forces. He also encloses that very little left-lateral movement has recorded in the upper thrust sheets.

Ouachita Mountains and the Arkoma Basin

The Ouachita orogenic belt was produced by intense tectonic stresses from late Atokan to early Missourian and Arkoma basin was formed as a result of these tectonic events of the Ouachita orogeny. Many workers studied the tectonic evaluation of the Arkoma Basin and the Ouachita Mountains (Walper, 1977; Cox, 1988; Haley and Stone, 1995; McBee, 1995; Brown; 1995).

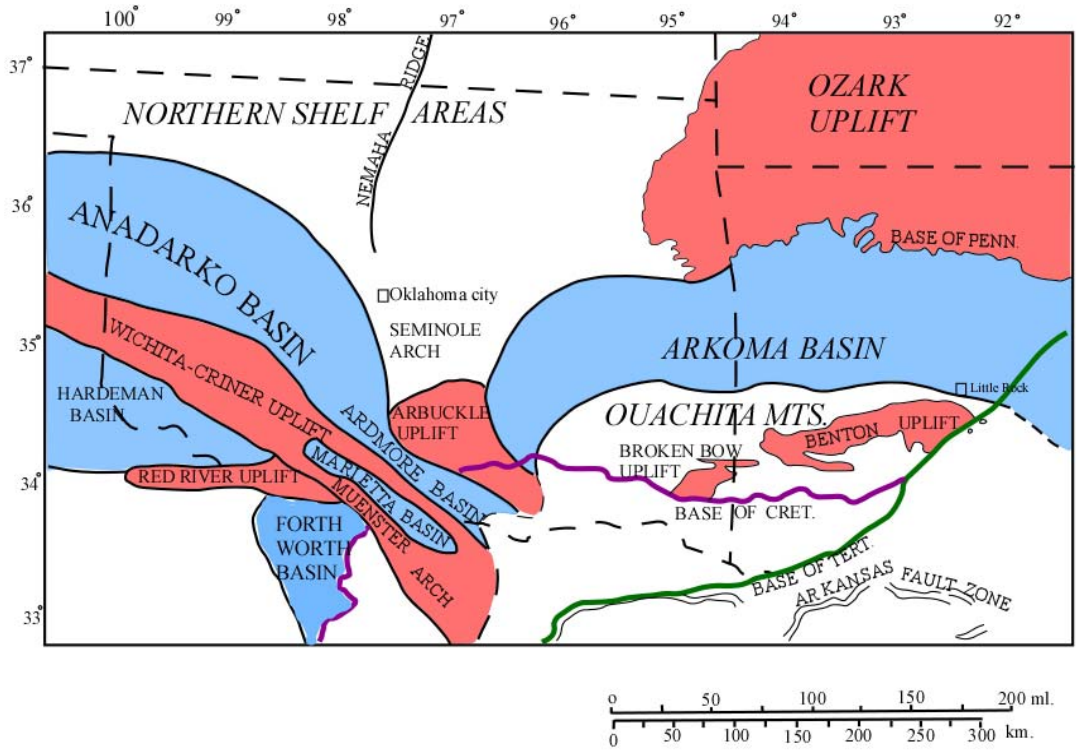

Figure 18. A general schematic picture of the Arkoma Basin and Ouachita Mountains.

In late Precambrian, after the rifting of the Paleozoic supercontinent Rodania, south edge of the North America became a passive continental margin with opening of the Iapetus ocean. Carbonates and sandstones of shallow marine to non-marine deposited on the shelf while to the south, deeper marine sediments such as; shale were deposited. Plate motion reversed and tectonic plate convergence began in late Ordovician. The ocean continued closing during Devonian and Mississippian due to the development subduction zone along the southern margin of the North American plate. The North American plate subducted beneath the Afro-South America plate and as a result oceanic crust was eliminated. Along the oceanic margins of the basins, a fold-thrust belt developed while tectonism and sedimentation was proceeding. In late Mississippian time, subduction of the oceanic crust completed. During the late stage of plate convergence, the folded and faulted nappes and slices of the oceanic crust were thrusted further and as a result Ouachita and Marathon core areas were formed. Deep marine sediments of Ouachita basin were scraped off and cropped out in the core of Ouachita Mountains. The uplift of the subduction complex and sediments were eroded and accumulated in basins In the late Atokan time, the subduction complex was pushed northward and thrusting dominated along the Ouachitas. Carbonates, shales and sandstones of late Cambrian through earliest Atokan (Spiro) age sediments deposited in the Arkoma Basin. The strata presented in the Arkoma Basin extend beneath the Ouachita core area (Fig. 20).

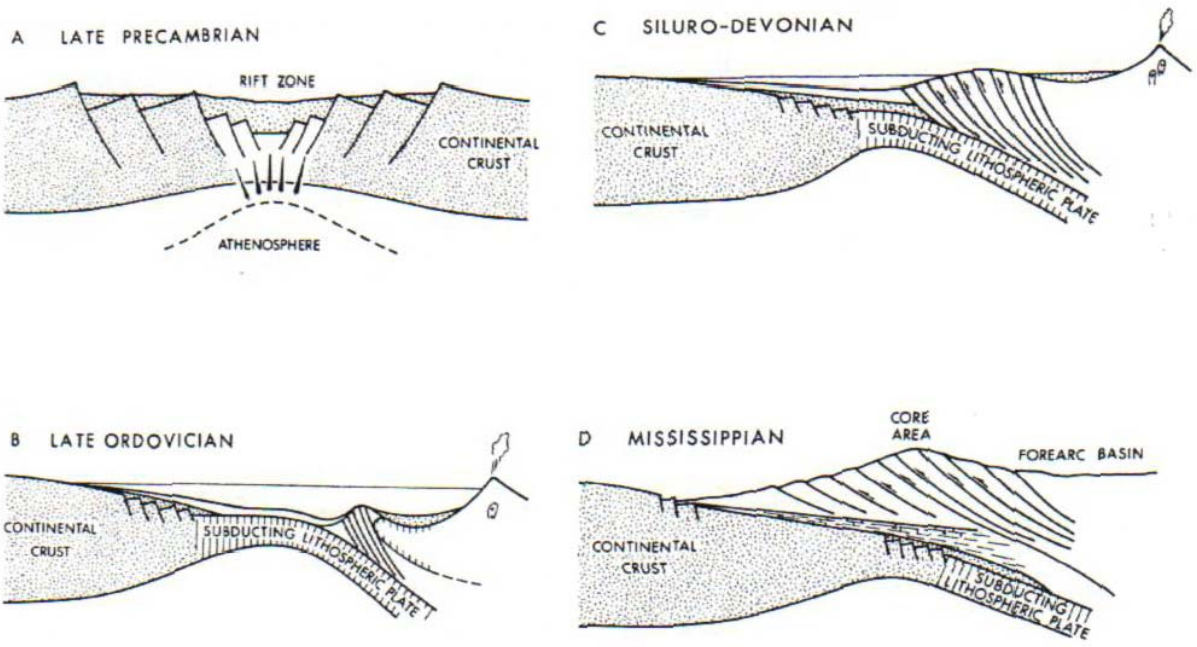

Figure 19. Diagrammatic cross section showing the tectonic evolution of the Ouachita System (From Walper, 1977).

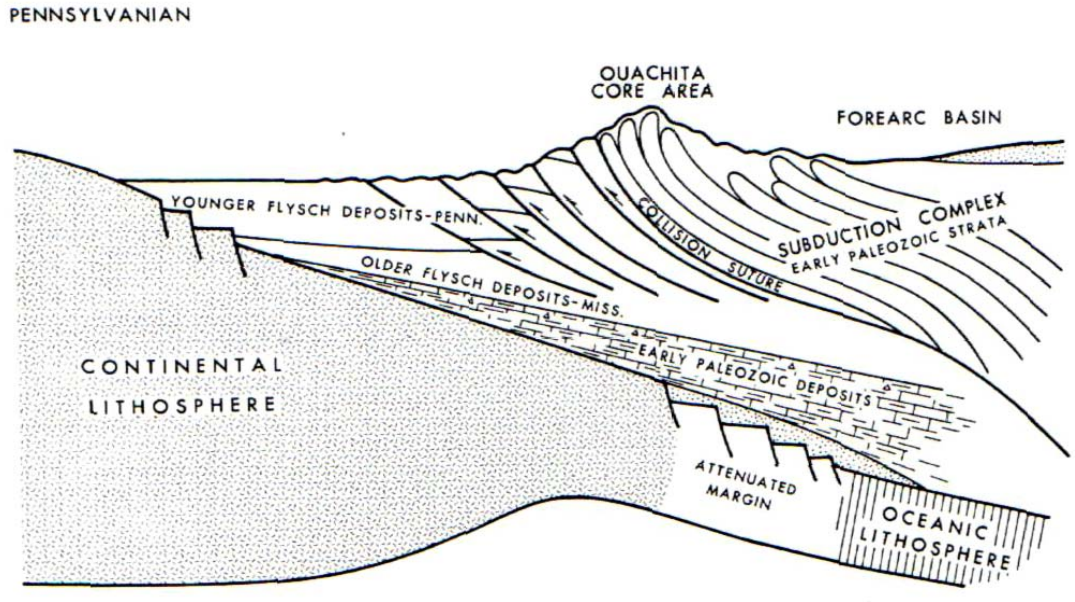

Figure 20. Diagrammatic cross-section (Pennsylvanian) showing development of foreland basin, fold-thrust and basin sedimentation (from Walper, 1977)

The compressive stresses were initiated by plate convergence and they were affected throughout the North American continent. These compressive stresses were formed and reactivated northwest directed faults. Vertical and strike-slip movements of these faults were resulted with rising of several uplifts. In the Southern Oklahoma aulacogen, the compressional forces produced the Amarillo-Wichita-Criner Hills uplift and the faulted and folded Arbuckle anticline. They also played a major role on evaluations of Anadarko, Ardmore and Marietta basins. All these basins are elongated parallel to the direction of maximum principal stress. According to Walper (1977) the direction of principal compressional stress was north-west-southeast in Texas and southern Oklahoma. These north-west-southeasts directed compressional stresses produced the Amarillo-Wichita-Criner Hills uplift in the southern Oklahoma. Later, central Texas came under influence of northeast-directed compressional stresses by convergence of the Pacific plate movement, and Ouachita orogenic belt formed.

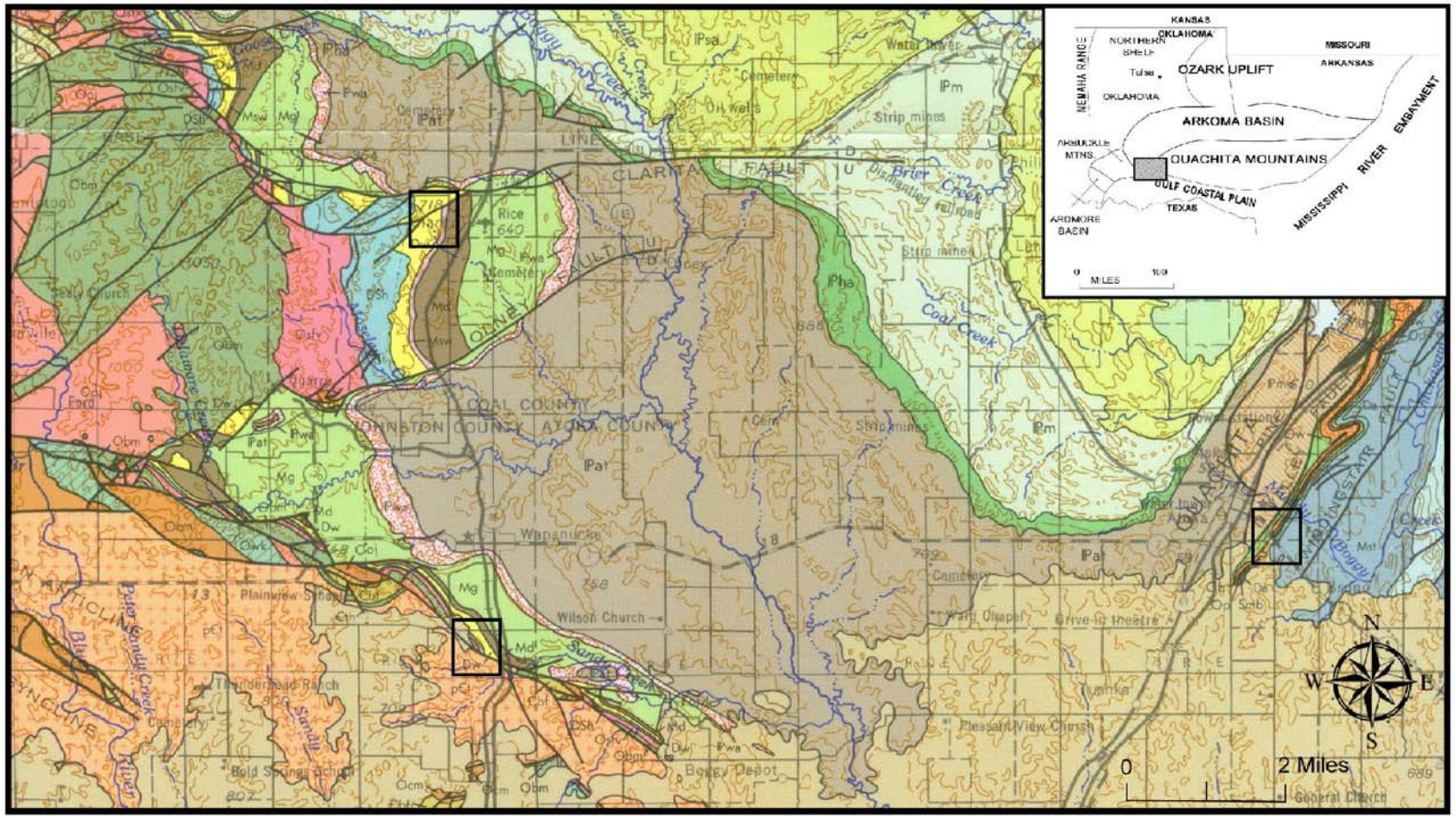

Figure 21. Geology map of the study area in the Ouachita region showing the outcrop locations.

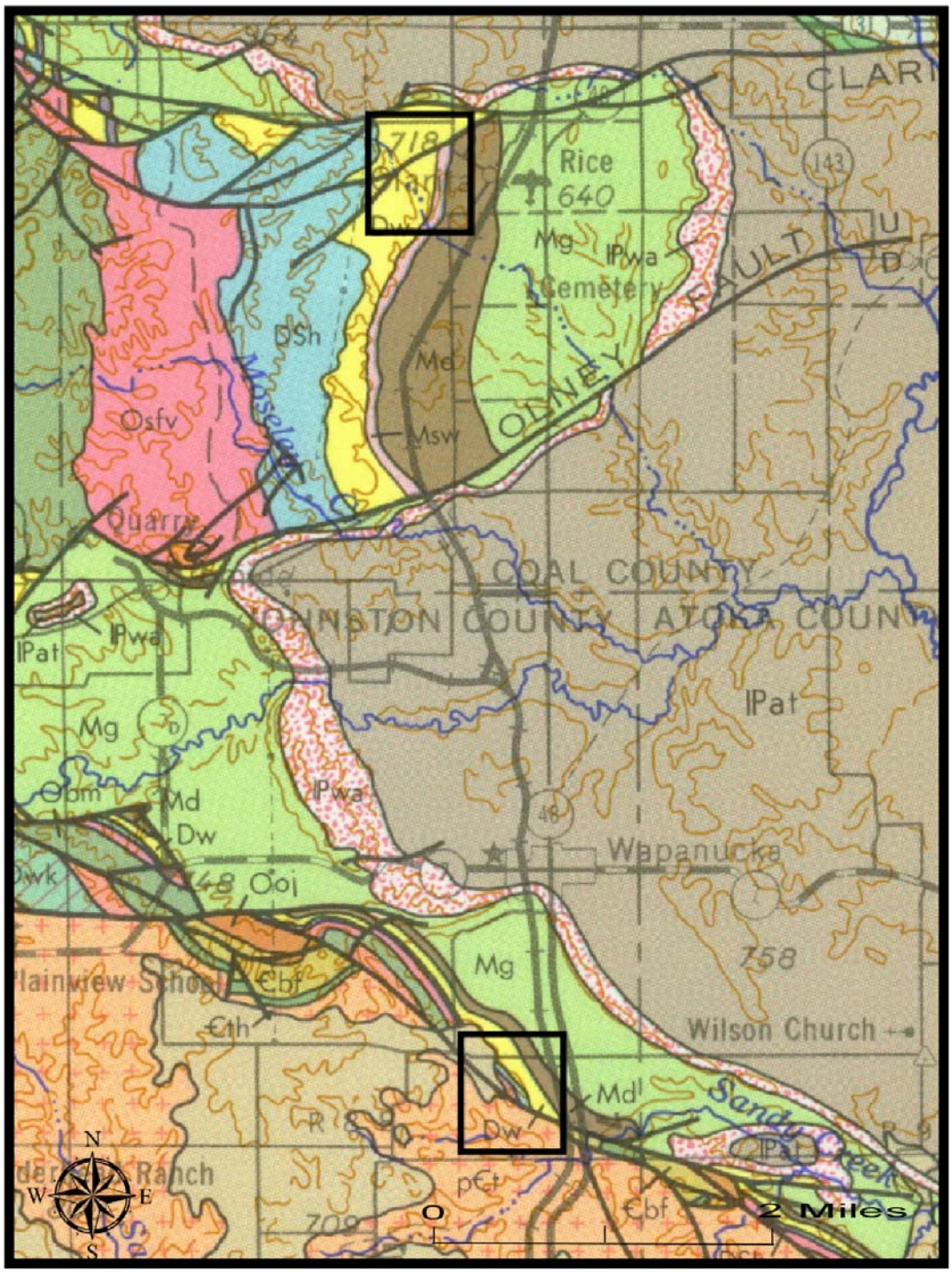

Figure 22. The Woodford Shale exposures at (1) the Clarita Shale Pit and (2) the Wapanucka ShalePit outcrops.

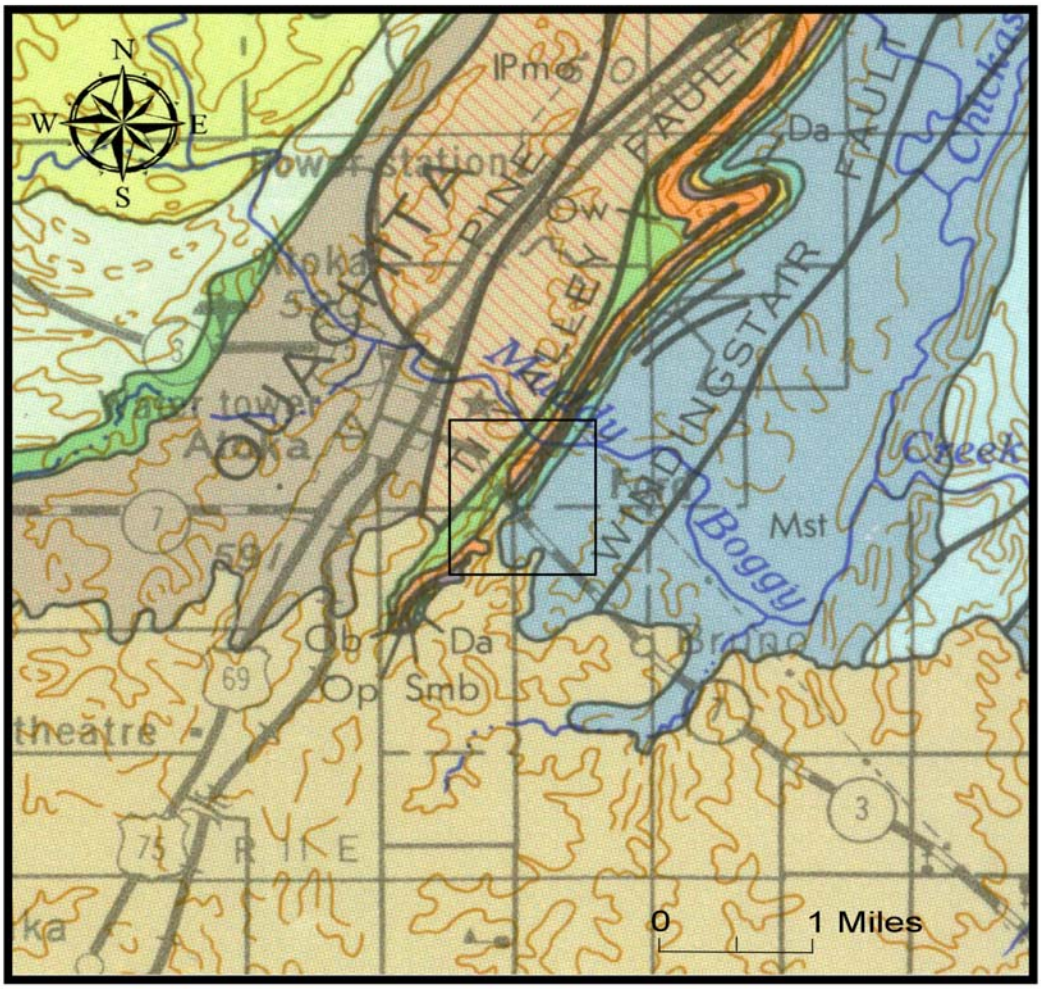

Figure 23. Scratch Hill/East Atoka outcrop is located on the hanging wall of the Choctaw fault

CHAPTER IV

FINDINGS

Fracture orientations and dips were measured for the Woodford Shale at four outcrops in Southern Oklahoma. Measurements gathered from the complete outcrop to reduce the effects of localized deformation and identify dominant fracture sets. Dominant fracture sets were chosen for measuring every fracture, because the Woodford Shale contains random and non-systematic fractures. Dominant fracture sets were difficult to identify at some outcrops due to accessibility and thereby they are not seen on diagrams. As a result, the fracture population of a specific fracture set on diagrams may not indicate the dominance of that fracture set. Stereonet diagrams were created in order to show fracture sets with the same orientation but different inclination. However, in McAlister Shale Pit, Scratch Hill/East Atoka Road Cut, Wapanucka Shale Pit and Clarita Shale Pit outcrops, rose diagrams were created because fractures are not as indiscriminate as in the Arbuckle Anticline. Fracture sets, relationship between sets and characteristics were examined and recorded. Systematic fracture sets were defined based on their orientations and the positions on the bedding planes.

Additionally, fracture measurements from other formations were used to verify dominant fracture sets and avoid misinterpretations, because characteristics and orientations of fracture sets are more consistent and clear for the other units. Shear or tension fracture indicators such as; tail cracks, tensional jogs or hackle marks were not observed in the outcrops; hence the deformation mode of the fractures was not absolutely defined. However, the structural positions of the beds and the stresses associated with the evolution of the Arbuckle Anticline to support the formation of both tension and shear mode fracture.

Mechanical stratigraphy inventory were used to delineate the area of fracture measurement. These squares were oriented perpendicular to bedding in most cases In McAllister Shale Pit outcrop; an inventory square was located on a bedding plane. A total of 11 mechanical stratigraphy inventory squares were used on seven outcrops. They were positioned at different stratigraphic levels and the intervals where are straight and solid within the boundary of each inventory square, the number and the thickness of the beds, the number of fractures effecting each bed and fracture spacings were recorded. Vertically and laterally continuous fractures were included in fracture density measurements. However, highly and randomly fractured ductile organic rich beds were not included in fracture density calculations because they are not fractured systematically and thereby they do not give coherent results. The package of thin laminas, in which fractures are vertically and laterally continuous fractured together, were recorded as if a single thick bed.

Samples were taken from organic rich and silica rich units and fissile and non-fissile units in order to make thin sections and conduct X-ray diffraction analyses. Thin

sections were examined in terms of color, constituents, microfractures and fracture filling cements. X-ray diffraction analyses were conducted in order to examine the effect of composition on the rock brittleness and ductility. Also, clay types were identified.

Lake Classen Spillway Outcrop

The Lake Classen Spillway outcrop is located at 34°27'38.10"N latitude; 97° 9'11.09"W longitude. It is located on the forelimb of the Arbuckle Anticline. Woodford Shale along the Lake Classen Spillway outcrop strikes approximately N30W and dips 85° NE. The bedding planes are nearly vertical, but not overturned as in the I-35 North Limb outcrop. An overview of the outcrop is shown in Figure 24.

Figure 24. An outcrop image from the Lake Classen Spillway.

Fracture Measurements

Fracture populations were sampled primarily from the lower and middle sections of the Woodford Shale at the Lake Classen Spillway outcrop because access to the upper interval is difficult due to cover. A total of 64 fracture measurements were taken from Woodford Shale at the Lake Classen Spillway outcrop.

Fracture orientations observed at the Lake Classen outcrop can be explained by with the fold-related fracture patterns. According to Stearns and Friedman (1972), there are two common fracture patterns associated with a fold (Fig. X). These fracture patterns consist of two conjugate shear fractures and a tension fracture. A total of six fractures can exist and the angle between these fractures can vary. The relative ages of two fracture patterns can not be determined however the pattern 1 should begin to form earlier during fold evolution. This ordering supported by the existence of the first pattern on low-dipping folds without much cross-sectional curvature in which pattern 2 is absent (Stearns and Friedman, 1972). However, both the fracture patterns can overlap in time and can be found in the same bed. In addition to this, a fracture belonging to either pattern can terminate several fractures from the other pattern. Stearns and Friedman (1972) propose that pattern 2 fracture more commonly develop during late fold evolution.

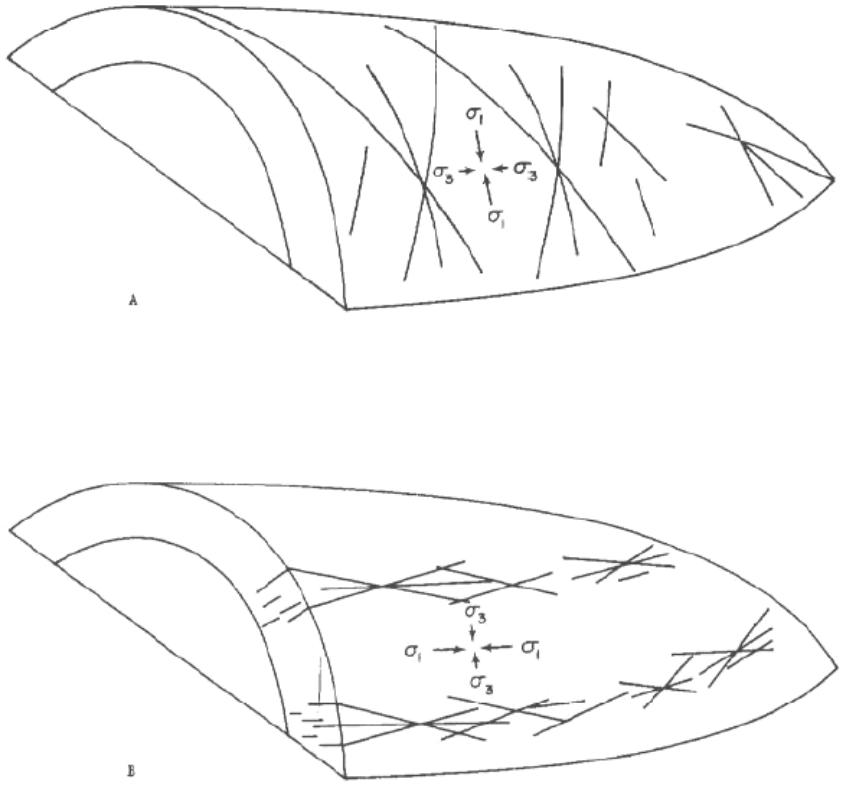

Figure 25. Schematic illustration of the most common fracture patterns associated with a fold. (A) Pattern I and (B) Pattern II are both maintain consistent to bedding (Stearns and Friedman, 1972).

The two common fracture patterns were observed at the Classen Lake outcrop. A stereonet diagram was created to include the dip data and to plot the fracture sets (Fig. 2). Set I, II and III have the same striking attitude; however the dip directions of set I and set II are different. The strike of the Set I, II and III fractures is approximately N60E,which is near perpendicular to the bedding strike. The reason of the same striking attitude is the almost vertical bed dip and development of fracture perpendicular to bedding. The Classen Lake fracture pattern is unique among the other outcrops. The angle between set I and set II fractures varies from place to place on the outcrop and, thereby they show

both orthogonal and conjugate fracture patterns. The dip angles of these shear fracture planes range from 20° to almost vertical. We plot correspondingly on the stereonet. These fractures belong to either first or second dominant fracture patterns and are shear fractures. In addition, set III fractures are almost vertical. They have also a perpendicular orientation to the strike of bedding planes. Set III fracture plots accumulate near the center of the stereonet. These are interpreted as tension fractures belonging to the fracture pattern 1 determined by Stearns and Friedman (1972). Set IV fractures are also related to fold-related fracture pattern. However they are the least available fracture sets to measure because of scariness due to limited outcrop exposure. They oriented parallel to the strike of the bedding planes and dip is between 0° and 15° NE. These fractures are tension fractures belonging to fracture pattern 2.

In summary, the relationship between fracture sets suggests the two major fold-related fracture patterns are present in the Woodford Shale at Classen Lake Spillway. The two dominant patterns developed throughout the exposed Woodford, indicating the effects the late fold evolution.

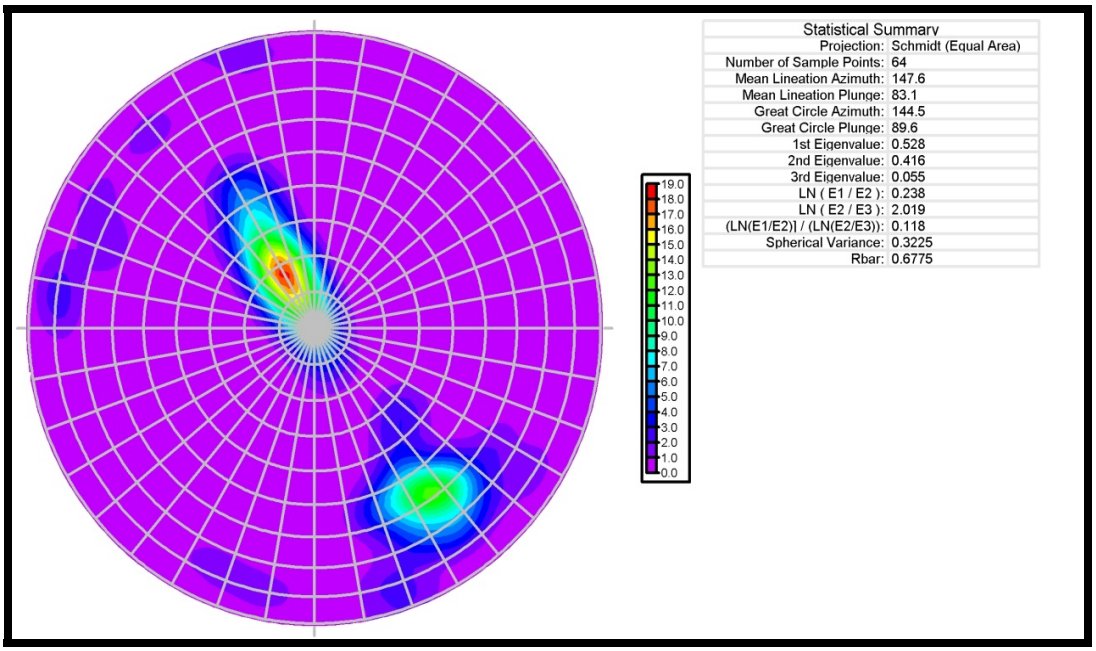

Figure 26. Fracture patterns in the Lake Classen Spillway outcrop. Set I fractures dip approximately N30W, while Set II fractures dip S30E. Both are strike perpendicular to the strike of the bedding plane.

Mechanical Stratigraphy Measurements

Fracture density measurements were conducted in two square-shaped (50x50cm) inventory areas located at the different stratigraphic positions (Fig. 3, Fig. 4). Bed thicknesses, the number of beds, the number of fractures on each bed and fracture spacings were recorded. Beds in the upper inventory square are thicker than in the lower inventory square and most range between 5cm to 12cm thick. The beds are seemed to have more ductile constituent in the upper inventory square. The lower inventory square consists of thin and likely brittle silica-rich beds and laminations. Bed thickness in the lower sequence and lamination thicknesses range from several millimeters to 4 cm thick. The mechanical stratigraphy analysis shows that the mean fracture spacing is 5.8 cm and

the fracture density 0.18 f/cm in the upper inventory square; whereas the average fracture spacing is 2.8 cm and the density 0.5f/cm in the lower inventory square (Fig. 7, Fig. 10). These results suggest a correlation between bed thickness and fracture numbers, and that thicker beds have fewer fractures (Fig. 5, Fig. 8). In addition, fissile laminations could cumulatively behave as a thicker bed, absorb, accommodate strain and contain fewer fractures.

Figure 27 Lake Classen Outcrop: Inventory Square 1 with thicker and non-fissile beds. With a range of thicknesses change from 3 to 8 cm.

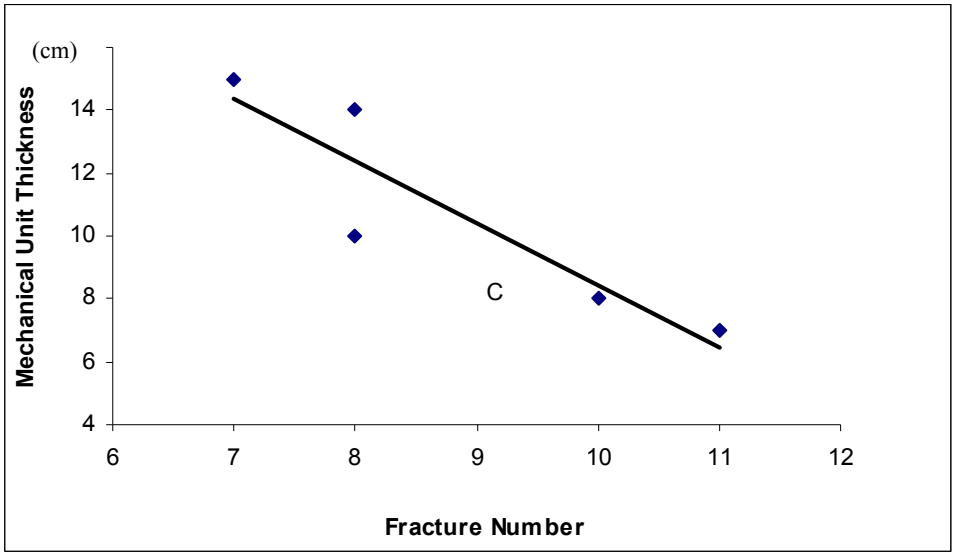

Figure 28.Mechanical unit thickness v. Fracture numbers from the upper inventory square at the Lake Classen Spillway outcrop. Fracture population is decreasing with mechanical unit thickness decreases.

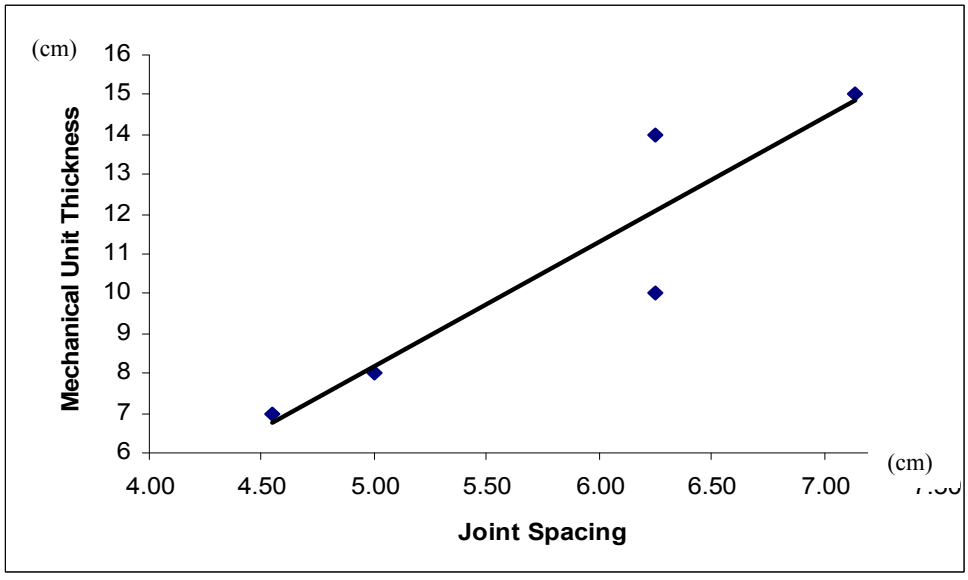

Figure 29.Mechanical unit thickness v. Fracture Spacing from the upper inventory square at the Lake Classen Spillway outcrop. Joint spacings are increasing while mechanical unit thickness increase.

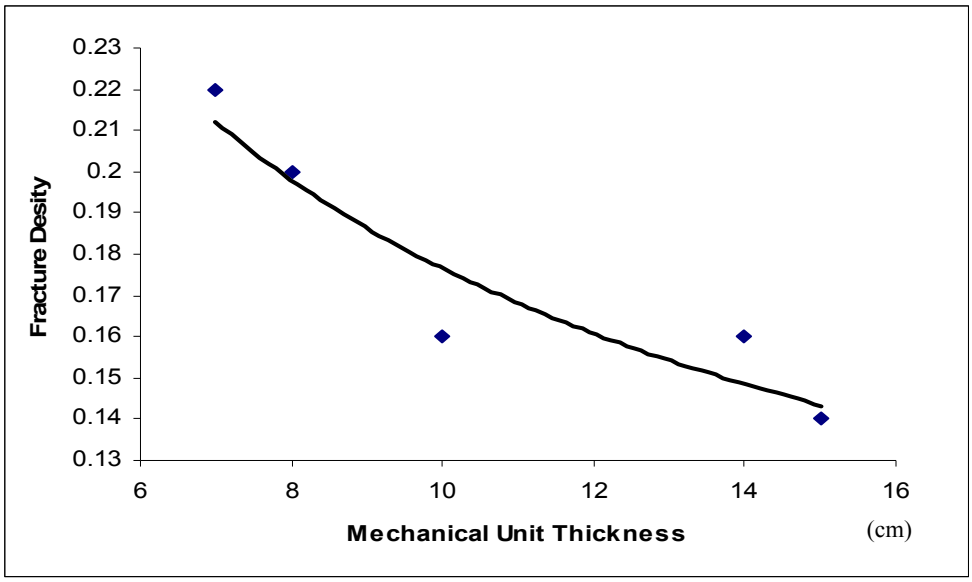

Figure 30. Fracture density (f/cm) vs. Mechanical unit thickness from the upper inventory square at the Lake Classen Spillway outcrop. Fracture density decreases while mechanical unit thickness increase.

Figure 31. Lake Classen Outcrop: Inventory Square 2 with non fissile and the fissile units. The non-fissile units have more radiolarians and the silica-rich compared to fissile units. The fissile units are darker colored , clay rich and contain less radiolarians than the silica rich beds.

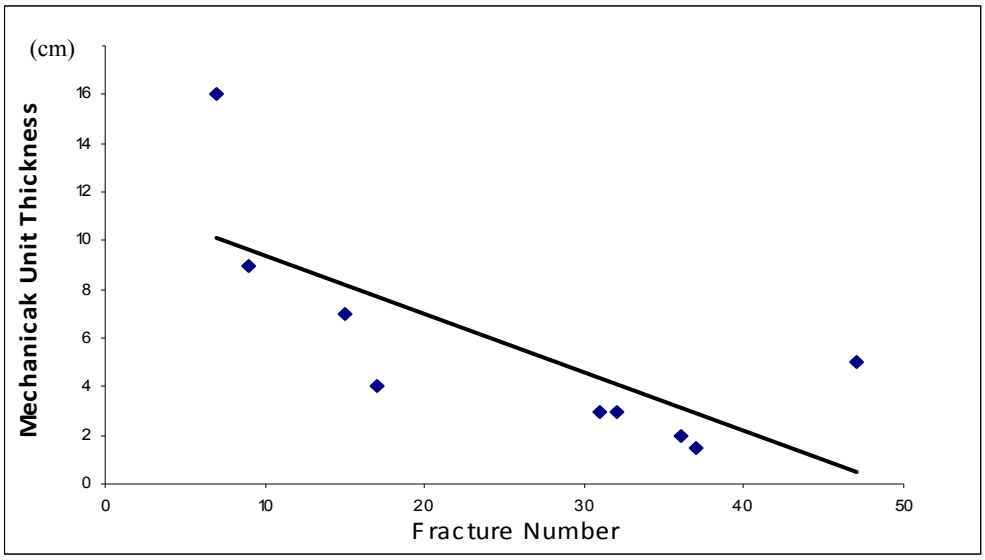

Figure 32. Mechanical unit thickness v. number of fractures for beds in the lower inventory square, Lake Classen Spillway outcrop. Notice that beds are thinner than CLO. However, number of fractures decreases while bed thickness increases.

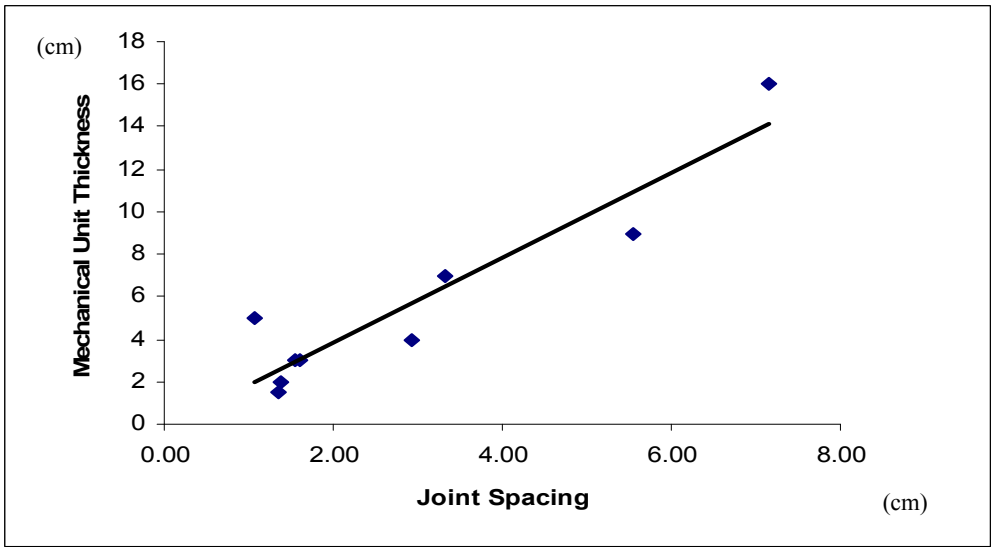

Figure 33. Mechanical unit thickness v. joint spacing for beds in the lower inventory square, Lake Classen Spillway outcrop. Joint spacings increase while mechanical unit thickness increase.

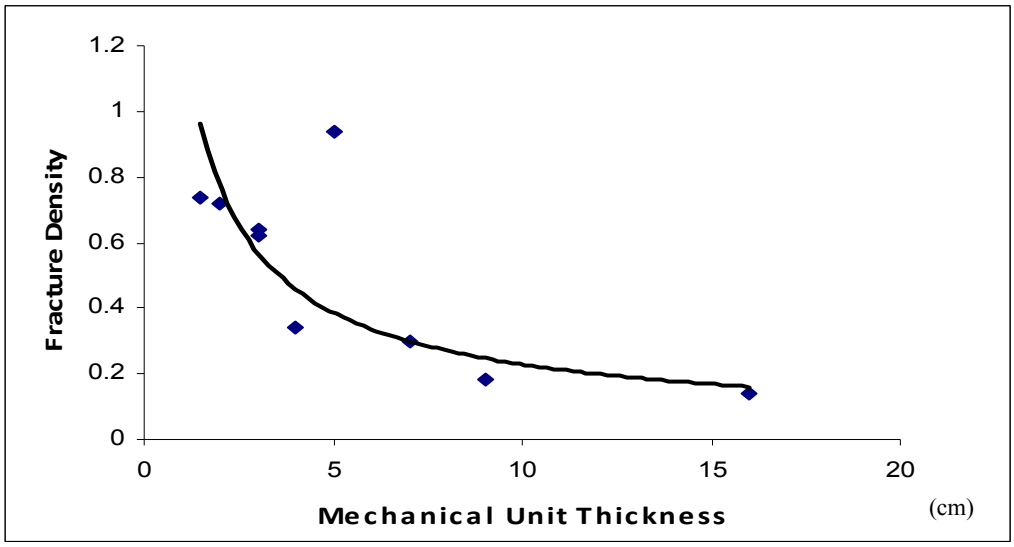

Figure 34. Fracture density (f/cm) v. mechanical unit thickness from the lower inventory square at the Lake Classen Spillway outcrop. Notice sharp decrease in fracture density. Fracture density decreases while mechanical unit thickness increases.

Thin Section and X-ray Diffraction Analyses

Three samples from the Classen Lake outcrop were analyzed using powder X-ray diffractometry and thin section microscopy. The samples were chosen based on brittleness, fissility, bed thickness and color. The samples are identified as: (1) CL-0; light brown colored, 3 to 9cm bed thickness, non-fissile unit, (2) CL-1; dark brown to black colored, 2 to 4cm bed thickness, non-fissile unit, and (3) CL-2; dark colored, average 2mm bed thickness, fissile unit.

Sample 1: CL - O

The rock is brown to dark colored shale with somewhat visible lamination. The reddish brown color is typical of the more organic-rich part of the Woodford Shale.

Natural fractures are rare, however, a few fractures occur mostly parallel to bedding planes. These fractures are commonly partially or completely healed with silica cement. Thin section analyses indicate that mall sponge spicules occur oriented subparallel to bedding planes. Silt-sized quartz grains, dark material interpreted as bitumen and wisps of phosphate occur. However, only a few radiolarians have identified in the thin section.

X-ray analysis shows that the sample is primarily quartz, and illite clay. Qualitative analysis suggests that the relative abundance of quartz reflects the relative abundance of radiolarians. Illite reading is relatively high. Lower quartz readings and high illite readings suggest higher percentage of clay and ductile behavior for this sample. This was confirmed by the lesser number of fractures in beds in this inventory square.

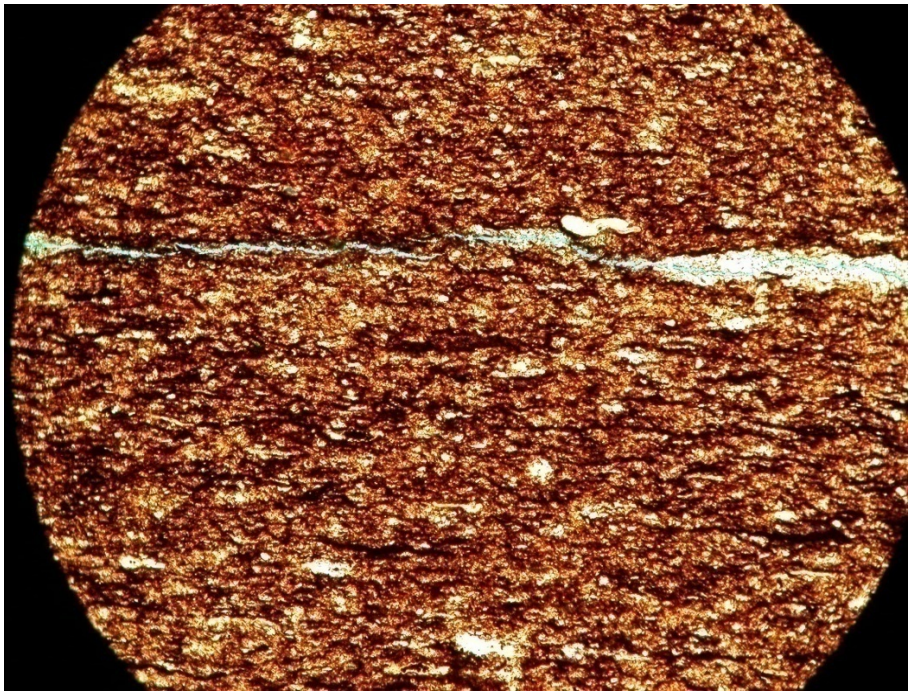

(a)

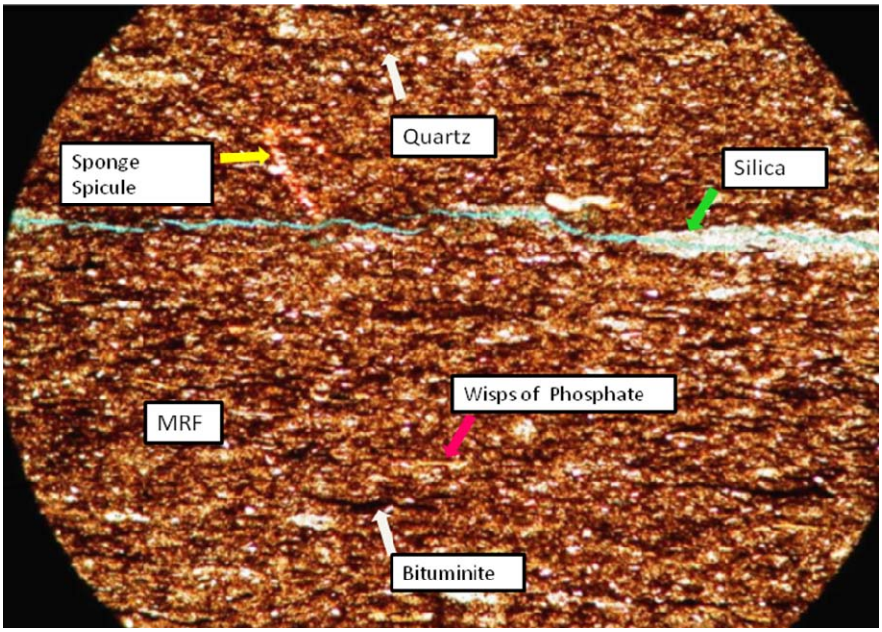

(b)

Figure 35. The thin section photographs of the CL0 sample from the Lake Classen Spillway outcrop. (a) PPL - X10 – (b) XPL - X10

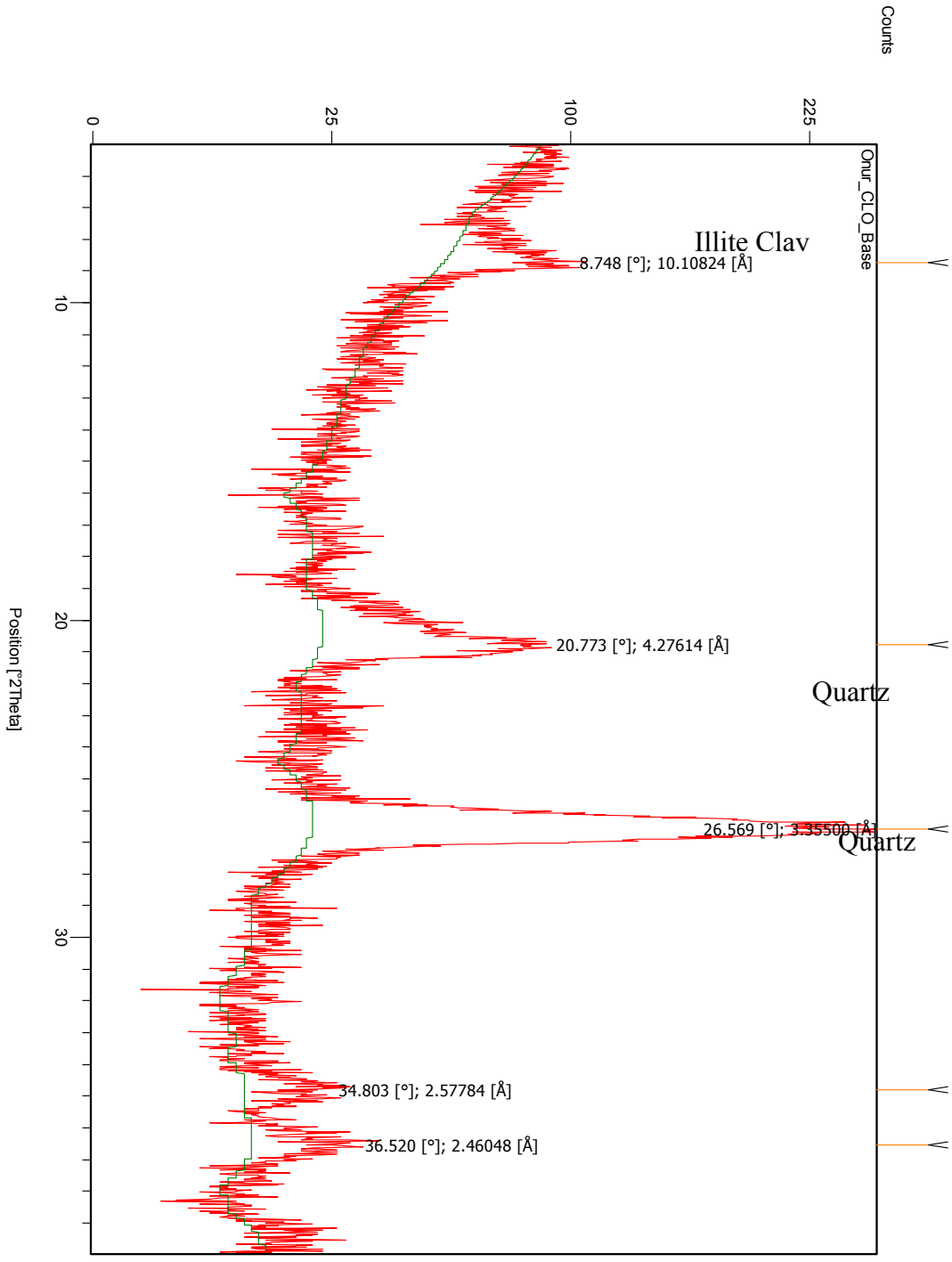

Figure 36. Powder X-ray diffractogram of sample CL0, Classen Lake. Note illite peak at 8.7 (2θ) and quartz peak at 26.6 with 20.2, repectively

Sample 2: CL - 1

This sample shale is darker colored than sample CL-0. There are no visible pores in the thin section. However, some healed microfractures were detected. The number of radiolarians increases in this sample relative to CL-O and the percent of quartz increases well. The roundness of the radiolarians indicates minimal compaction and ductile deformation during deposition. Glauconites replace some fossil fragments. Small blebs of pyrite are evident. Laminas are not readily apparent and alignment of grains is less obvious than in sample CL-0.

Sample CL-1 has a higher percentage of quartz based on peak height from X-ray diffraction analysis. The percentage of quartz and the number of radiolarians appear to be proportional. The lack of any scarceness clays and high amount of quartz suggest this will be a brittle bed included a higher frequency of fractures that reflect the increased brittleness.

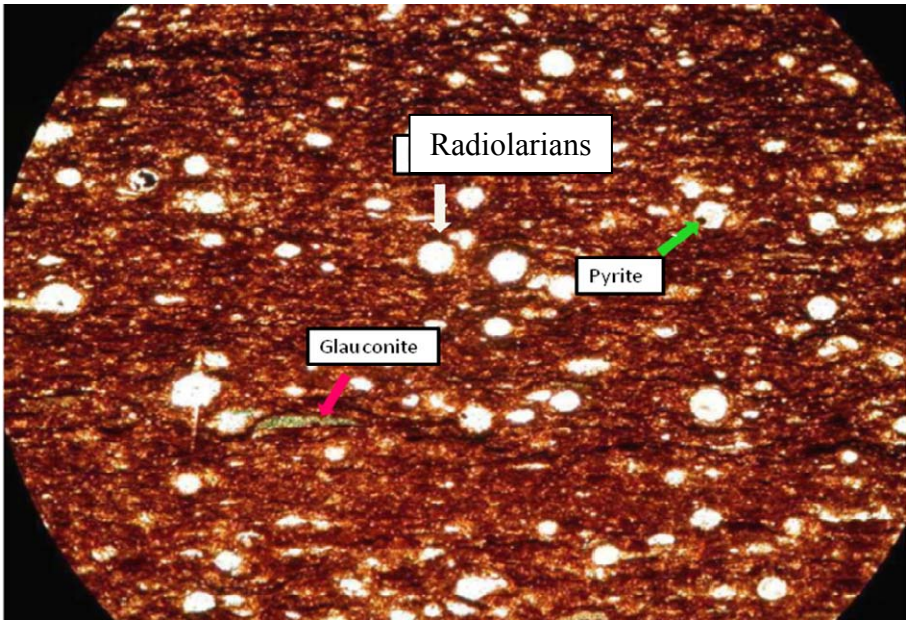

(a)

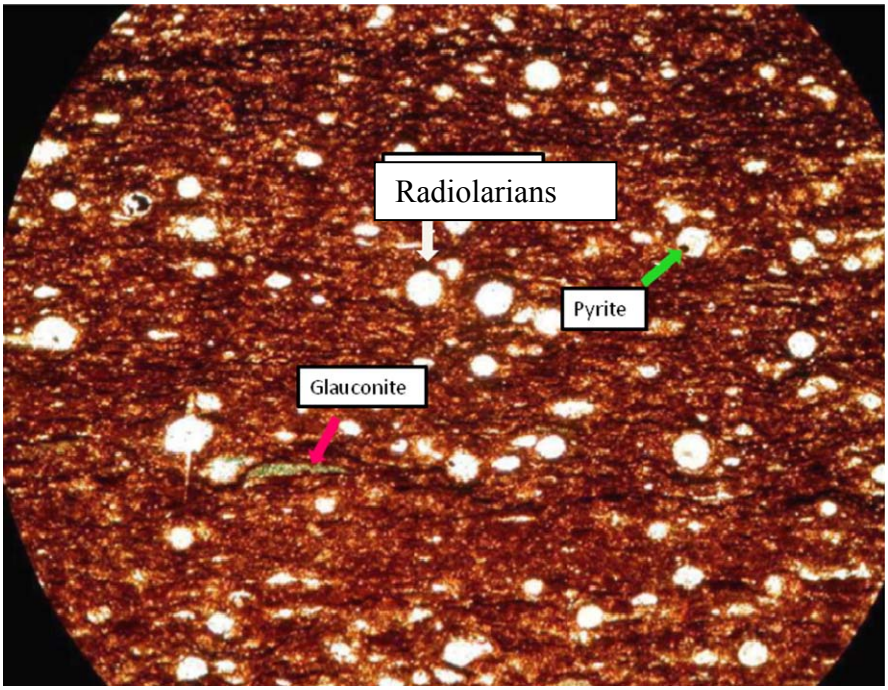

(b)

Figure 37. Thin section photomicrographs of the CL1 sample from the Lake Classen Spillway outcrop. (a) PPL - X10 – (b) XPL - X10.

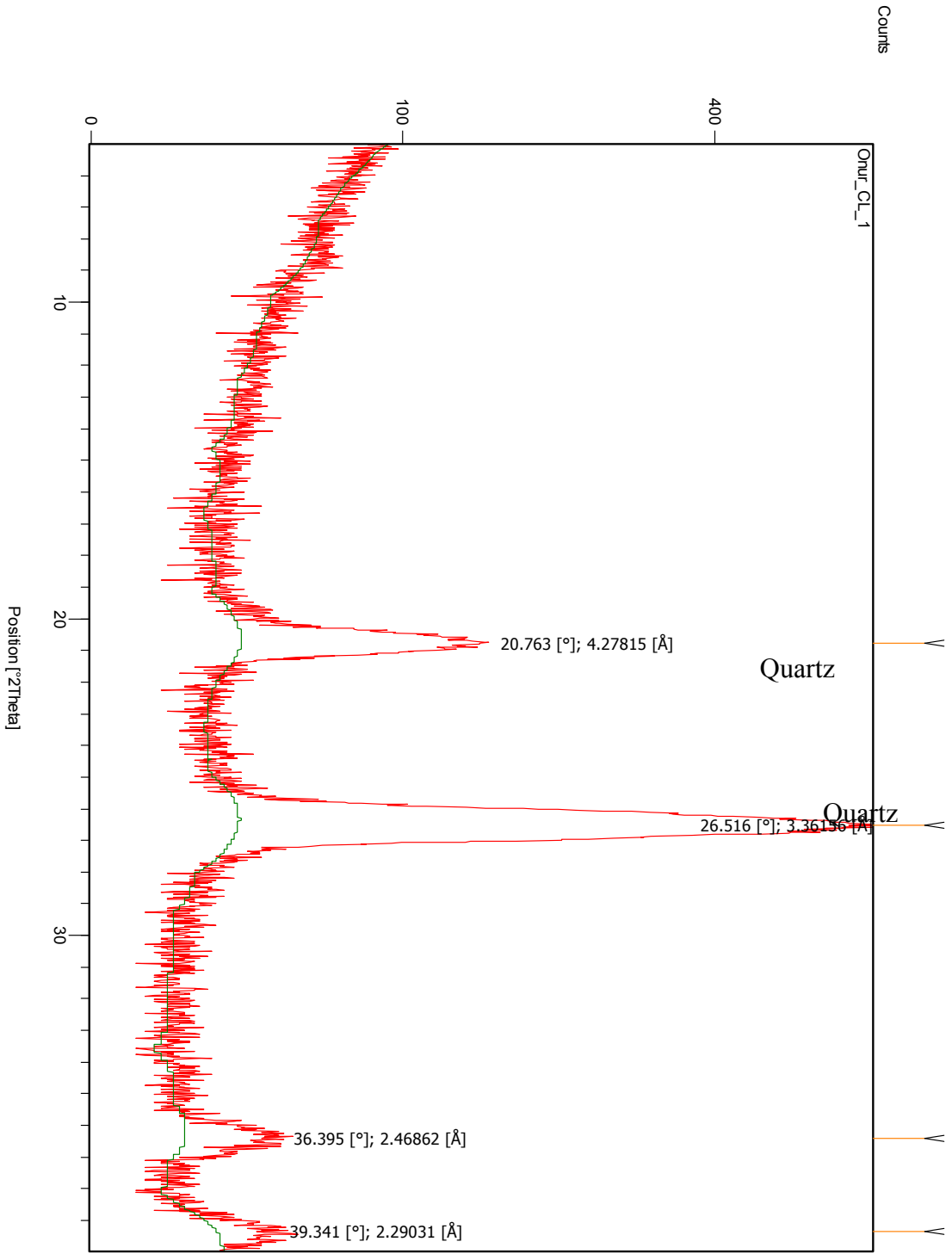

Figure 38. Powder X-ray diffractogram of sample CL1, Classen Lake. Note quartz peak at 20.7 with 26.5, repectively

Sample 3: CL – 2

Sample CL-2 is very dark colored organic rich shale with no apparent no porosity except a few tiny fractures. Most fractures are cemented with calcite. The fissility of thin shale contributes to the separation along laminas during thin section preparing process. The sample contains a few flattened radiolarians, wisps of phosphate, silt and clay. In clay rich samples, radiolarians are flattened because of the compaction of mud-rich sediment during lithification. The number of radiolarians in CL-2 is fewer compared to the other two samples taken from the Classen Lake outcrop.

X-ray analysis shows that the sample consists primarily of quartz and illite. The population of the radiolarians is quite low and as a result the quartz readings are low compared to other samples. Illite is relatively abundant. The bed would display ductile behavior and contain fewer fractures. No fracture perpendicular to bedding was captured in thin section.

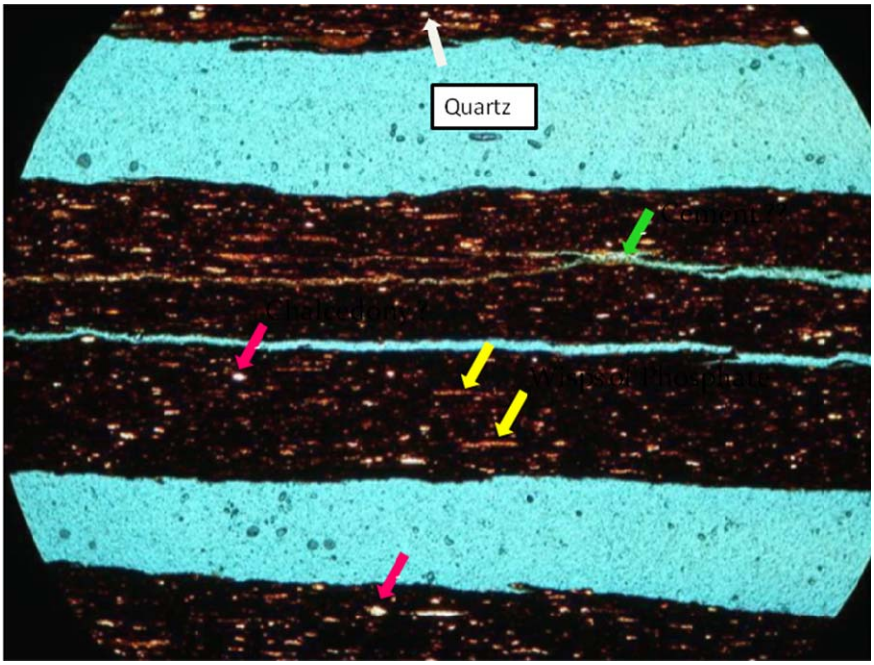

(a)

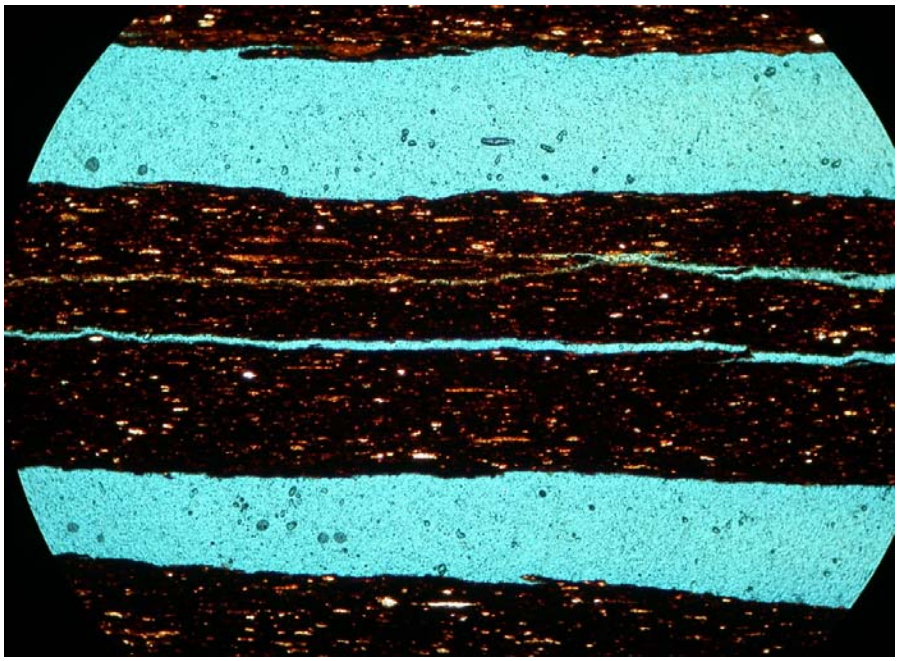

(b)

Figure 39. The thin section photographs of the CL2 sample from the Lake Classen Spillway outcrop. (a) PPL - X10 – (b) XPL - X10. The clay rich sample separated along bedding planes during thin sectioning.

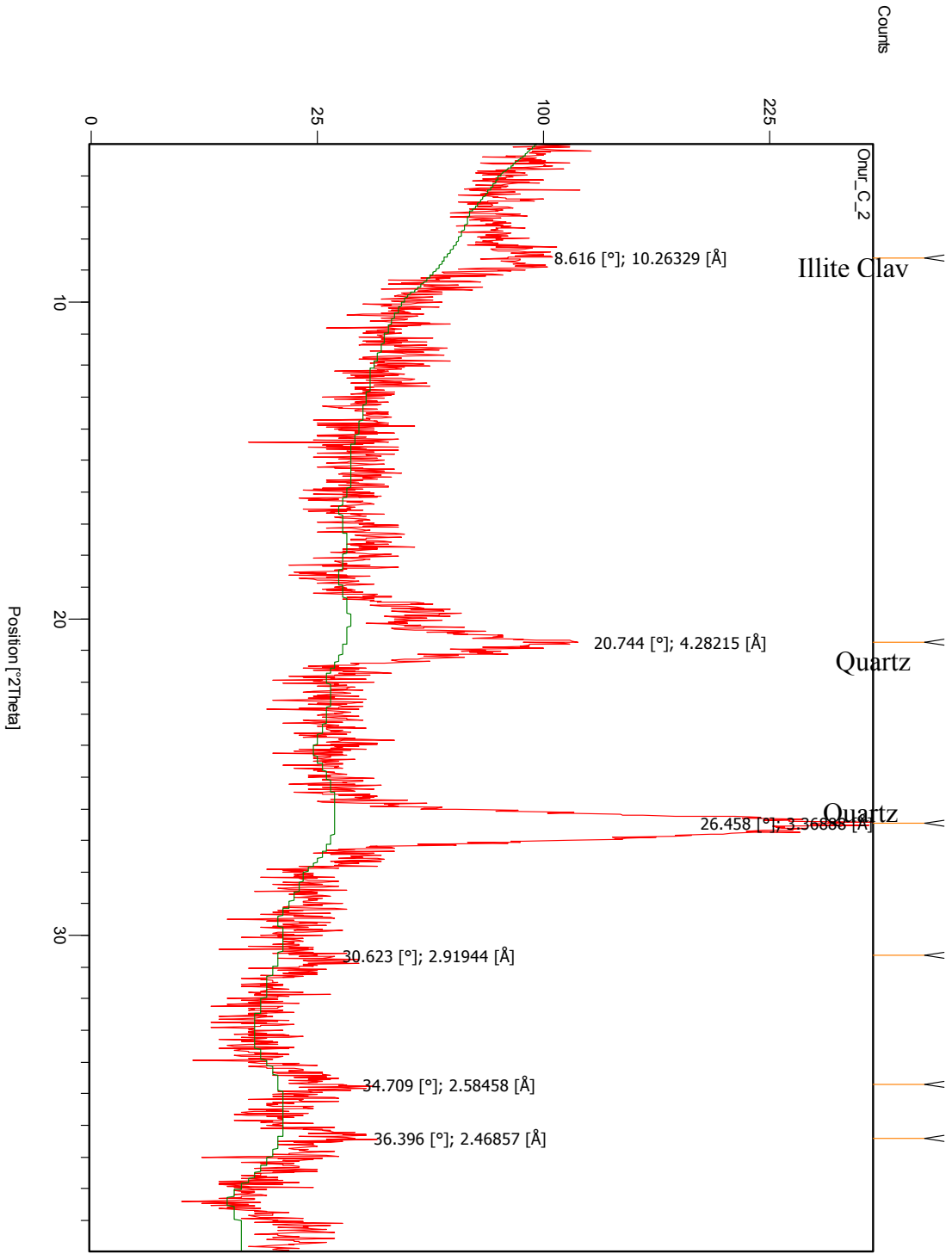

Figure 40. Powder X-ray diffractogram of sample CL2, Classen Lake. Note illite peak at 8.6 (2θ) and quartz peak at 26.4 with 20.7, repectively. Also there are unidentified mineral peaks.

I-35 North Limb Outcrop

The coordinates of the I-35 North Limb outcrop are 34°26'41.86"N latitude; 97° 7'55.40"W longitude. The beds of the Woodford Shale are overturned, strike between N55W and N65W, and dip 75°SW. The North Limb outcrop is the most densely and randomly fractured outcrop among the four. This is believed to be result of the late fold evolution in which more complex stresses and strains caused the development of higher density and randomly oriented fracture patterns.

Figure 41. A portion of the outcrop photograph o Woodford along the I-35 North Limb.

Figure 42. The I35N/77D outcrop contains the most densely fractured among all outcrops. Increased fracturing is likely the result of the stresses related to late fold evolution.

Fracture Measurements

Fractures populations were sampled across the entire Woodford outcrop and plotted on a stereonet. A total of 118 fracture measurements were recorded. The fracture attitudes recorded for the 77D/I-35 North Limb outcrop appear to be similar to the fracture attitudes recorded for the Classen Lake outcrop. However orientations of the fracture sets on stereonet are not as clear as those for the other outcrops. Late fold evolution and extreme bed rotation (overturned) believed to be caused of increment fracture density.

The dominant fracture pattern observed at the I-35N outcrop comparable with the Classen Lake fractures. Set I and II fractures are dipping with variable degrees to the NW and E-NE directions . The dip directions have slightly changed compared to Classen Lake fractures because the beds are overturned and dipping to SW. The angles between these two fracture sets vary. Thereby, they display both conjugate and orthogonal fracture patterns on bedding planes and appear to belong to the two common fracture patterns determined by Stearns and Friedman (1972). They are the shear fractures of both common patterns and the offsets are recorded at some levels of the Woodford Shale. The average strikes of the fracture planes at 77D/ I-35 N are shifted about 30°west when compared to the fractures at the Lake Classen Spillway outcrop. The reason for this shifting is the difference in the bedding attitudes of the Woodford Shale at the two outcrops. Although the 77D/ I-35N set I and II fractures have similar attitudes as the Classen Lake set I and II fractures, they are striking oblique to the bedding planes because the beds are not vertical as in the Classen Lake outcrop. As a result, Set I is striking approximately N30E and Set II is striking between N-S and N15W. Fracture set III has a perpendicular orientation whereas Fracture set IV has a parallel orientation to the strike of bedding planes. Fracture set III is tension fractures belong to the common fracture patterns 1 and 2, respectively. As at the Classen Lake, all fracture sets are related to folding and fold-related fracture patterns are observed along the outcrop.

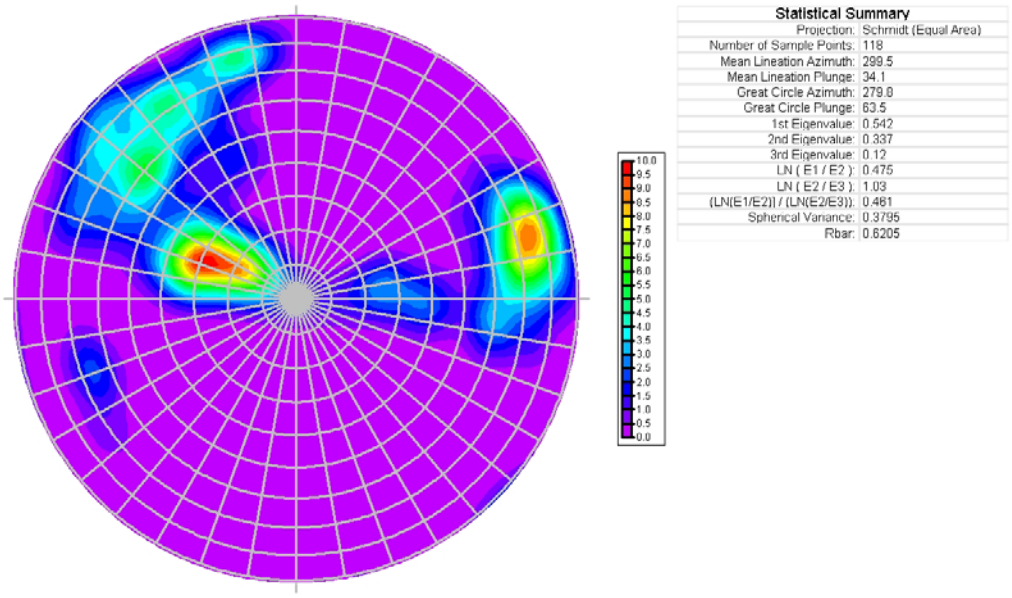

Figure. 43. Fractures orientations at I-35 North Limb outcrop. Set I and II fractures are dipping at variable angles to the NW and E-NE directions

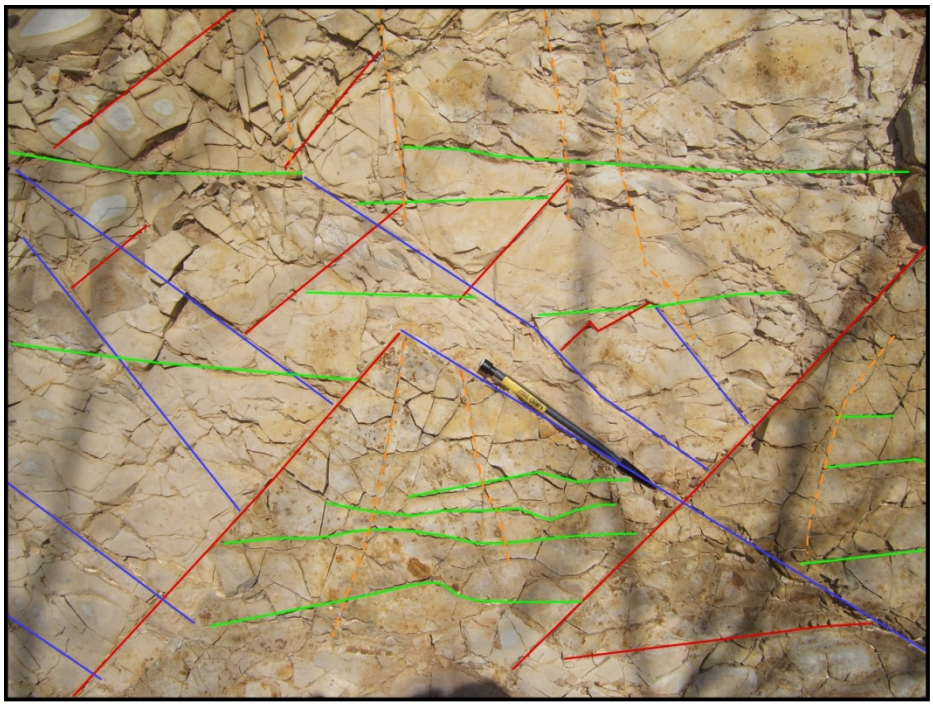

Figure. 44. Dominant fracture patterns within the I-35 North Outcrop. The two dominant fracture patterns are evident in this picture (Red: Set I. Blue: Set II, Orange: set III, Green: set IV.

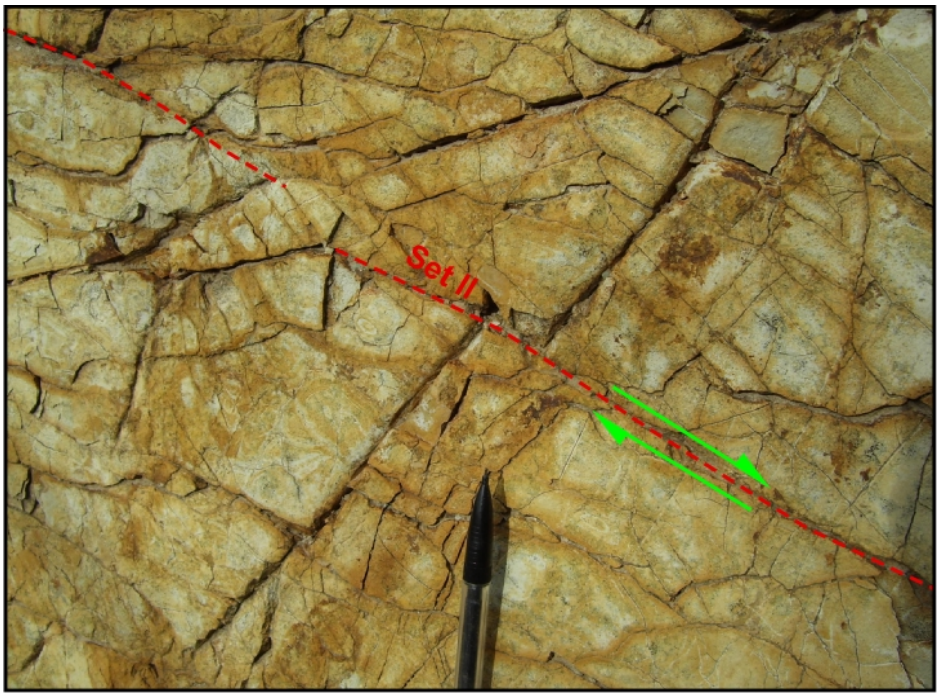

Figure. 45. Shear displacement along the Set II fractures in the I-35 North Outcrop.

Mechanical Stratigraphy

The I-35 North limb is the most densely and randomly fractured outcrop and contains both systematic and non-systematic fractures. Systematic and non-systematic fractures are observed at the outcrop. Non-systematic fractures often die out within the systematic fracture patterns and the lengths of non-systematic fractures are controlled by the spacing of systematic fractures. Systematic fractures behave like a boundary to non-systematic fractures and non-systematic ones terminated against them. As a result, fracture properties at 77D/ I-35N are the most complicated among the four Woodford shale outcrops. Late fold evolution and bed rotation past vertical may be responsible for complicated fracture patterns at 77D/ I-35N. Mechanical stratigraphy measurements were completed in two inventory squares. Fracture density measurements show that the average fracture spacing (Xa) is 2.18 cm and the fracture density (λ) is around 0.575f/cm

(Fig. 20). The organic rich beds are predictably more ductile than silica rich beds and as a result, they contains less fractures per unit of length. Fractures generally terminate against organic-rich beds. Furthermore, as in the Classen Lake outcrop, the thin beds at 77D/ I-35 N cumulatively behave as a thick bed and the fracture density in these beds can be very low (Fig. 19).

Figure 46.77D/ I35 North Outcrop: Inventory Square 1. that is perpendicular to bedding planes. This inventory square contains the organic-rich and the silica rich beds. Thin sections of the dark colored beds could not be prepared because of bed fissility and weakness.

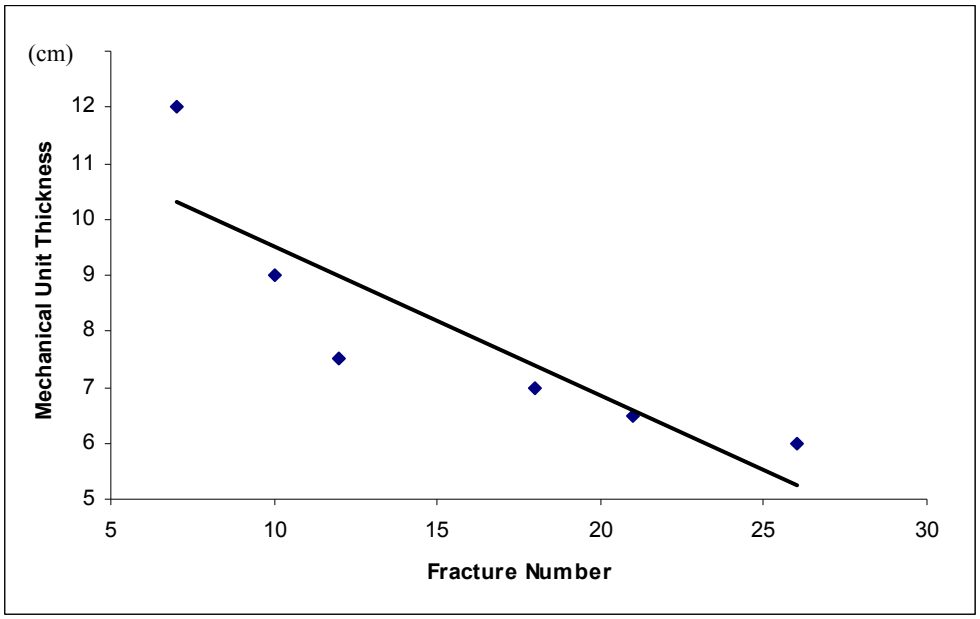

Figure 47. Mechanical unit thickness v. fracture numbers from the inventory square at the I-35 North Limb outcrop. While mechanical unit thickness decreases, fracture numbers increase.

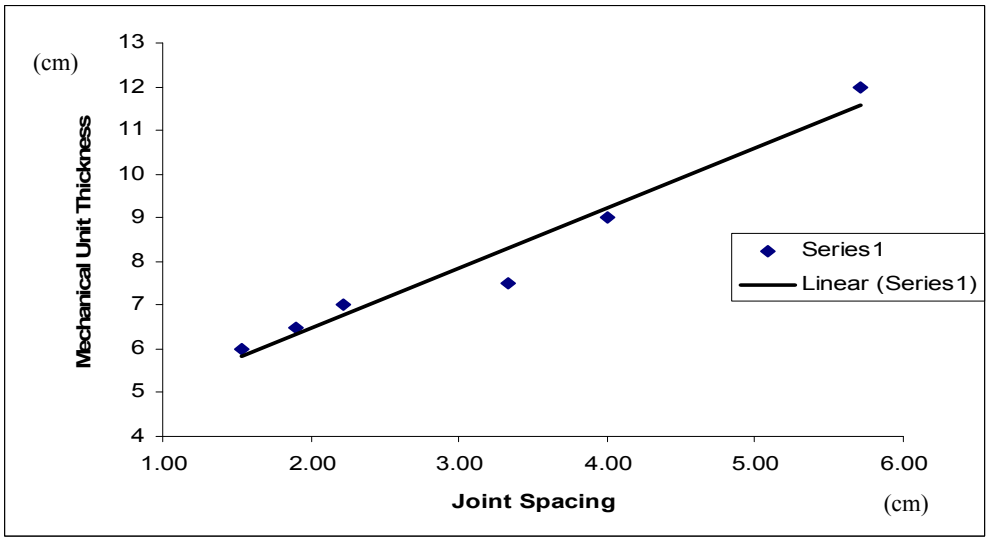

Figure 48. Mechanical unit thickness v. Joint spacing from the upper inventory square at the I-35 North Limb outcrop. Increment in mechanical unit thickness causes longer fracture spacings.

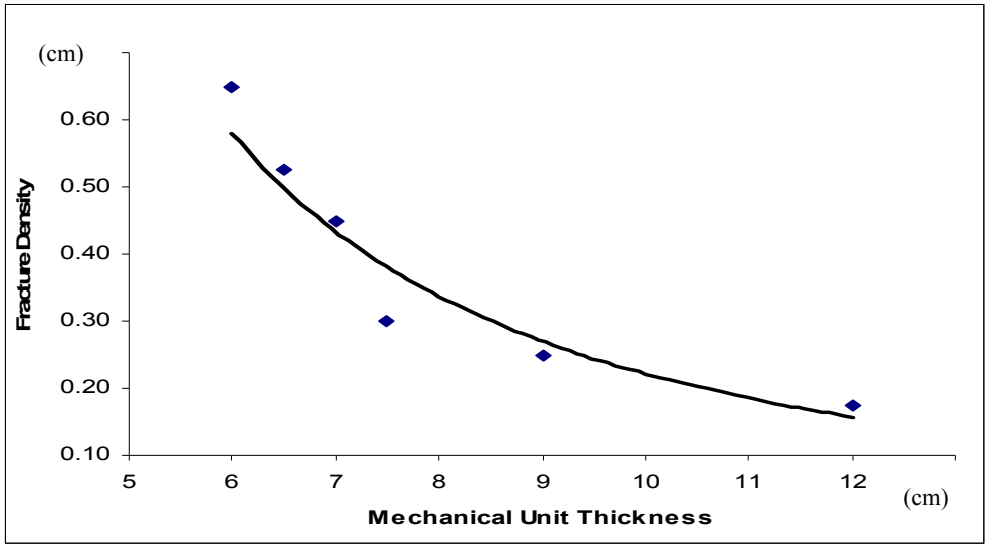

Figure 49. Fracture Density v. mechanical unit thickness, upper inventory square,77D/I-35 North Limb outcrop. Fracture density decrases with increment in mechanical unit thickness.

Thin Section and X-ray Diffraction Analyses

Because of the high fissility of clay-rich beds, only one sample was prepared for thin section analysis from the 77D/I-35 outcrop. This sample was also x-rayed.

Sample 1: I-35N

Sample 1 is reddish brown to brown colored and contains partially healed fractures. Fractures are mostly curved and transact the sample. Although these fractures are partially healed, they may be open enough to transport fluid. The fractures appear to be cemented with silica and limonite. Pyrite, phosphate and phosphate nodules are present. Detrial quartz silt occurs in minor amount and few radiolarians were identified.

The quartz peak value readings are relatively low on the X-ray diffractogram analysis and an illite peak is present. It is expected that this bed will contain fewer fractures due to the presence of illite.

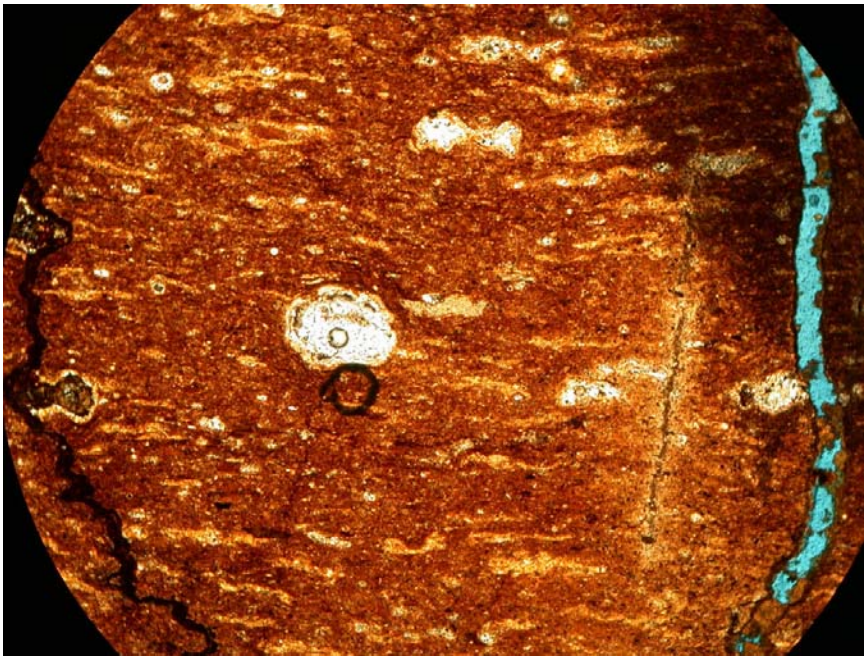

(a)

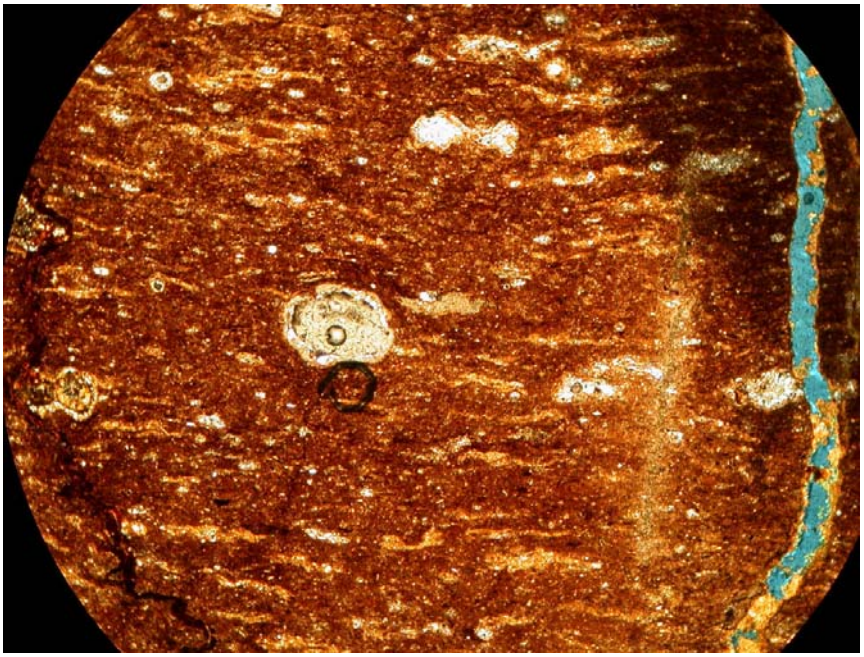

(b)

Figure 50. The thin section photomicrographs of the N2 Sample from the I-35N North Limb outcrop. (a) PPL - X10 – (b) XPL - X10. Notice the partially cemented vertical microfracture on the right side.

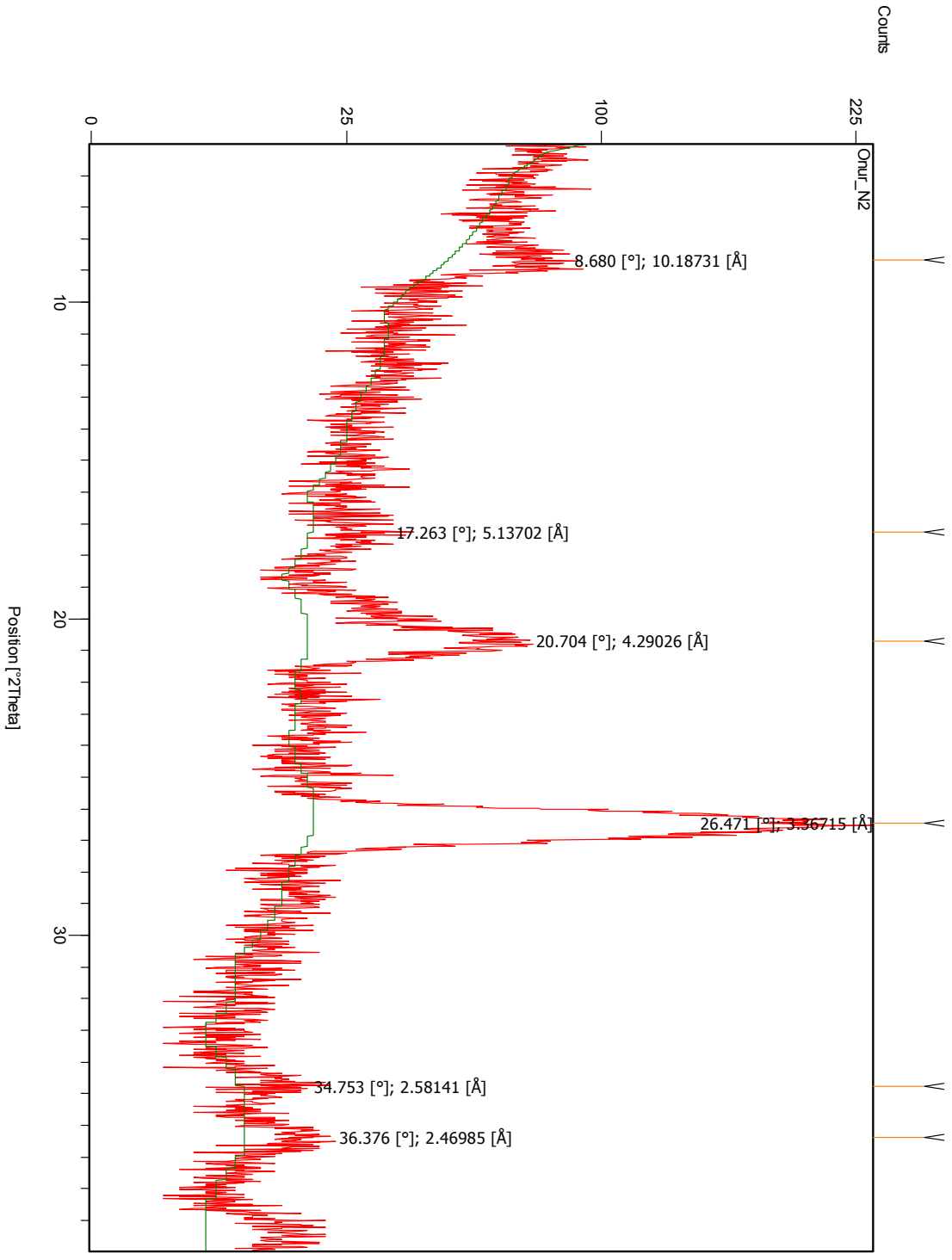

Figure 51. Powder X-ray diffractogram of sample N2, I35N Limb. Note illite peak at 8.5 (2θ) and quartz peak at 26.4 with 20.7, repectively. Also there are unidentified mineral peaks

I-35 South Limb Outcrop

The coordinates of the I-35 South Limb outcrop 34° 4'39.77"N Latitude; 97° 9'15.48"W. Longitude is located on the backlimb of the Arbuckle Anticline and the beds strike. This outcrop approximately N45W to N55W, and dip between 55SW to 70SW. This outcrop is dominated black colored, organic rich, fissile and non-fissile units in the middle section, whereas more gray colored, cherty, non-fissile units with phosphate nodules occur in the upper section. Fracture measurements were recorded from the upper and middle intervals of the Woodford outcrop. This outcrop is the least deformed and contains the most consistent fracture patterns of all outcrops. An overview of the Woodford Shale beds is shown in Figure 52.

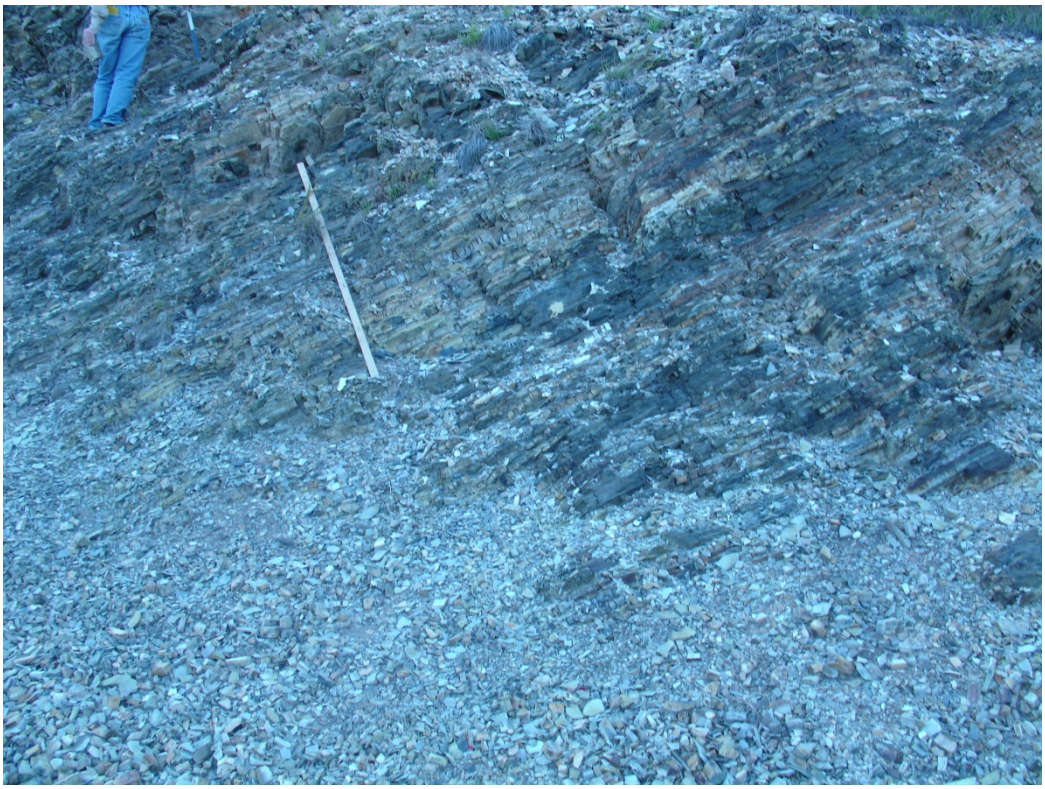

Figure 52. The Photograph of the middle member of the Woodford Shale at the I35 South Limb Outcrop.

Fracture Measurements

The I-35 South Limb outcrop provides an ideal exposure to collect fracture data. Fractures are able to be sampled from upper and middle levels of the Woodford Shale. A total of 148 fractures were measured along the Woodford Shale (Fig. 22) Fractures measured on the backlimb are very similar to fractures on the forelimb. Fracture orientations and the stereonet show an excellent consistency with the fold-related fracture pattern 1. However, the pattern 2 fractures are recorded less than those of the pattern 1. Low-dipping beds and less deformation on the backlimb compared to forelimb outcrops are the primary reasons for the absence of pattern 2 fractures. Set I and Set II fractures have a conjugate pattern and the angle between them remains near 60°. Set I fractures dip around N35E,at 60°. They align oblique to strike of the bedding planes. Set II fractures dip approximately E-NE at 75° and have an oblique orientation to the strike of the bedding planes. Both sets of fractures belong to the fold-related pattern 1 fractures. The set III fractures, which are tension fractures are clustered at the center of the stereonet. They trend approximately between N35W and N45W and dip perpendicular to the strike of the bedding planes.

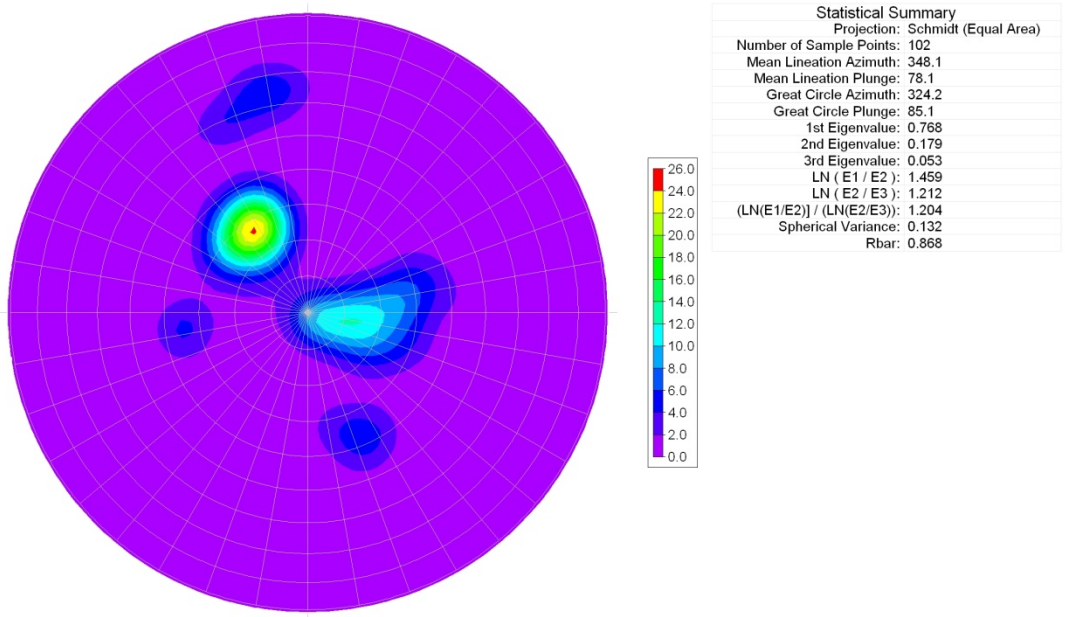

Figure 53. The dominant fracture sets along the I-35 South Limb outcrop. Fracture sets are more consistent compared to the north limb outcrops. Low-dipping beds and less deformation compared to forelimb outcrops are the primary reasons for the consistent fractures.

Mechanical Stratigraphy Measurements

Three mechanical stratigraphy inventory squares were conducted on the I-35 South Limb outcrop. The mean fracture spacing in the upper inventory square of the Woodford Shale is 2.05cm and the density is 0.38f/cm (Fig. 23). This section of the Woodford is more siliceous and cherty than the lower sections, and as a result, more fractured than the lower sections. In the middle inventory square, the mean fracture spacing is about 3 cm and (λ) is 0.38f/cm. This square imcludes most organic rich units. In the lower inventory square, the mean fracture spacing is 2.5 cm and (λ) is 0.6f/cm (Fig. 24). There is a systematic decrease in fracture density moving from cherty and silica rich shale to organic rich shale. Additionally, many fractures die out within the organic-rich

or/and fissile shale, however a few fractures do transact both silica-rich organic-rich beds. (Fig.28).

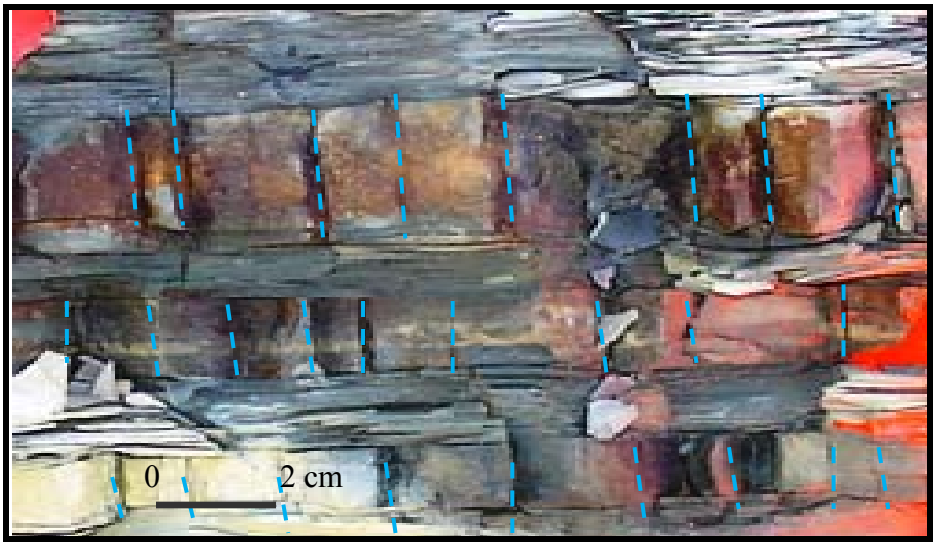

Figure 54. Bedding perpendicular fractures within the non-fissile cherty/silica rich units that terminate against the fissile, organic-rich beds.

Figure 55. The upper level inventory square for the Woodford Shale I-35 South outcrop. The Phosphatic horizon with phosphate nodules and the cherty-silica rich beds are densely fractured. Notice that non-fissile units contains abundant amounts of perpendicular fractures.

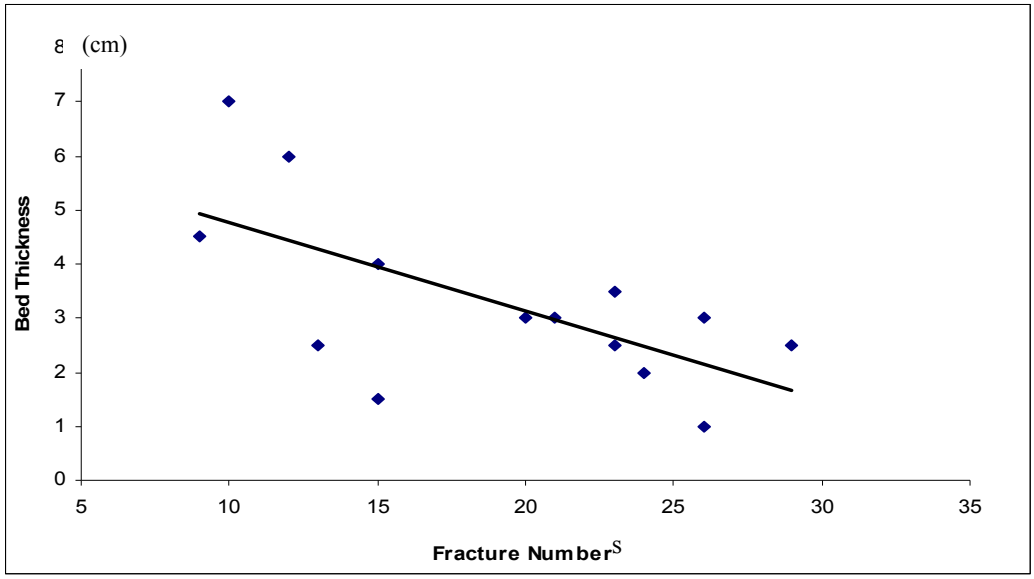

Figure 56. Bed Thickness v. fracture numbers from the upper inventory square at the I-35 South outcrop. Although data points are scattered, the graph shows that while bed thickness decrease, fracture numbers increase.

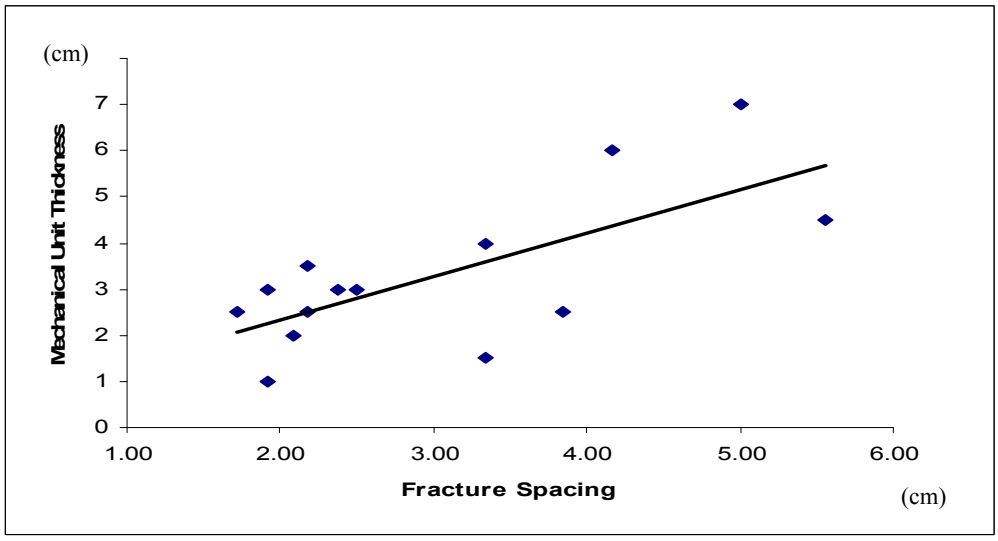

Figure 57. Mechanical unit thickness v. Fracture spacing from the upper inventory square at the I-35 South outcrop.

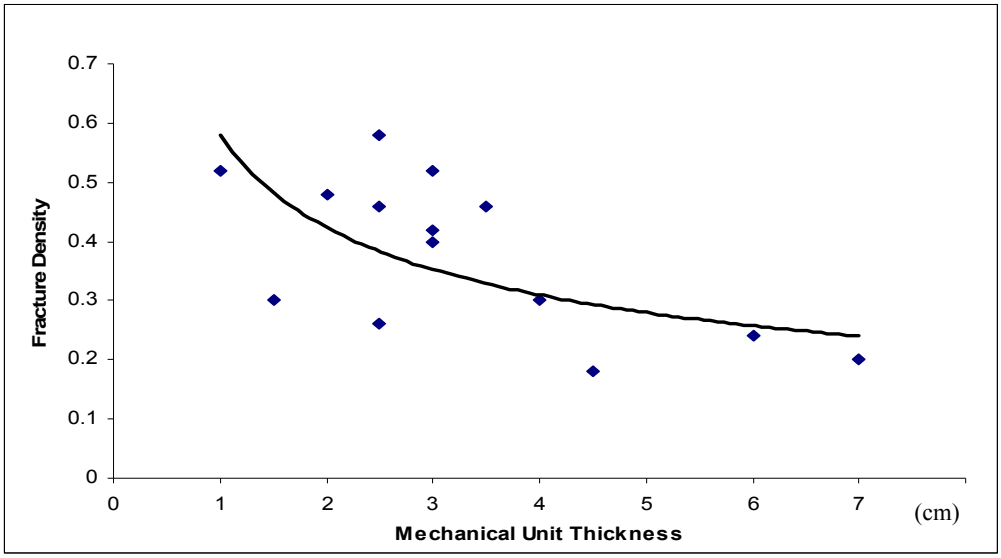

Figure 58. Fracture Density (f/cm) v. Mechanical unit thickness from the upper inventory square at the I-35 South outcrop. Fracture density decreases while mechanical unit thickness increases.

Figure 59.The lower level inventory square I-35 South Outcrop. The Fissile units and non-fissile units are darker colored than that of the upper inventory square. Non-fissile units are more silica-rich than fissile ones. Also notice that fissile unit fracture are rare and align oblique to bedding whereas non-fissile unit fractures are more common and perpendicular to bedding.

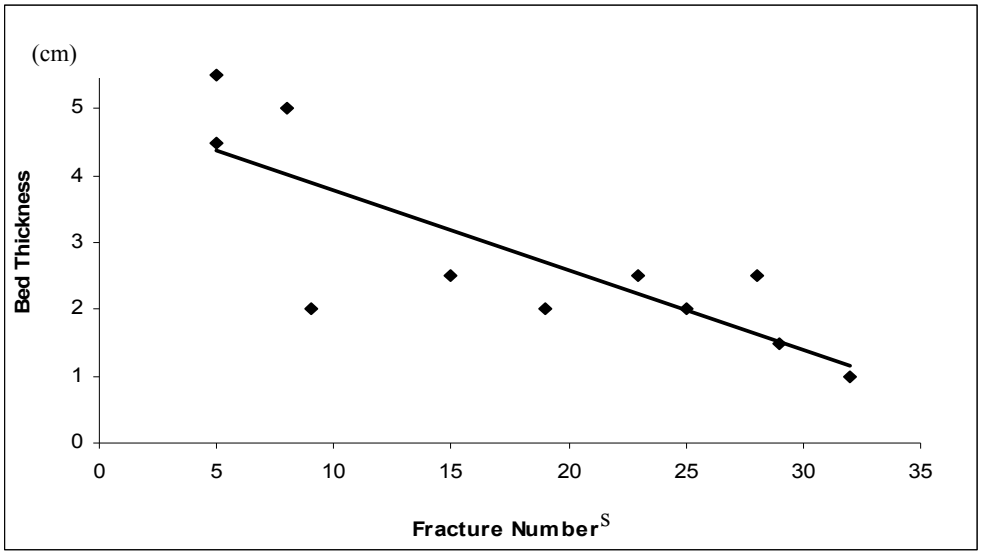

Figure 60. Mechanical unit thickness v. Fracture numbers from the lower inventory square at the I-35 South Limb outcrop.

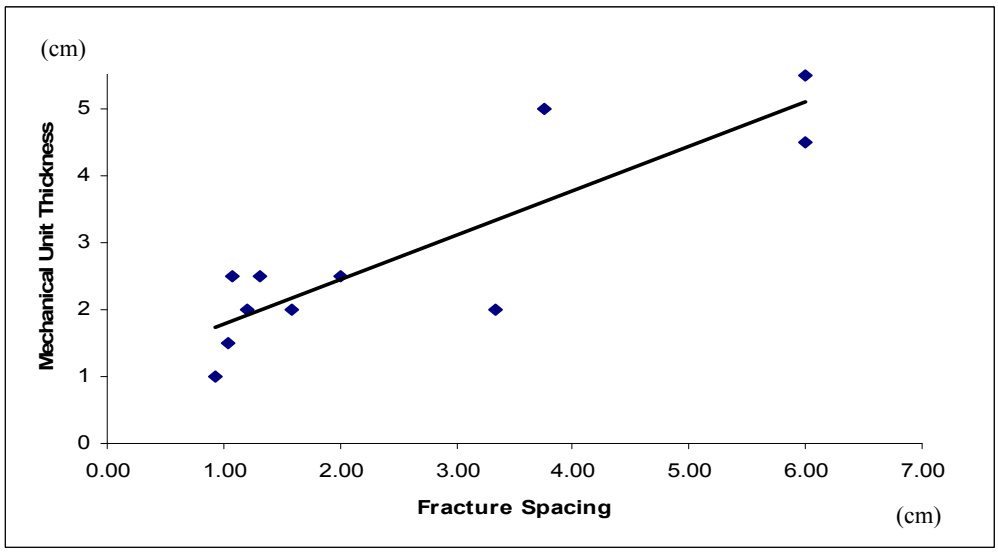

Figure 61. Mechanical unit thickness v. Fracture spacing from the lower inventory square at the I-35 South outcrop.

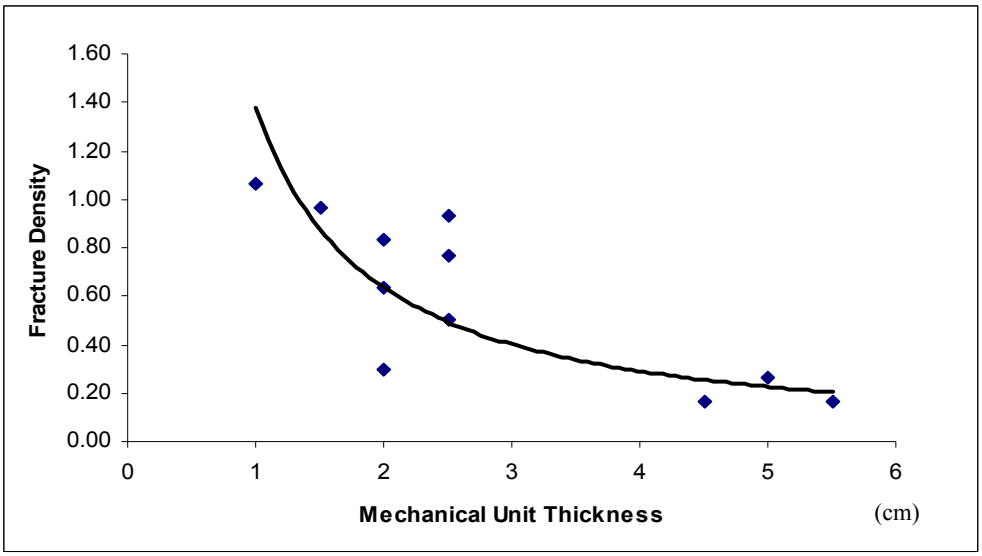

Figure 62. Fracture Density (f/cm) v. Mechanical unit thickness from the lower inventory square at the I-35 South outcrop.

Thin Section and X-ray Diffraction Analyses

Three rock samples were collected from I-35 South outcrop for laboratory analyses. The first sample came from the upper phosphatic horizon of the Woodford Shale and is a very light colored, highly fractured, silica rich, cherty bed. The thicknes is approximately 7cm and it is bounded by thinly laminated ductile beds. The other two samples are dark colored and also highly fractured, however one is fissile and the other one is non-fissile. The thickness of the fissile unit is a few millimeters and the non-fissille unit is approximately 3.6cm thick. The fissile unit was not competent enough for thin sectioning, however it was x-rayed.

Sample 1: I35 - S1

Sample I-35-S1 is light gray colored in hand sample and light brown color in thin section. Several micro-fractures were identified in this sample that appears to be open. They are generally bedding perpendicular and micro-fracture die out at the intersection with phosphate nodules or bend around the nodules. Sponge spicules, radiolarians, chalcedony and pyrite were identified in the thin section.

As expected, x-ray analyses showed that the quartz readings are higher compared to the other two samples from the I-35 South Limb outcrop; illite was not detected.

(a)

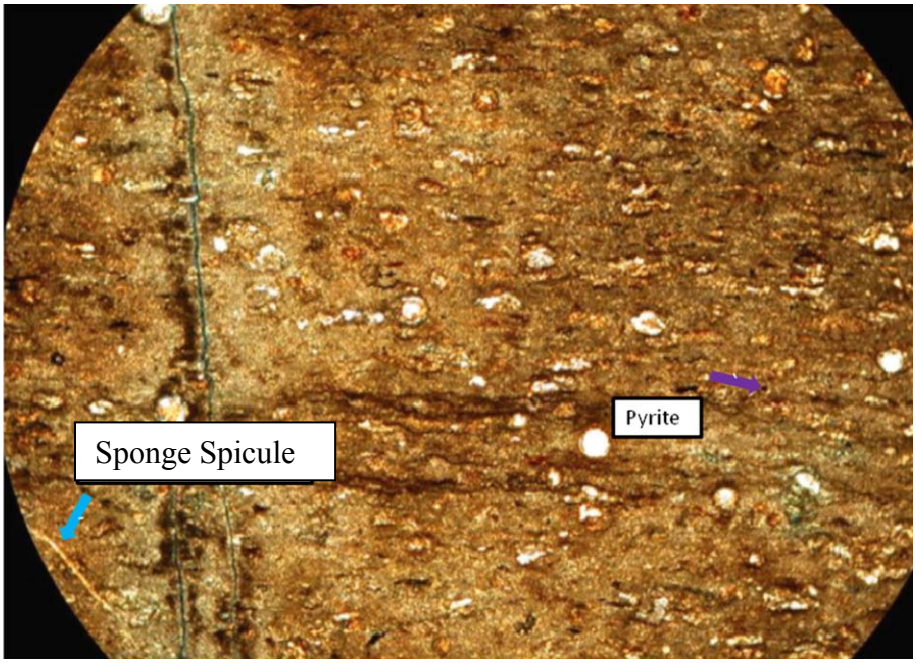

(b)

Figure 63. Thin section photomicrographs of the I35 - S1 sample from the I-35S South Limb outcrop. (a) PPL - X10 – (b) XPL - X10

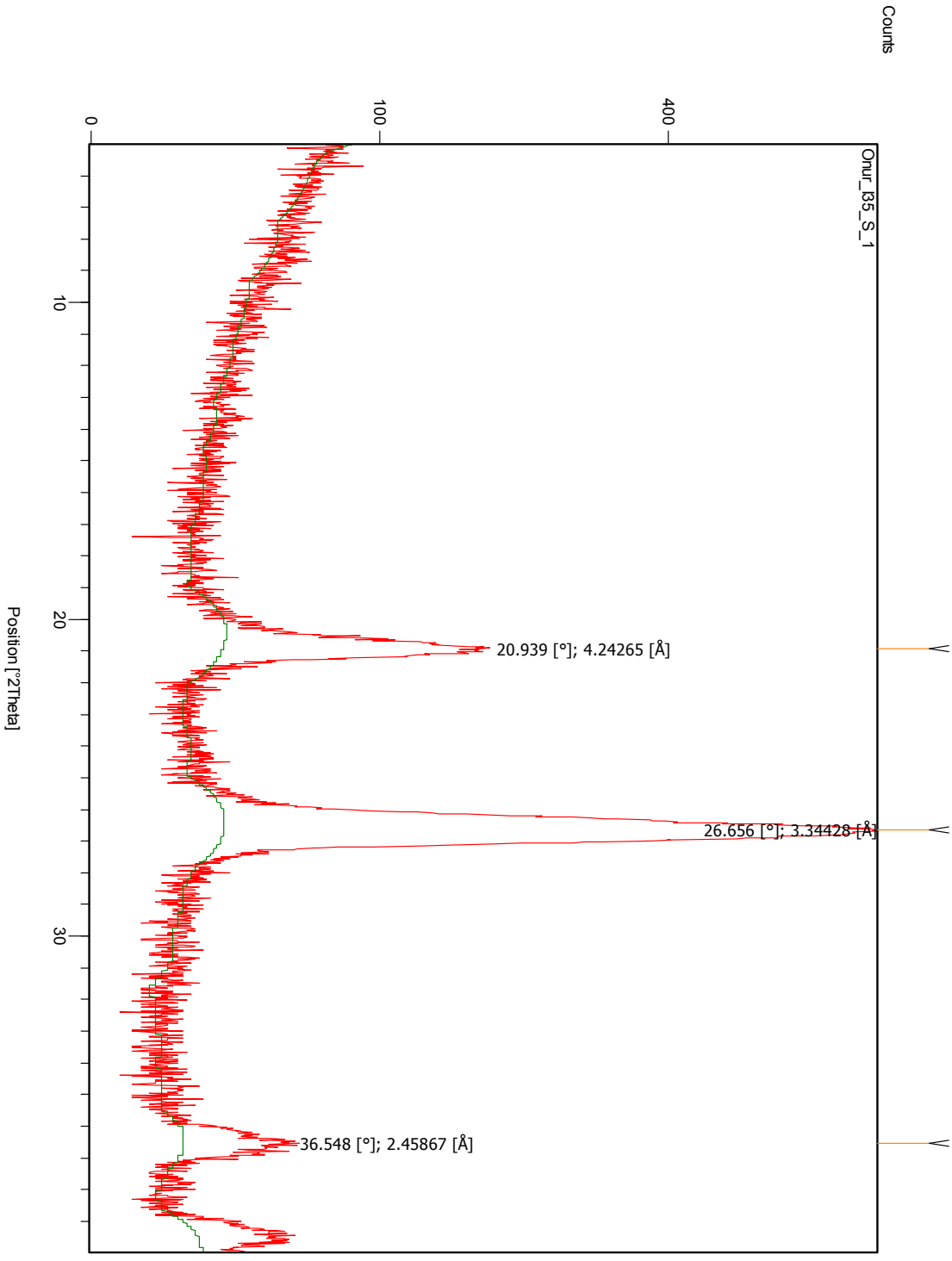

Figure 64. Powder X-ray diffractogram of sample 1, I35 South Limb. Note the absence of illite around 8.6 (2θ) and strong SiO2 peaks at approximately 26.7 and 20.9 (2θ) .

Sample 2: I35 – S2

The I-35-S2 sample colored both in the hand specimen and thin section. It contains micro-fractures, the majority of which are perpendicular to beddings. Most of the micro-fractures are healed. An abundance of radiolarians suggests a high of silica-content. Phosphate, pyrite and unidentified fossil fragments were evident in the thin section.

Total rock X-ray analysis of shows that the sample is primarily quartz, which is expected based on the abundance of radiolarians.

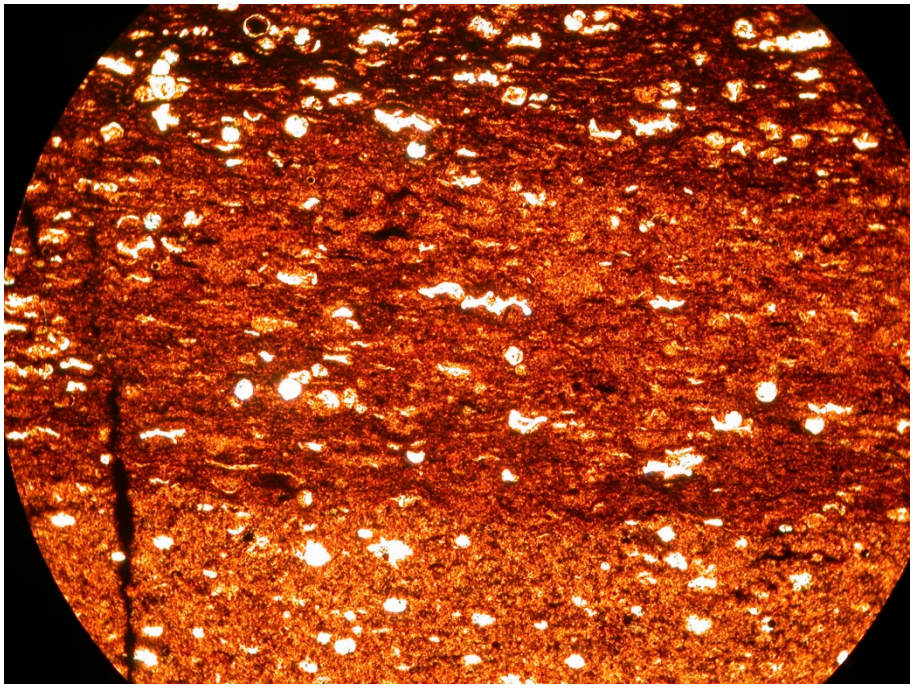

(a)

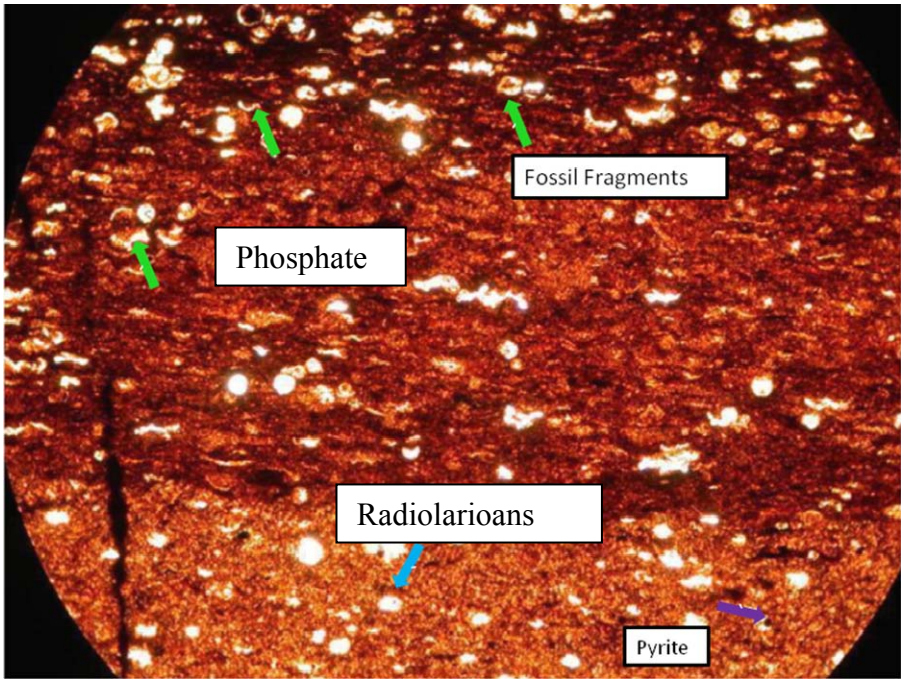

(b)

Figure 65.Thin section photomicrographs of the I35 – S2 sample from the I-35S South Limb outcrop. (a) PPL - X10 – (b) XPL - X10

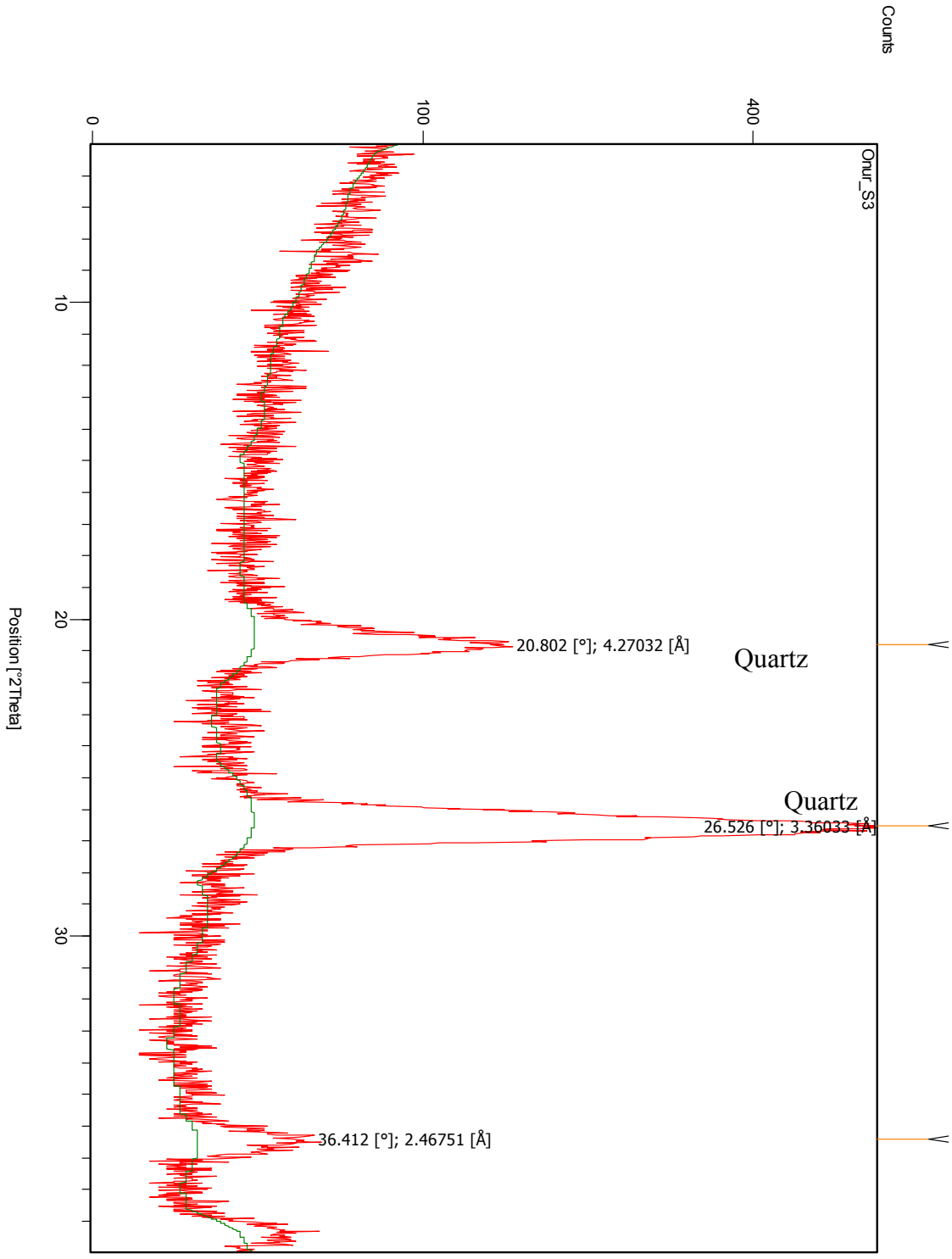

Figure 66. Powder X-ray diffractogram of sample 2, I35 South Limb. This sample is also quartz-rich and clay-poor.

Sample 3: I35S – S3

The quartz readings are relatively low in the X-ray diffraction analysis. Illite peaks and another unidentified mineral are also present in the graph. Low quartz readings and presence of illite is compromised with the fissility of the hand sample. However, the brittleness of the sample is not clear.

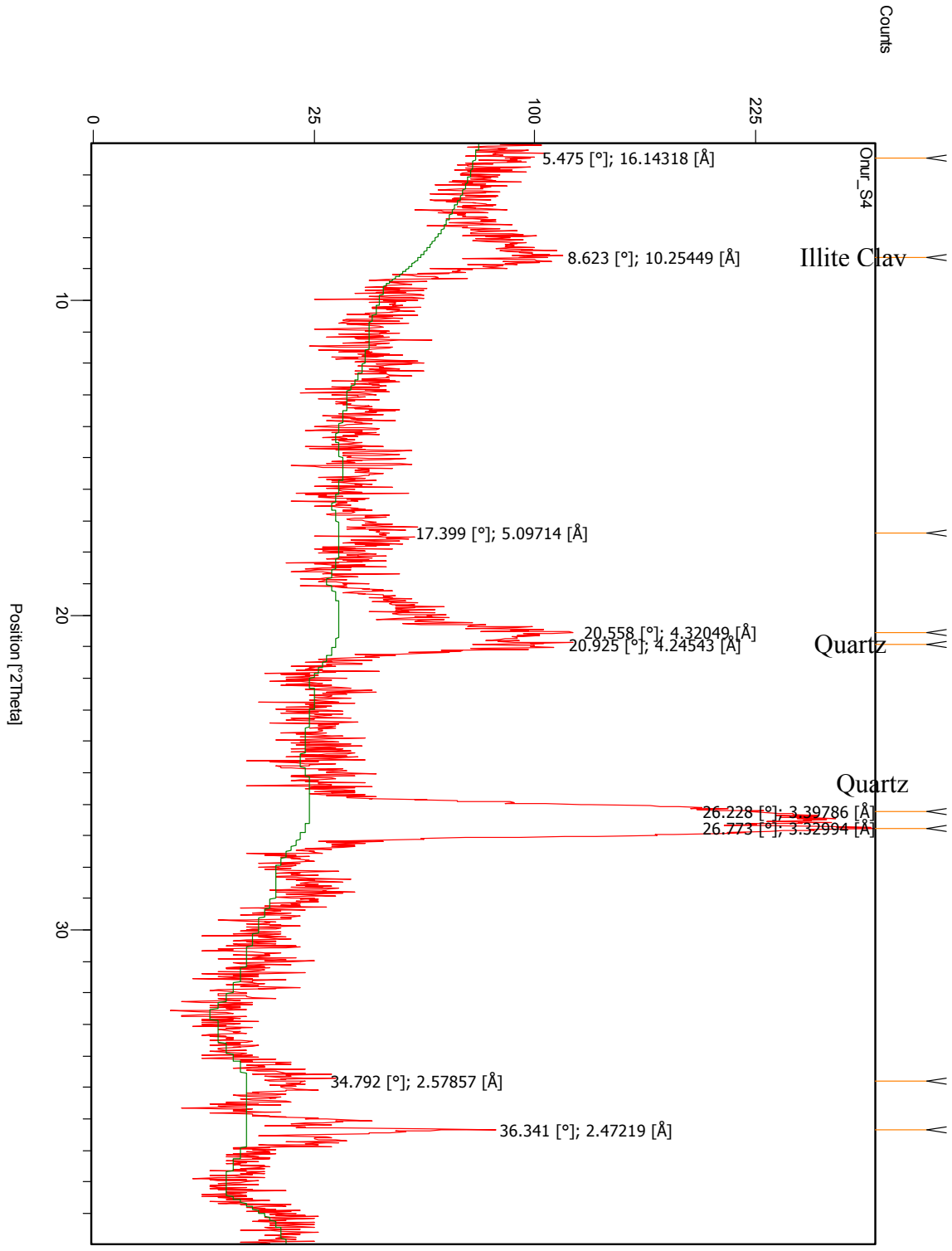

Figure 67. Powder X-ray diffractogram of sample 3, I35 South Limb. This sample shows an incerase in illite (8.6 2θ) and redeuced value of quartz (26.7 and 20.9 2θ respectively)

McAlister Shale Cemetery Pit Outcrop

McAlister Cemetery shale pit is located in the southern Criner Hills area (N/2 SW1/4, sec.36 T.5S. R1E) (Fig. 32). The Woodford beds strike N35W and dip 36 degrees to the northeast. The entire section of Woodford shale is exposed between the floor and highwall of the pit. The Woodford at this locality is more fissile at the base and towards the nodules. It transitions to thicker, siliceous blocky shale in the upper part and finally becomes finally light colored, altered shale with phosphate nodules.

Figure 68. A section from the middle of Mc Alister Cemetery outcrop. The interval is silica rich and contains fissile and the non-fissile units. These units are fractured; and contain dead oil within the fracture sets.

Fracture Measurements

Fracture measurements were obtained for the entire section of Woodford Shale. A total of 308 fracture orientations were recorded. Because of the bedding attitudes and limited outcrop accessibility, the fracture orientations were determined from a bedding perpendicular view. Bedding surface fractures were measured in the middle section.

Two dominant fracture sets were observed across the entire Woodford Shale outcrop. However, on the bedding plane surfaces, additional cross fractures and buckling fractures were recorded. These fracture sets may exist in other intervals of the Woodford, but were not detected because of the limited exposure at bedding plane surfaces.

In the McAlister pit, set I fractures strike N40E, whereas set II fractures strike N70E (Fig. 34). Both fracture sets were observed throughout the Woodford section. These fractures have strikes that are oblique to the strike of the bedding, and dip 74°NW and 78°SE respectively. The two fracture patterns are conjugate sets that align with an angle to bedding that they show a conjugate pattern in the bedding perpendicular view (Fig. 35). Set III fractures trend parallel to the strike of the bedding planes. Outcrop observations indicate that these fractures have a shear displacement and buckling is the primary mechanism for their development (Fig. 36). The last fracture set, (set IV), intersects set I fractures at right angles on the bedding plane.

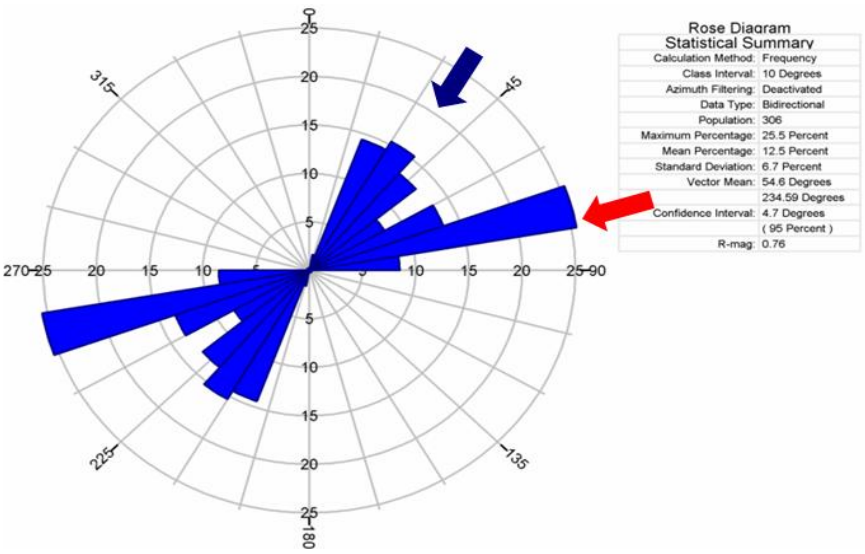

Figure 69. Fracture set I and set II orientations along the entire Woodford outcrop in McAlester Shale Pit outcrop.

Set I and set II fractures are extremely planar and very consistent in orientation. However in contrast to set I and set II fracture orientations, set III fractures are sub-planar, irregular and curved. Fracture spacings for set III are not consistent those for set I fractures. Orientation of fracture set IV is the least consistent among all fracture sets. Although, their orientation often seems parallel to set II fractures, the cross-cutting relationship of set IV to set II indicates that they are completely different most set IV fracture die out within the fracture set I. In contrast, set II fractures transect fractures of set I. The outcrop observations show that bedding oblique fracture sets formed at the beginning of fold evolution. However, set III and IV fractures formed later of folding.

In addition to the crosscutting relationship, dead oil resides within oil fracture sets except set III. This relationship is infegailed evidence that set III fractures developed later than other fracture sets. A sketch of a bedding plane surface at McAlister Cemetery Shale Pit outcrop displays many of the features of joints at this outcrop (Figure 71).

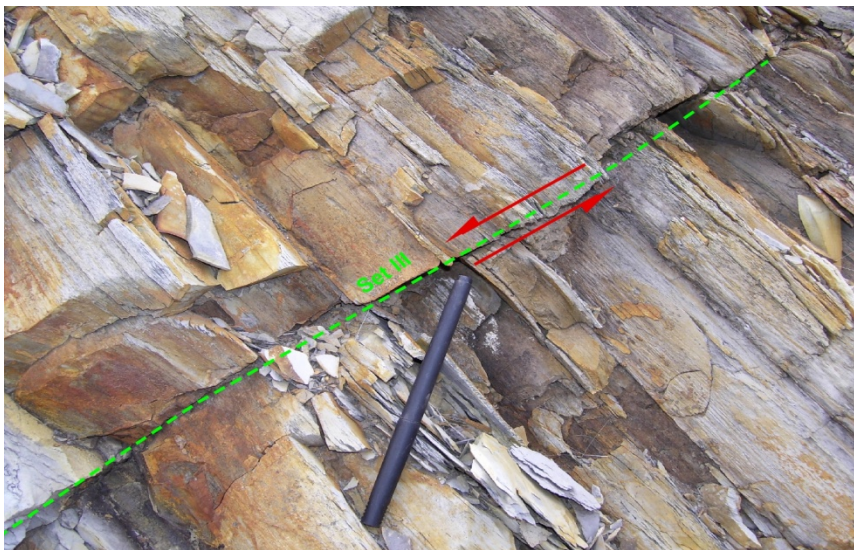

(a)

(b)

Figure 70. Shear displacement along the set III fracture reflect locally developed bending or buckling process along the middle Woodford Shale. (Bedding perpendicular view).

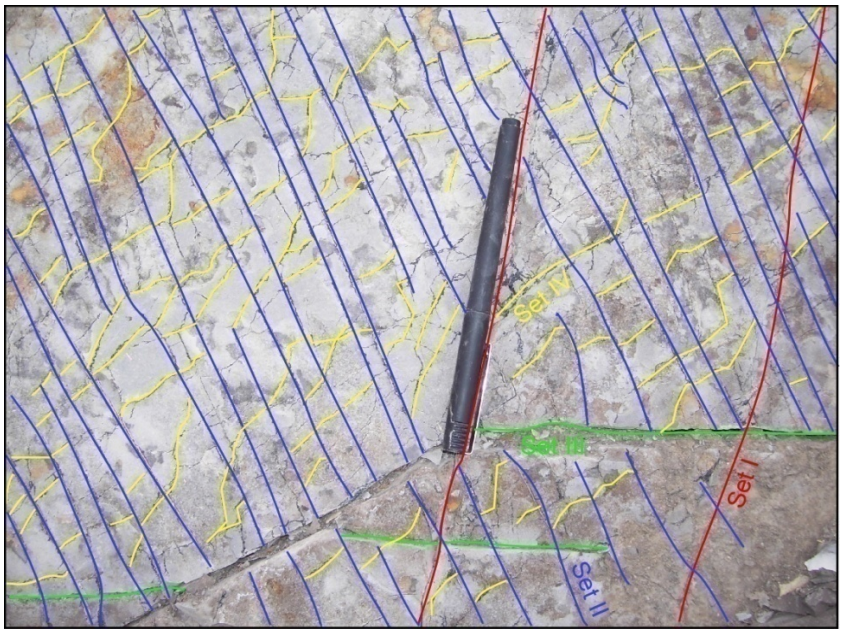

Figure 71. Fracture patterns within the McAlister Shale Pit outcrop. Set I and Set II are dominant fracture sets with an oblique orientation to both bedding planes and each other. Set III fractures are parallel/sub parallel to bedding planes and the least available set to measure. Set IV fractures are aligned orthogonal to set I fractures on the bedding plane.

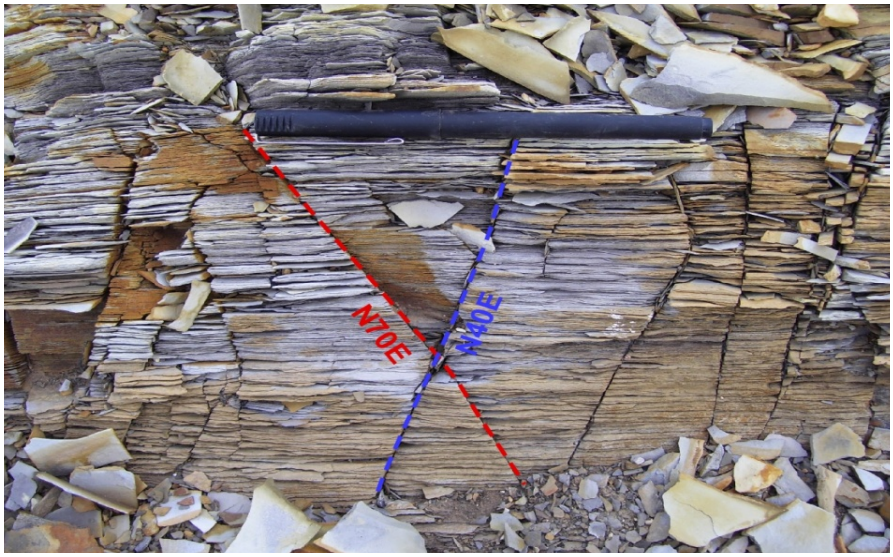

Figure 72. Dominant fracture sets striking N70E and N40E intersect at an acute angle within the bedding.along the Woodofrd Shale at Mcalister Shale pit outcrop.

Figure 73. Dead oil within the N70E set and N40E set.

Mechanical Stratigraphy Measurements

The inventory squares were located the dip shape to give a bedding plane view. The cumulative measured lengths of the fractures in the inventory square were divided by the area of the inventory square to give fracture density. The results show the average fracture density is $3.27cm^{-1}$ for the Woodford in the McAlister Cemetery Shale Pit. Set I fractures cut all beds (thick or thinly bedded) and their fracture spacings are less than those for Set II fractures. The average fracture spacing for Set 1decreases to 1.5 cm^{-1} within thin laminations and some intervals. Additionally, their spacing is always smaller than the spacing for set II fractures.

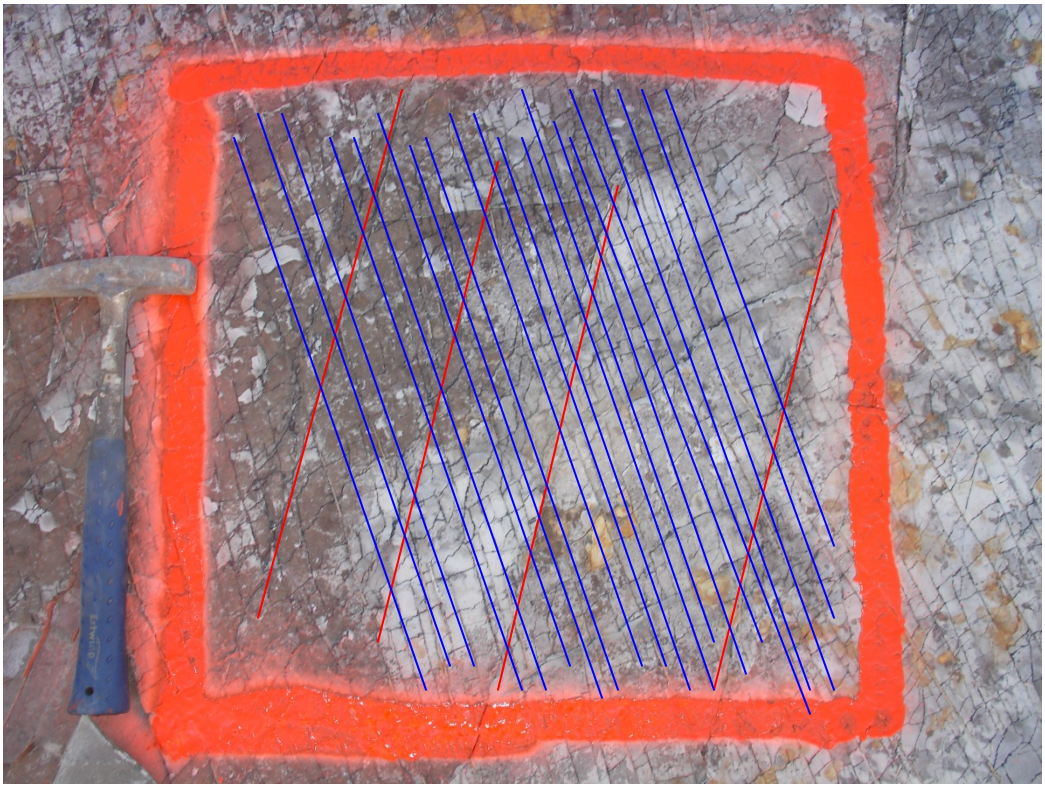

Figure 74. Inventory Square; Mc Alister Cemetery Shale Pit. The average fracture spacing for fracture set I is 1.68 and 5.7cm for the fracture set II.

Thin Section and X-ray Diffraction Analyses

Samples were collected across the Woodford interval for this section and X-ray analysis. A representative sample McAl from the silica-rich, light gray colored beds was especially chosen from the fractured interval containing dead oil.

Sample 1: McAl

The matrix of McAl is quite dark in the thin section, though the hand sample is light gray. McAl contains abundant radiolarians that appears round and undeformed by compaction. This sample appears to contain clay, but is radiolarian rich; therefore the

brittleness of the sample is expected to be relatively high. Some of the micro-fractures are filled with dead oil (Figure 75) Other constitutes include pyrites, whereas is disseminated.

The X-ray diffractogram (figure) for McAl show high peaks of quartz, which reflects the radiolarian concentration. Illite and chlorite are present and in higher concentration compared to other silica-rich samples. The hand sample is brittle and it appears the presence of illite and chlorite do not impact noticeable ductility.

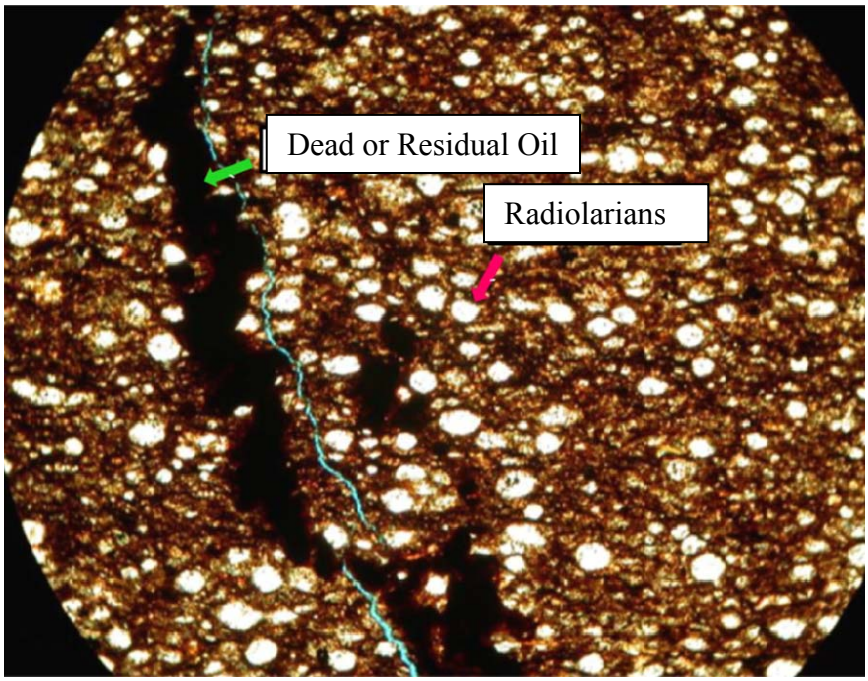

(a)

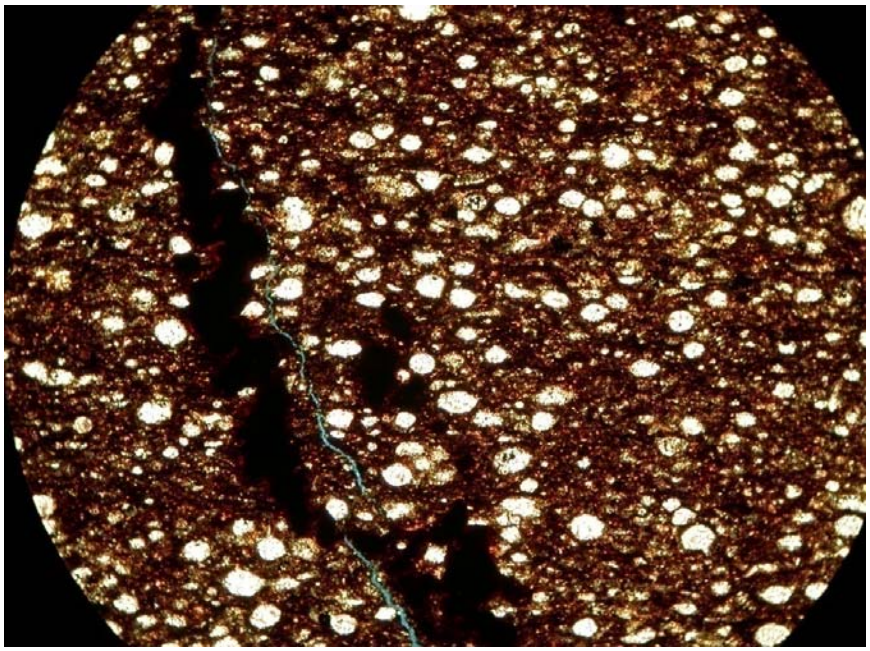

(b)

Figure 75. Thin section photomicrographs of the McAl sample from the McAlister Cemetery I-35S South Limb outcrop. (a) PPL - X10 – (b) XPL - X10. Round white objects are radiolarioans and black vertical linen is dead oil-filled fracture.

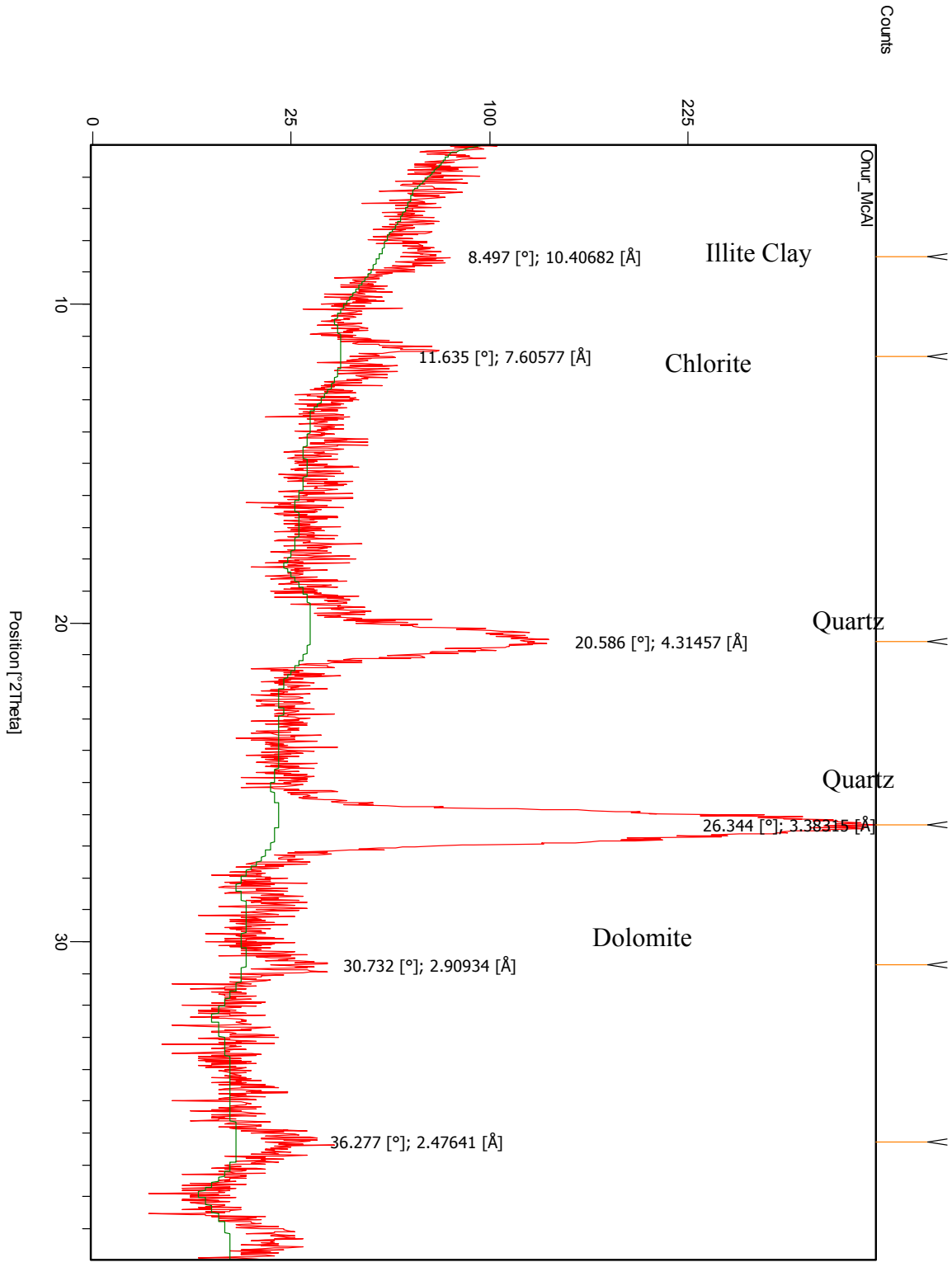

Figure 76. X-Ray Diffractogram from sample McA1 from McAlister Cemetry Shale pit.

The peak at approximate 2θ value 36.8 indicates that dolomite is present.

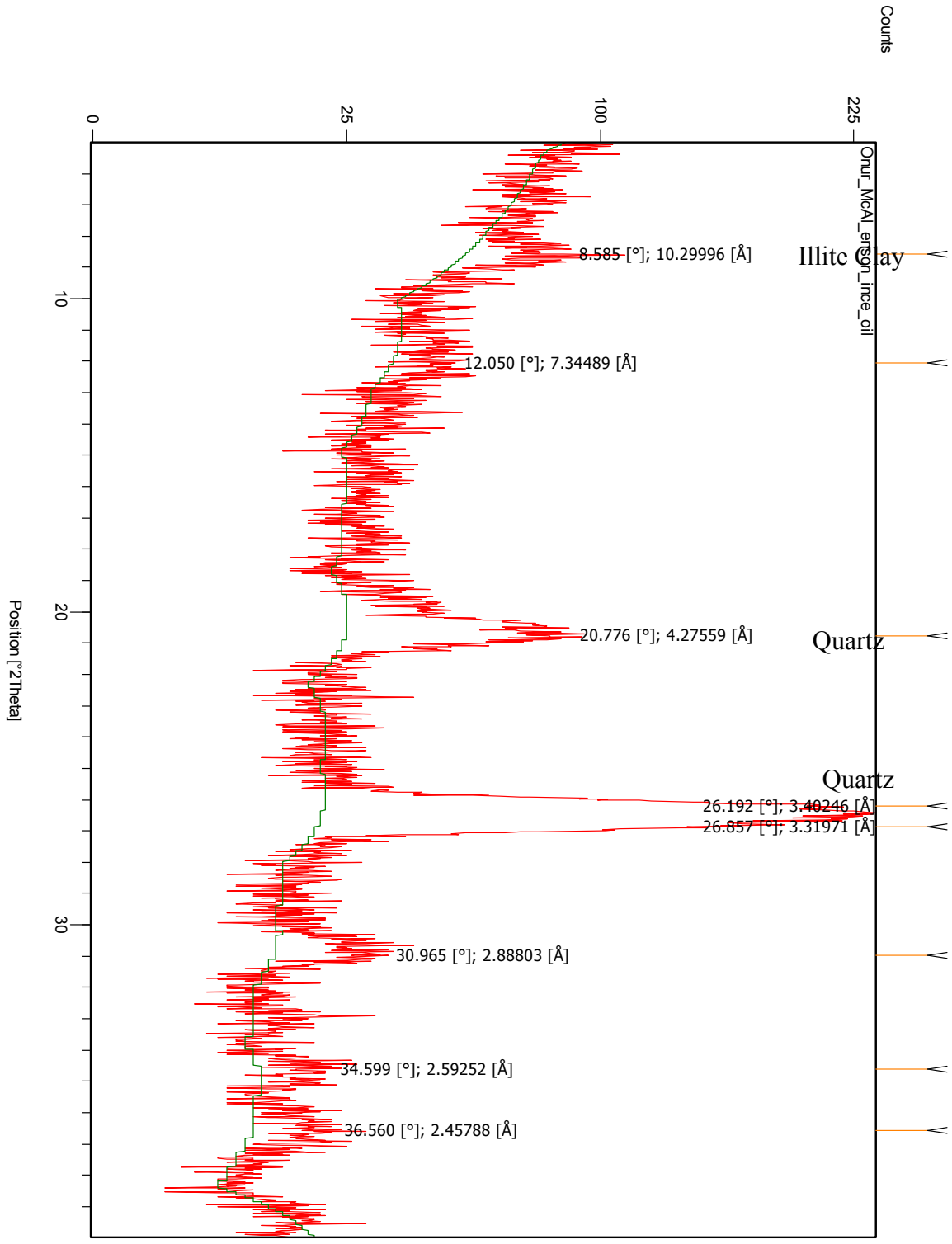

Figure 77. X-Ray Diffractogram from sample McA12 from McAlister Cemetry Shale pit.

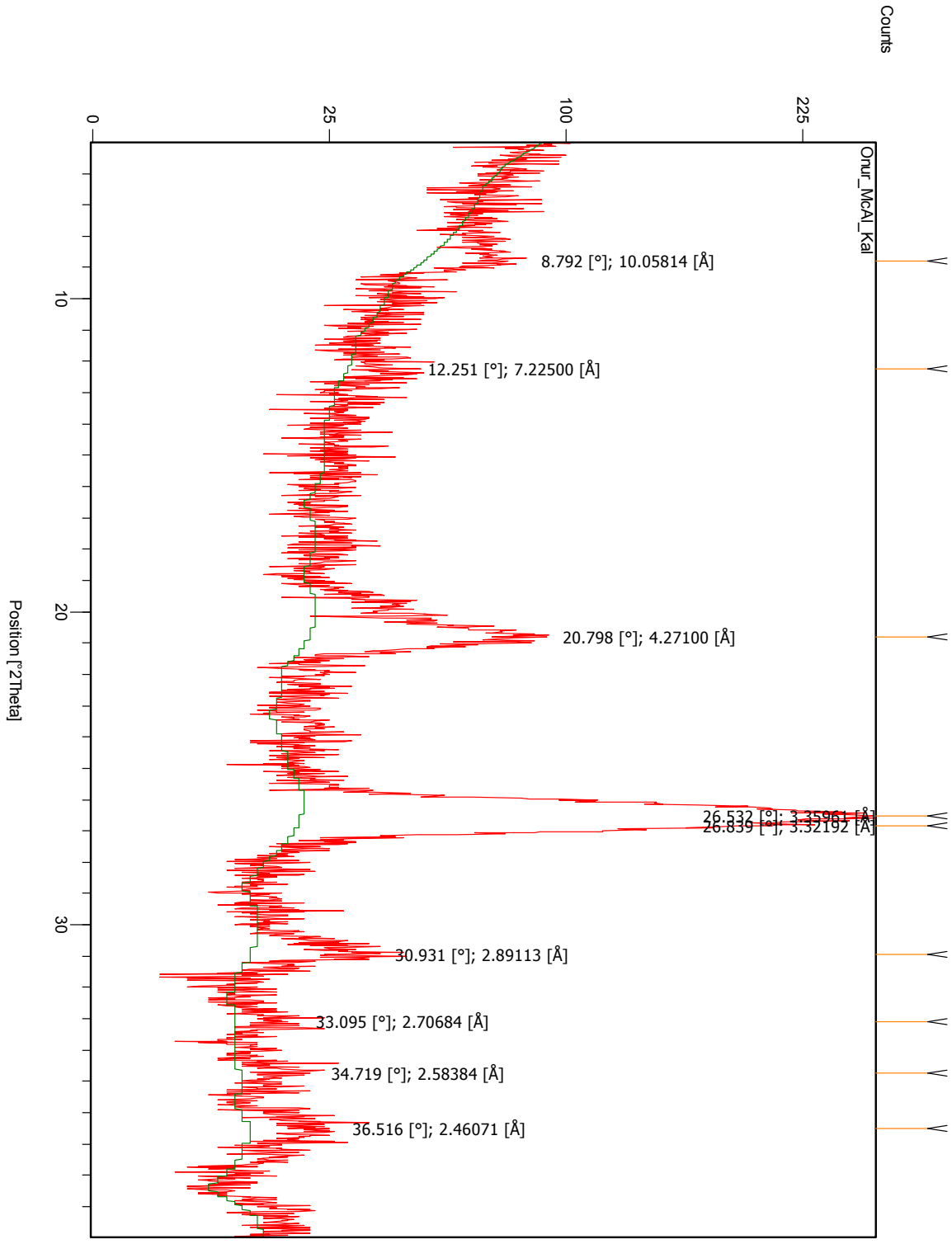

Figure 78. X-Ray Diffractogram from sample McA13 from McAlister Cemetry Shale pit.

Scratch Hill/East Atoka Road Cut outcrop

The Scratch Hill/East Atoka Road Cut outcrop is located at N34º22'32.1", W096º06'34.4" in the Arkansas Novaculate which is in part time equivalent to the Woodford (Fig. 39). The beds are highly inclined and deformed as inclined by localized faulting and folding. The beds in most of the down part of the lower part of the section strike approximately N31E and are steeply dipping to vertical. However, the bedding attitude changes as a result of local structures and faults and the beds in the upper part of the section strike between N43E and N52E.

Figure 79. An outcrop image from Scratch Hill outcrop

Fracture Measurements

Fracture populations were measured across the outcrop area; however access to all stratigraphic levels is difficult. The fracture sets within the same bed are not consistent

in terms of their strike, which was influenced by local faults and folds. Strike for a single bed may change as much as 15° in less than a few hundred meters so the strikes of the fractures change accordingly. Three rose diagrams were created that illustrate fracture orientation. The first two rose diagrams show the Strach Hill (middle and lower Novaculate) and East Atoka road cut upper Novanclate outcrop respectively. The third rose diagrams show the combined fracture measurements for the entire outcrop (Fig. 53). The two dominant fracture sets found within the Scratch Hill segment strike (I) N72E and (II) N56W (Fig. 42). Set I fractures are dipping NW at around 30° and set II dip to NE and SW around 62°. The two fracture sets create a new orthogonal pattern. (Fig. 43) These fractures primarily bedding-perpendicular fractures. The second rose diagram was created to show the fracture sets across the upper Novaculate. The two fracture sets strike (I) N34E and (II) N76W (Fig. 50). Set I fractures are dipping SW, whereas Set II fractures dip NE at variable degrees. Other fractures are not systemically developed that do not have as consistent strikes as the previous two sets. These inconsistent fractures with variable strikes and dip are most considered further for this study, but do indicate the impact of localized tectonics on fracture frequency and orientations.

Figure 80.Close up view of well developed fracture sets. Notice that their dip change along the length of the fracture.

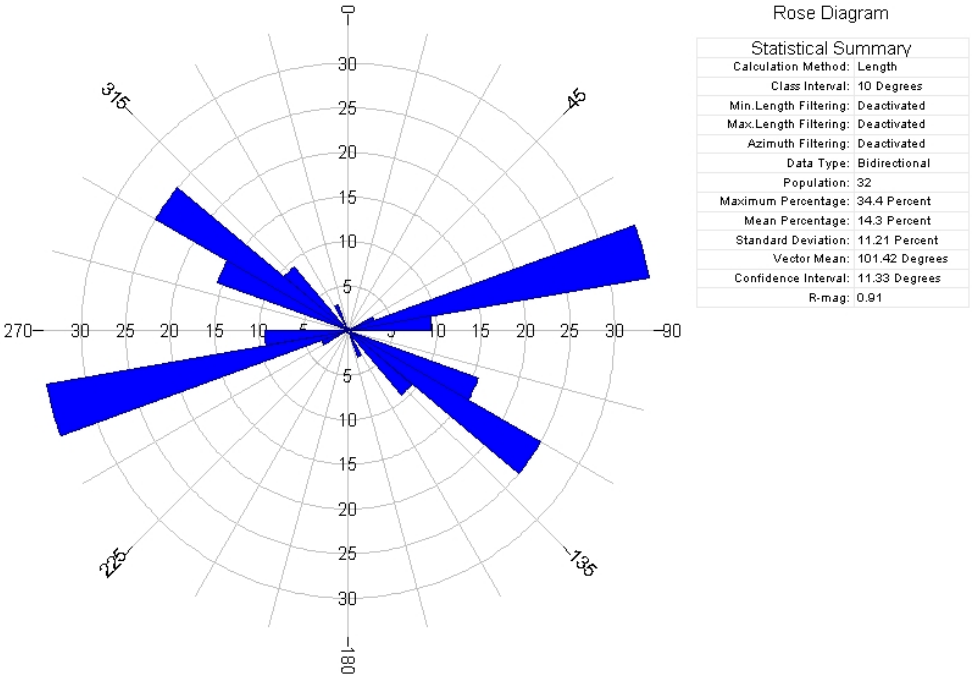

Figure 81. Orientation of Set I and Set II Fracture, lower and middle Novaculate Scratch Hill outcrop.

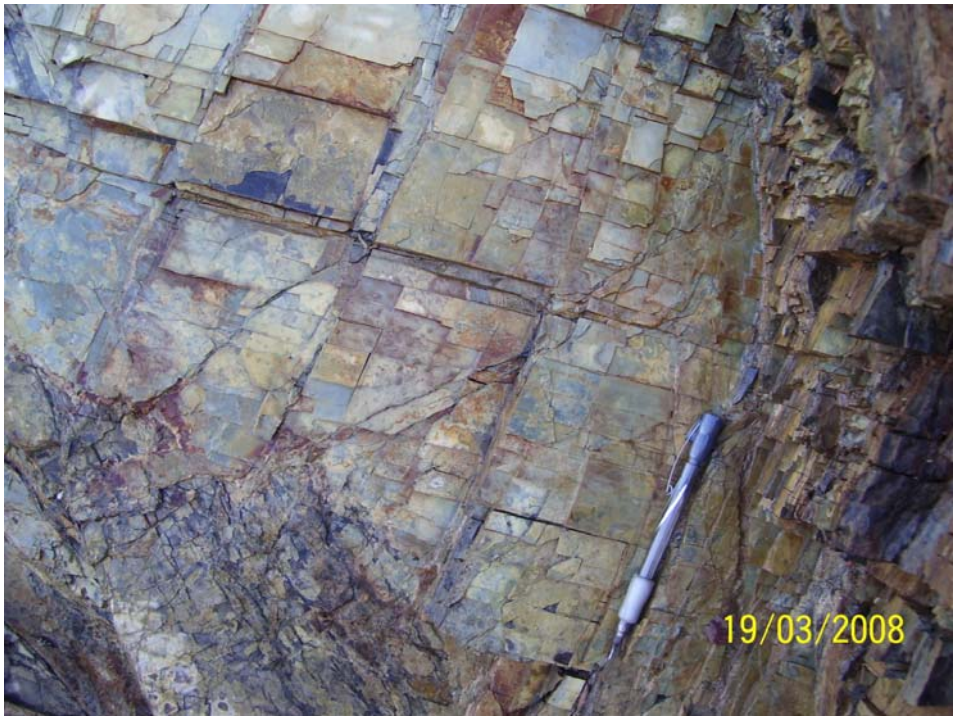

Figure 82. Fracture sets that display a near orthogonal pattern.

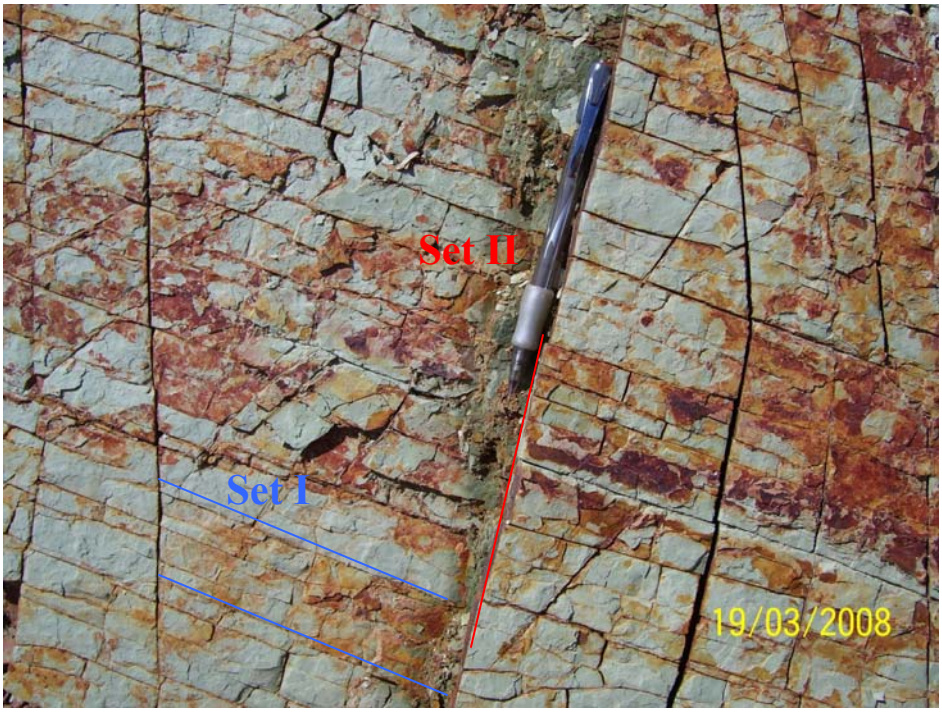

Figure 83. Set I fractures with a lesser fracture spacing than set II fractures.

Figure 84. Fractures from middle to upper Novaculate in the East Atoka Road Cut outcrop.

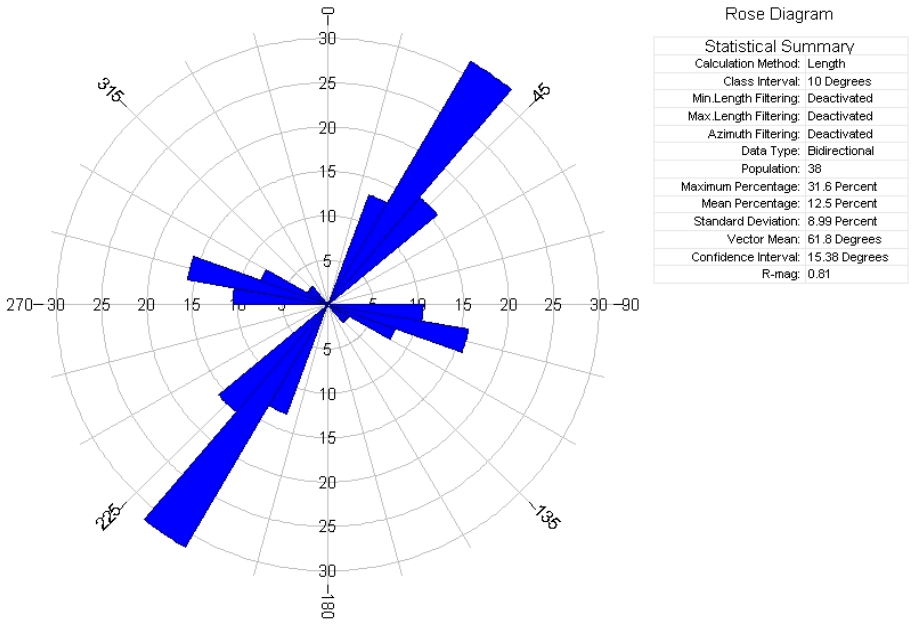

Figure 85. Orientation of set I and set II fracture,East Atoka Road Cut outcrop.

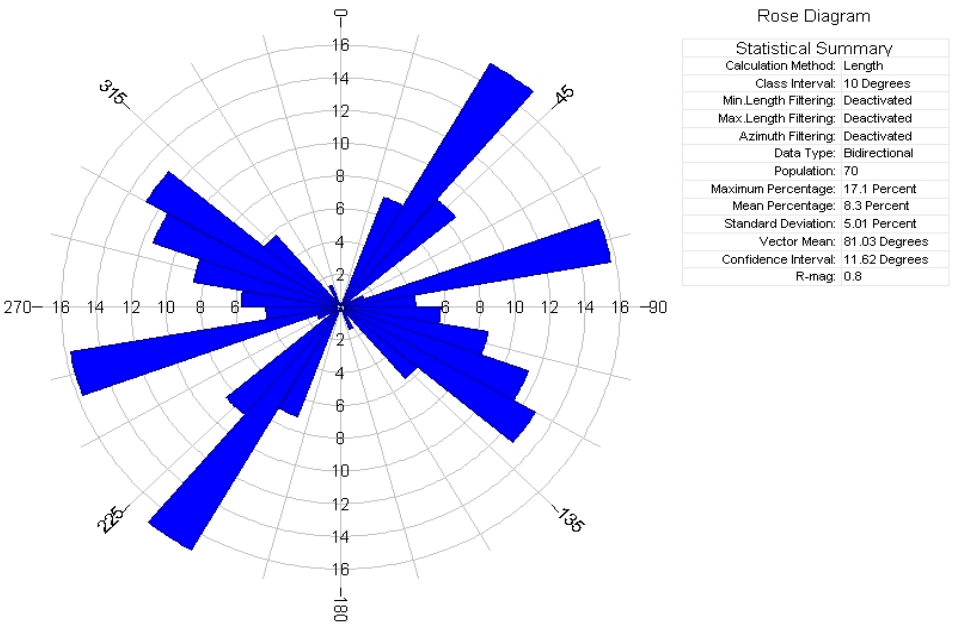

Figure 86. Orientation of the combined fracture measurements from the Scratch Hill/ East Atoka Road Cut outcrop.

Mechanical Stratigraphy Measurements

Mechanical stratigraphy analysis was completed on the Scratch Hill/East Atoka Road Cut outcrops. Alternatively silica-rich and clay-rich units of variable thicknesses are present (Fig. 52). Silica-rich units are generally thicker than the clayey units and as a result, clayey units are more densely fractured than silica-rich ones. Mechanical stratigraphy analyses were not attempted on clayey laminations. (Fig. 53). The brittle, silica rich thicker beds have fewer fractures than thinner laminations. In brittle units, the average spacing between fractures is 4.1 cm and the average fracture density is 1.05 f/cm. Clayey, silica-rich and organic-rich units exhibit different mechanical properties. Fractures terminate within the organic rich beds; however the number of the fractures

increases within the clayey units. Moreover the silica rich units have the widest fracture arrays.

Figure 87. Fracture distribution for different mechanical units. Bed thickness is the major factor controlling the fracture distribution and development.

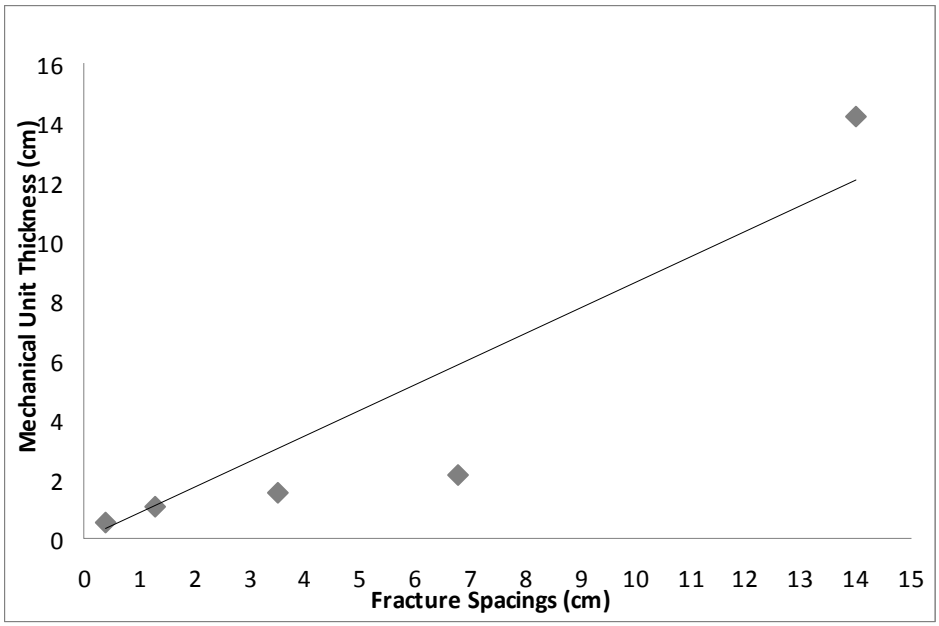

Figure 88. Mechanical unit thickness v. fracture spacings for the Arkansas Novaculate. Beds are mostly 1 to 3 cm thick however thicker units (13cm) are also present at the outcop.

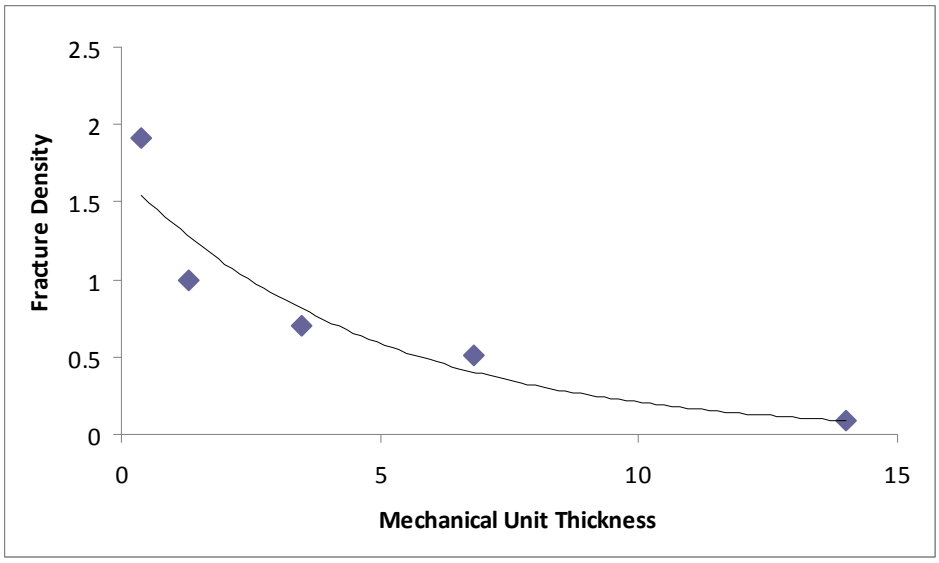

Figure 89. Fracture Density(f/cm) v. Mechanical unit thickness, Arkansas Novaculate. Fracture density decreases while mechanical unit thicknesses increase.

Figure 90. Densely fractured clayey units within the Arkansas Novaculate.

Wapanucka Shale Pit

The Wapanucha Shale pit outcrop is located at approximate attitude of N34º20'46.4", and longitude of W096º26'0.26". The beds strike between N33W and N41W and dip 25NE. The bedding attitudes are more consistent and they dip shallower than the Scratch Hill/East Atoka Road Cut outcrop.

Fracture Measurements

Measurements showed that two fracture sets dominate the outcrop; (I) E-W and (II) N15E fractures (Fig 56, Fig. 59). The two dominant fractures form orthogonal patterns however the angle between these sets sometimes decreases and the fracture sets

can show a conjugate relationship as well (Fig. 57). The deformation of the sets seems to be tensioned mode; however small amount of offsets along set I fractures are traceable (Fig. 58). Set II fractures generally have smaller spacings and fracture arrays, their strike is very consistent and planar. In addition, there are other fractures that strike parallel and perpendicular to the strike of the bedding planes. These are less abundant than the two dominant fracture sets. One group the strike perpendicular fractures are not consistent as others and their strike and dip dissection curve along their lengths.

Figure 91. Fracture patterns for the Woodford Shale, Wapanucka Shale pit. Set II strikes N15E and Set I strikes E-W to form an orthogonal pattern. Notice the curve of strike perpendicular fractures and strike parallel fractures.

Figure 92. Fractures sets forming a conjugate pattern. In this cases the strike perpendicular fractures have not developed. The absence of strike perpendicular fracture may be because of the shear movement along the fracture sets.

Figure 93. The shear movement along the set I fractures in the Woodford Shale. This movement might prevent the strike perpendicular fractures from forming.

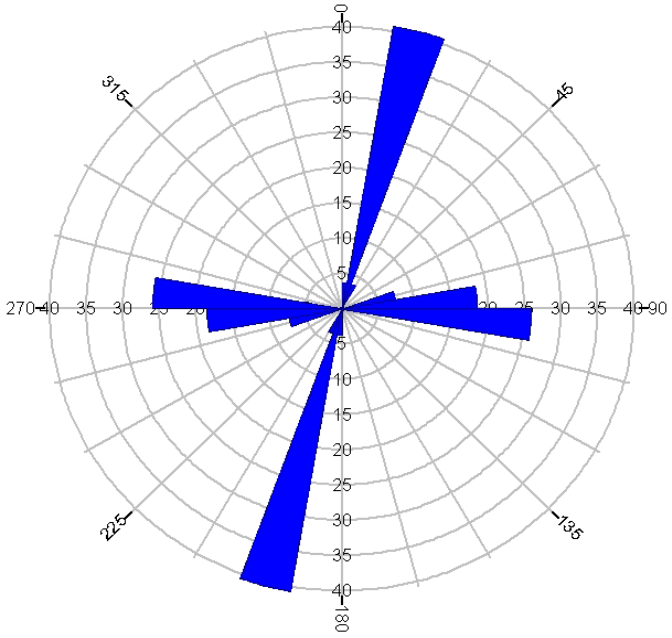

Figure 94. Dominant fracture orentations at the Wapanucka Shale pit outcrop. The two dominant directions are E-W and N 15E

Mechanical Stratigraphy

Mechanical stratigraphy analysis was conducted in an inventory square oriented perpendicular to bedding (Fig. 60). Bed thicknesses, number of fractures, fracture spacings, fracture fillings and lithology recorded. Thinly laminated shale units behave as a thick bed, so they contain fewer fractures than individual thick beds. The fractures are mostly open, but a few of them are cemented by calcite cement. The average fracture density is 0.5f/cm and the average fracture spacing is 1.9 cm within the inventory square. Silica-rich beds are more fractured than clayey beds.

Figure 95. Inventory Square;Wapanucka Shale Pit.

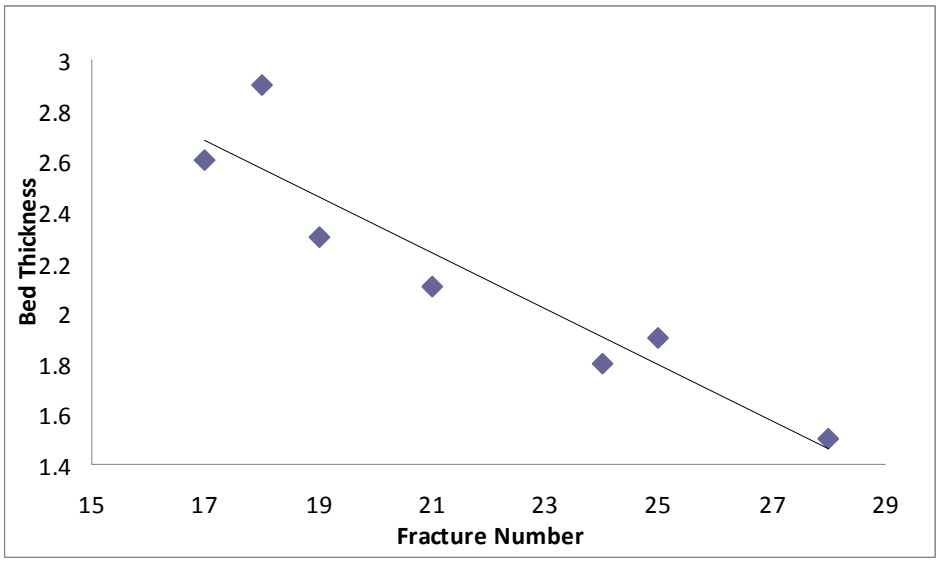

Figure 96. Mechanical unit thickness (cm)s v. fracture numbers from the inventory square, Wapanucka Shale Pit Fracture number increases as bed gets thinner.

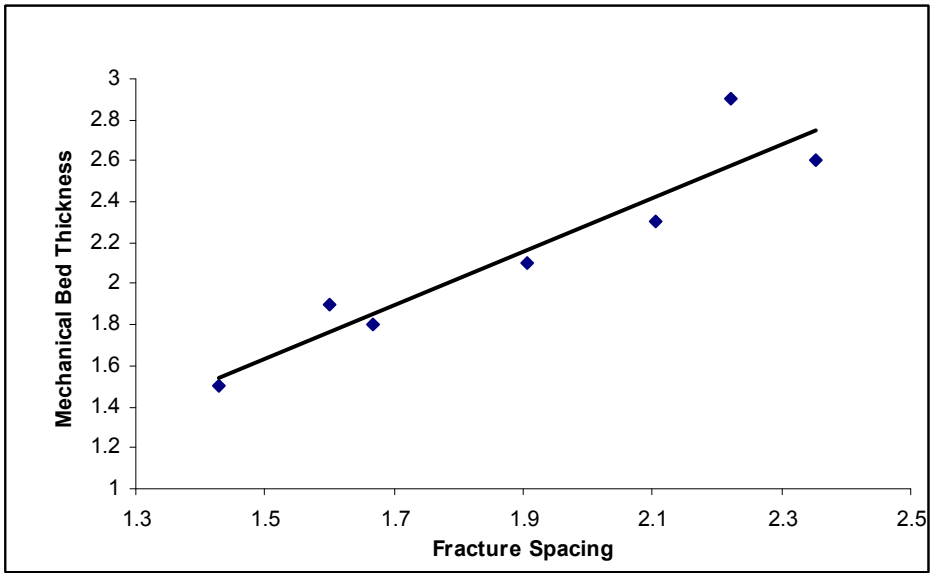

Figure 97. Mechanical unit thickness (cm) v. Fracture spacings (cm) within the inventory square. Notice that the beds are up tp 3-4 cm thick at the outcrop.

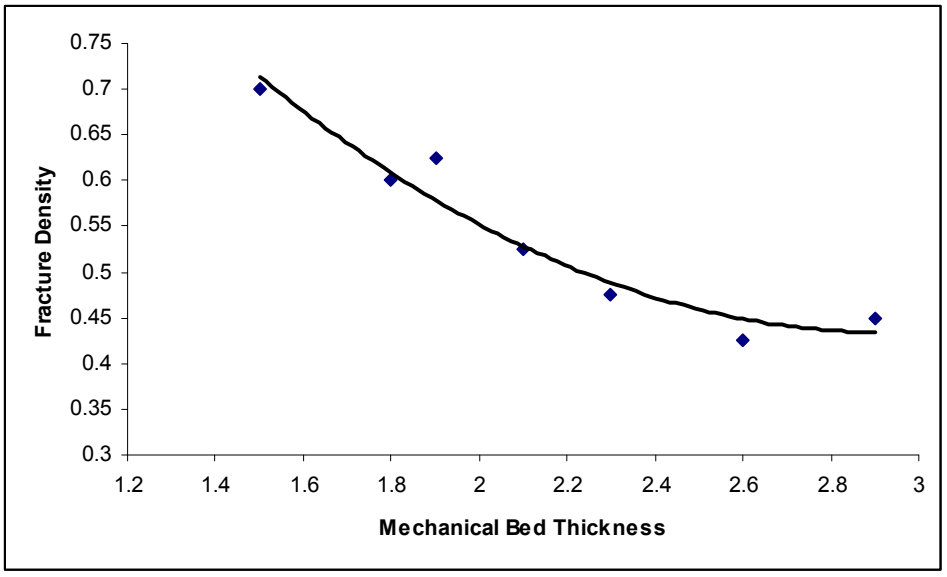

Figure 98. Fracture Density (f/cm) v. Mechanical unit thicken (cm)s within the inventory square. Woodford Shale, Wapanucka Shale Pit. Upper Fracture density decreases as bed thickness increases.

Clarita Shale Pit

The Clarita Shale pit outcrop is located at a latitude as wN34º28'17.9", and longitude of W096º27'59.8". This outcrop is the least deformed one in the study group (Fig. 64). The beds strikes N15E and they dip very gently to SE (6º). The bedding surfaces are widely exposed and different stratigraphic levels are easily accessible for fracture measurements.

Figure 99. General outcrop view of the Clarita Shale Pit outcrop. Spacing between fracture in set I approach 70cm.

Fracture Measurements

The fracture sets at Clarita Shale pit are strike (I) E-W and (II) N25E (Fig 66). The fractures are oriented perpendicular to bedding and form an orthogonal pattern. There is no detectable offset or extensional feature evident in the fracture sets. However the structural position of the beds and their orientations still

suggest tension mode. In addition gape of, several millimeters along the fracture trace arrays suggests a tension mode. Set I fractures are more consistent and planar when compared to set I fractures. Set I spacings approach 70 cm and decrease to 3 to 4 cm within specific stratigraphic intervals (Fig. 65). The fracture array also can approach 4-5 mm when the spacing is around 70cm wide (Fig. 67). It might be an evidence for power-law.Set II fracture consistently have smaller fracture arrays and spacings than fracture set I, but they are not developed within some stratigraphic intervals. Both of the fracture sets transect 8 cm to 12 cm thick beds(Fig.8).

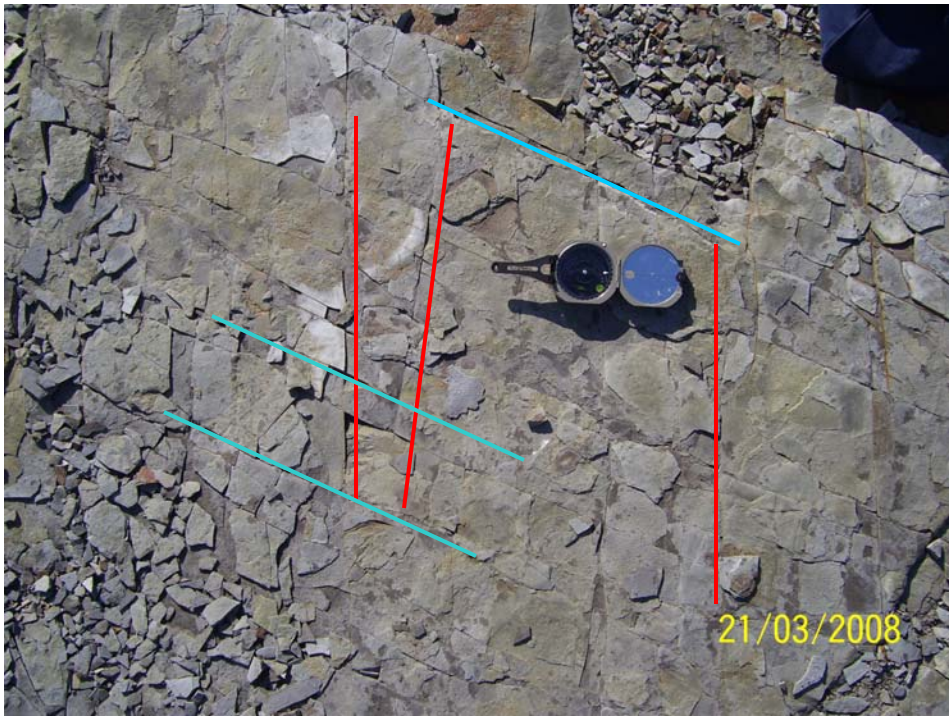

Figure 100. Fracture sets I (red) and II (blue) forms conjugate fracture patterns. Note that the fracture spacing has decreased to several centimeters for set I.

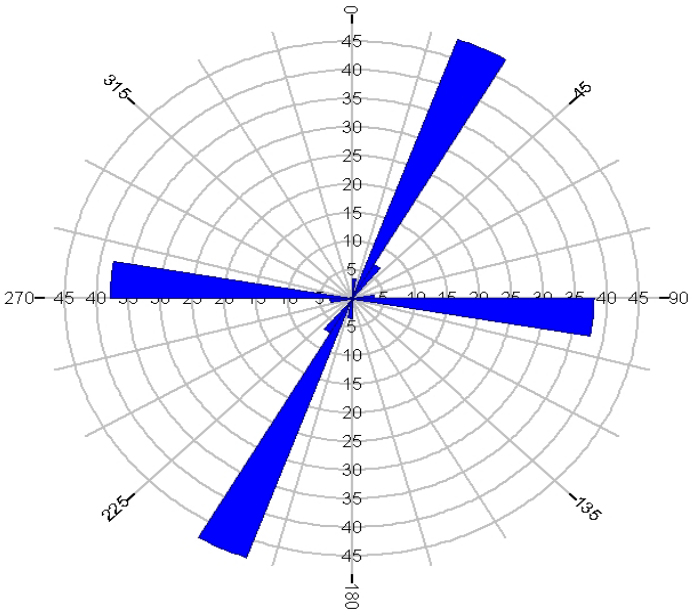

Figure 66. Fracture orientations in the Clarita Shale pit. The N25E and E-W orientations are similar to those for the Wapanucka Shale pit.

Figure 101. The fracture aperture of the Set I fracture. Clarita Shale pit 4-5 mm fracture aperture when the fracture spacing is around 70 cm.

Figure 102. Typical 8-12 cm thick bed of the Woodford Shale in the Clarita Shale pit. Set I and Set II fractures normally transect these beds. (Brunton for scale)

Fracture Pattern Interpretation

The systematic fracture sets found at the Arbuckle Anticline limbs are directly related to the evolution of the anticline. They are quite consistent with the fold related fracture patterns proposed by Friedman and Stearns (1972). Along the northern limb of the Arbuckle Anticline, two dominant fracture patterns were recorded. The vertical beds of the Lake Classen Spillway and the overturned beds of the I35 North Limb indicate that both of the outcrops were exposed to the late folding processes. Compared to the other outcrops exposed among the study area, beds located on the I-35 North Limb outcrop were significantly deformed during fold evolution, so this should be the reason for the more complex fracture pattern develop of those. The fracture sets that are present on the Woodford Shale suggest that the principal stresses and their direction should have changed during folding. The first common fracture pattern indicates that maximum principal stress (σ_1) was parallel to the dip direction at the beginning of folding, while the intermediate stress was normal to bedding and the least principal stress parallel to bedding strike. However, when the beds have gained inclination, the direction of principal stresses changed. Consequently, the secondary fracture patterns developed under reoriented principal stresses.

Fracture orientations and relationships are more complicated on the northern limb of the Arbuckle Anticline. Observations on the northern outcrops indicate an increase in fracture patterns and complexity with proximity to the hinge of the anticline. Late fold evolution caused the development of the two patterns on the northern outcrops and that not as scattered populations on the stereonets. However, the southern limb beds have not experienced the late fold evolution. For this reason; only the first fracture pattern

developed along the I35 South Limb outcrop. Fracture measurement populations are not scattered as much on the stereonets. Low-dipping beds and less deformation compared to the forelimb outcrops are the primary reasons for the absence of the second fracture pattern on the southern limb outcrop. In the McAlister Cemetery Shale pit outcrop, the dominant fracture sets developed in response to the same oriented regional forces. As a result of similar oriented stresses, fractures developed in the McAlister Shale Pit outcrop have similar orientations to those in the Arbuckle Mountains. The dominant fracture sets observed in the McAlister Cemetery Shale Pit outcrop are oblique to the strike of the beds, however the angle between set I fractures and the bedding strike is smaller than that of set II fractures. Therefore, the angle between set I fractures and regional stresses is smaller. Although the two dominant fractures are recorded on the same beds, fracture set I has smaller fracture spacings than that of set II fractures. The fracture spacing difference between two sets also indicates that set I fractures are developed more closely to the principal stress direction.

Based on the orientation of the fractures observed at the four outcrops and the previous studies about the structural styles of the Southern Oklahoma Aulacogen (Walper, 1977; Brown, 1995; Saxon 1998; Randel, 2008), the maximum principal stress is oriented in NE and W-NW directions. However, fractures are strongly influenced by local structures and the Arbuckle Anticline. Therefore, the proximity to local structures played a significant role in fracture development and orientations by changing the principal stress directions. In addition to this, after removing bedding dips, some fracture orientations are consistent with the regional principal stress directions and also with fractures orientations within the Ouachita outcrops. Therefore, there is a possibility of

some fracture development in response to regional stresses prior to the Arbuckle Anticline evolution.

In the Eastern Arbuckle and Ouachita outcrops, the fracture sets are less affected by local structures. In the Eastern Arbuckle Wapanucka and Clarita Shale pits, fracture orientations are very consistent to each other. Therefore, set I and set II fractures are regional fractures that developed under Ouachita tectonic stresses and principal stresses are not significantly disturbed by any local structures. However, in the Scratch Hill/East Atoka Road Cut outcrop, the Ouachita frontal fault zone, bedding attitudes change locally and local folds again disturb the principal stresses. Consequently, fracture orientations and properties show a response to local stress distortions and thereby have developed under different oriented principal stresses. To conclude, in both Ouachita and Arbuckle outcrops, fractures are developed under regional stresses however, evolution of local structures totally change principal stress directions and therefore fracture properties.

Fracture Density Interpretation

The fracture densities determined within inventory squares on four outcrops have been compared with facies distribution. A decrease in average fracture density for organic rich shale beds, compared to silica-rich/cherty beds, has been systematically observed. Minimum values were recorded on organic rich beds and fractures observed on silica-rich/cherty shale often terminate within the organic-rich beds. Very few fractures propagate through organic-rich and/or fissile shale beds. Therefore, the composition of the Woodford shale beds has a significant effect on fracture spacing. Consequently, a shale bed with more brittle constituents has a larger fracture population. Powder X-ray

diffraction analyses also show that the quartz is the primary brittle constituent within the Woodford Shale. The amount of quartz is strongly proportional to the number of radiolarians found within the bed. However, the presence of illite significantly decreases the brittleness of beds.

In addition to composition, the thickness of a shale bed is an important factor in determining fracture density. Thicker beds have fewer fractures compared to thinner ones. However, the fissile and thin laminations of the Woodford Shale, no matter if they are brittle or ductile, respond to stress loading together and because of this feature, they response as a thick bed and fracture densities decrease in these laminated units. Fissile-ductile beds of the Classen Lake outcrop, fissile-brittle beds of the I-35S and the McAlister Cemetery Shale Pit outcrops show this type of response. Powder X-ray diffraction analyses results show that fissile beds have decreased amounts of quartz. One explanation for the thicker bedding is that quartz plays a significant role in cementing and that quartz cement extends three dimensionally allowing thicker beds to form. In contrast, alternating clay, organic material and quartz form laminas with tabula flat-lying strength, but vertical weakness persists, generating fissility. These brittle beds, separated by ductile ones, tend to fracture easier than thicker ones. Thin section analyses reveal that, organic-rich beds tend to have bedding parallel micro-fractures. Grain orientation in fissile beds could be the primary reason for generating beds parallel micro-fractures. Silica-rich, cherty beds have more bedding perpendicular fractures; these cherty beds are dominantly non-fissile.

The fracture density comparison graph indicates that the most densely fractured outcrop is I-35 North outcrop (*Fig. 103)*. This is probably because of overturned beds and reactivated fractures during late stage anticline evolution.

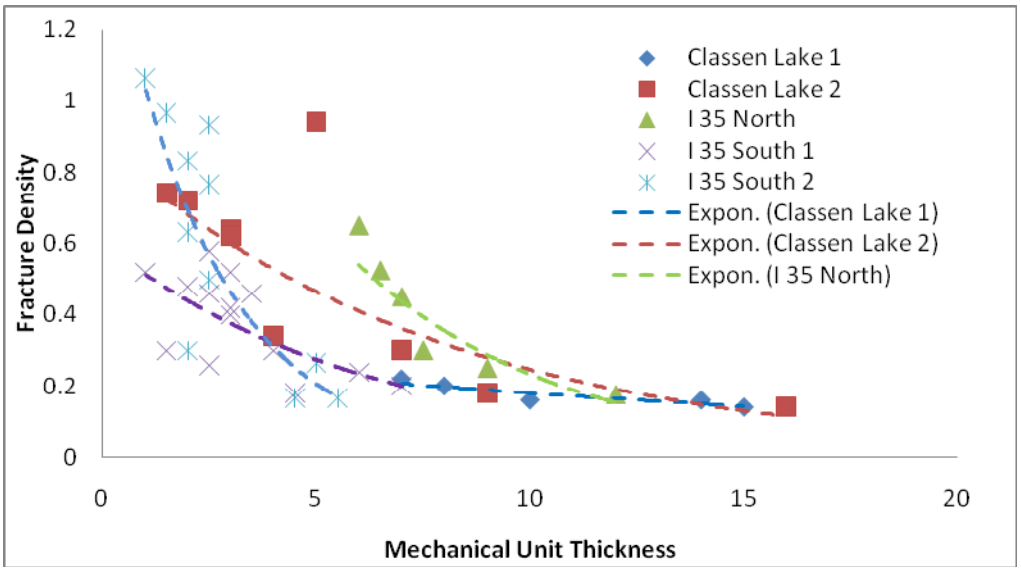

Fig. 103. Relationship between fracture density (f/cm) and mechanical unit thickness at all study sites.

Narr (1991) refer to the slope of the layer thickness-median joint spacing regression line as the *fracture spacing index (FSI)* computed with median fracture spacing as the dependent variable and greater fracture spacing index indicate higher fracture density. The FSI of Woodford shale is 0.94.

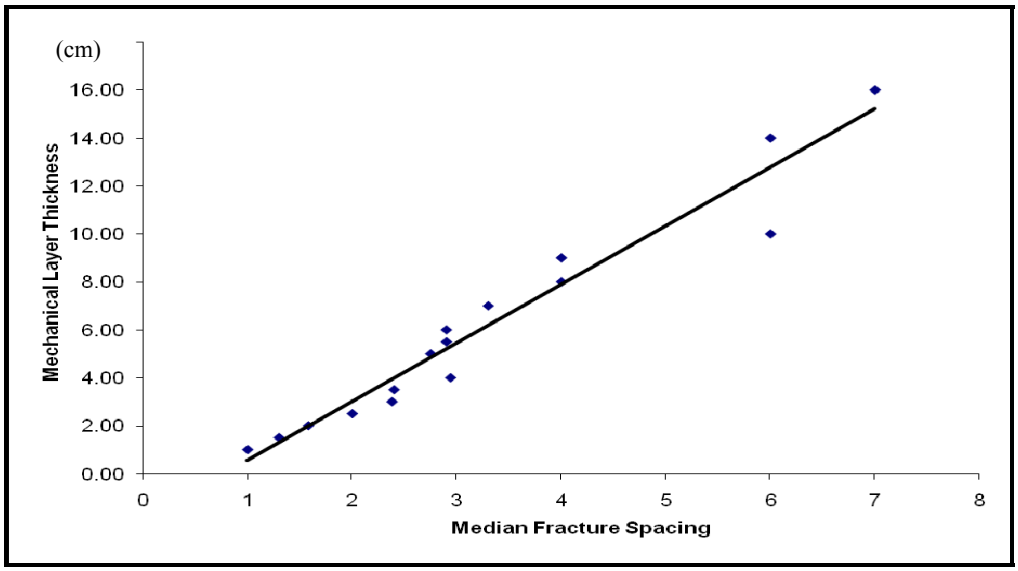

Figure. 104. Mechanical unit thickness v. median fracture spacing at all study sites.

CHAPTER IV

CONCLUSIONS

- The fracture patterns observed at the outcrops are related to the tectonic history of the region. Roughly, the NE-SW compressive stresses of the region are accompanied with the development of the fracture patterns on all outcrops.

- The fracture patterns developed at the limbs of the Arbuckle Anticline are related to the folding. However, some fracture orientations are consistent with the Ouachita fractures after bedding removal.

- The forelimb outcrops; the Lake Classen Spillway and the I-35 North Limb have vertical and overturned beds respectively. The beds are highly deformed compared to the other outcrops. As a result, they are intensely fractured compared to other outcrops.

- The late fold evolution, highly curvature and overturned beds are the main reasons for the high deformation and thereby for the development of early and late-fold-evolution related fracture patterns. However, at the backlimb of the Arbuckle Anticline, the Woodford Shale beds have not experienced strong deformation. As a result, a majority of the fractures developed under the early fold evolution stresses.

- The Lake Classen Spillway outcrop has both pattern 1 and 2 fractures. The shear fractures of pattern 1 and 2 have different dipping angles from almost horizontal to nearly vertical and they dip to the NW and SE. Because of the vertical bedding attitude, fractures are oriented perpendicular to the bedding strike. Tension fractures of pattern 1 strike perpendicular to the bedding strike due to the vertical bed attitude. However, the pattern 2 tension fractures strike parallel to the bedding strike.

- The I-35 North Limb outcrop has pattern 1 and 2 fractures. However the beds of the Woodford Shale are overturned and are dipping to the SW. For this reason, shear fractures of patterns 1and 2 have an oblique strike to the beds and are dipping approximately NW and E-NE. The strike of tension fractures of patterns 1 and 2 are perpendicular and parallel to the strike of the beds, respectively.

- The majority of fractures recorded at the I-35 South Limb belong to pattern 1. The shear fractures of pattern 1 dominate. The low intensity deformation of the southern limb compared to the northern limb accounts for the absence of pattern 2 fractures.

- In the McAllister Shale Pit outcrop, the fractures are not related to the folding. Set I fracture is the main fracture set and its orientation is closer to the direction of regional stresses. As a result, Set I fracture spacings are smaller those that of the fracture set II. Fracture set III developed due to buckling and formed last. In addition to this, cross-cutting relationship indicates that the fracture set IV developed after set I and set II fractures because die within the fracture set I and II.

- In the Eastern Arbuckle Wapanucka and Clarita outcrops, fracture orientations are not disturbed by local structures, and are strongly consistent with the regional stress directions.

- The brittleness of a bed is directly proportional to the amount of the quartz. Therefore, a systematic decrease in fracture density moving from cherty/silica-rich shale to organic-rich shale is observed. Additionally, the amount of quartz increases proportionally with the abundance of radiolarians within a bed.

- Fractures developed on cherty/silica-rich shale beds generally terminate against organic-rich beds. Highly and randomly fractured organic-rich shale beds do not have systematic fractures. Non-systematic fractures irregularly developed and have curvatures; thereby they do not have consistent orientation related to bedding.

- The presence of illite significantly decreases the brittleness of the beds and thereby the fracture density decreases.

- Bed thickness has a major effect on fracture density and distribution. Generally compositionally similar thinner beds have a higher fracture density than that of the thicker beds.
- Thickness and fissility are directly related to the amount of quartz. Thick and non-fissile beds contain more quartz than thinner, fissile beds.
- Fissile beds of the Woodford Shale respond to stresses as a thick bed. As a result they have low fracture densities.
- Micro-fractures tend to be parallel to bedding; however non-fissile beds tend to have more bedding perpendicular micro-fractures.
- The fracture spacing index (FSI) of Woodford shale is 0.94.
- The most densely fractured outcrop is the I-35 North outcrop. This reflects the tectonic history that overturned beds and reactivated fractures during late stage anticline evolution.

REFERENCES

Amsden, T., 1975, Hunton Group (late Ordovician, Silurian, and early Devonian) in the Anadarko Basin of Oklahoma: Oklahoma Geological Survey Bulletin 121, 214p.

Amsden, T., Denison, D., Fay, R., Rowland, T. L., 1978, Regional Geology of the Arbuckle Mountains, Oklahoma: AAPG, SEPM Annual Convention, Oklahoma City, Field Trip, 61 p.

Amsden, T., 1980, Hunton Group (late Ordovician, Silurian, and early Devonian) in the Arkoma Basin of Oklahoma: Oklahoma Geological Survey Bulletin 129, 136p.

Arbenz, J. K., 1989, Ouachita thrust belt and Arkoma basin, in R. D. Hatcher, Jr, W. A. Thomas, and G. W. Viele, eds., The Appalachian-Ouachita Orogen in the United States: Boulder, Colorado: The Geological Society of America, Geology of North America, v. F-2, p. 621-634.

Bixler, W. G., 1993, Structural analysis of the central Arbuckle Anticline, Southern Oklahoma: Baylor University, M.S Thesis.

Bellahsen, N., Fiore, P., Pollard, D. D., 2006, the role of fractures in the structural interpretation of Sheep Mountain Anticline, Wyoming: Journal of Structural Geology, v. 28, p. 850-867.

Bergbauer, S., Pollard, D. D., 2004, A new conceptual fold-fracture model including prefolding joints, based on the Emigrant Gap Anticline, Wyoming: GSA Bulletin, v.116, p. 294-306.

Brace, W. F., 1961, Dependence of fracture strength of rocks on grain size: Pennsylvania State University Mineral Export Station Bulletin, v. 79, p. 99-103.

Brown, W., Grayson, R., 1985, Tectonism and Sedimentation in the Arbuckle Mountain region, Southern Oklahoma Aulacogen: Baylor Geological Society, AAPG Student Chapter, 43p.

Cardott, B. J., 1985, Thermal maturation by vitrinite reflectance of Woodford Shale, Anadarko Basin Oklahoma: AAPG Bulletin, v. 69, p. 1982-1998.

Curtis, B., C., Lambert, M. W., 2002, Fractured shale-gas systems: AAPG Bulletin, v. 86, no. 11, p.1921-1938.

Comer, J., Hinch, H., H., 1987, Recognizing and quantifying expulsion of oil from the Woodford Formation and age-equivalent rocks in Oklahoma and Arkansas: AAPG Bulletin, v. 71, no. 7, p. 844-858.

Comer, J., 1992, Potential for producing oil and gas from the Woodford Shale (Devonian-Mississippian) in the southern Mid-Continent, USA: AAPG Bulletin, v.76, i. 4, p.574.

Comer, J., 1985, Thermal Maturation by vitrinite reflectance of Woodford Shale, Anadarko Basin, Oklahoma: AAPG Bulletin, v. 69, i.11, p.1982-1998.

Corbett, K., Friedman, M., Spang, J., 1987, Fracture Development and Mechanical Stratigraphy of Austin Chalk, Texas: AAPB Bulletin, v. 71, p. 17-28.

Cox, R. T., VanArsdale, B. R., 1988, Structure and Chronology of the Washita Valley fault, Southern Oklahoma Aulacogen: Shale Shaker, July, August, p.2- 13.

Dennis, T. G., 1972, Structural geology,. Ronald Press Comp. New York.

Dewey, J.F., and Burke, K., 1974, Hot spots and continental break-up: implications for collisional orogeny: Geology, v. 2, p. 57-60.

Dunham, R. J., 1955, Pennsylvanian conglomerates, structure, and orogenic history of Lake Classen area, Arbuckles Mountains, Oklahoma: AAPG Bulletin, v. 39, p. 1-30.

Gale, J., Reed, R. M., Holder, J., 2007, Natural fractures in the Barnett Shale and their importance for hydraulic fracture treatments: AAPG Bulletin, v.91, p.603-622.

Gross, M., 1993, The origin and spacing of cross joints: examples from the Monterey Fromation, Santa Coastline, California: Journal of Structural Geology, v. 15, n. 6, p. 737-751.

Gross, M., Fischer, M., Engelder, T., Greenfield, R., 1995, Factors controlling joint spacing in interbedded sedimentary rocks: integrating numerical models with field observations from the Monterey Formation, USA: GSA special publication, v.92, p. 215-233.

Grayson, R., 1985, Tectonism and Sedimentation in the Arbuckle Mountain region, Southern Oklahoma Aulacogen: Baylor Geological Society, AAPG Student Chapter, 43p.

Ham, W.E., 1951, Structural geology of the southern Arbuckle Mountains: Tulsa Geological Society Digest, v. 19, p. 68-71.

Ham, W.E., and others, 1973, Regional geology of the Arbuckle Mountains, Oklahoma: OGS Special Publication 73-3, 61 p.

Hardie, W.E., 1990, Subsurface structural study of the buried Ouachita thrust front, southeastern Oklahoma: Oklahoma City Geological Society, Shale Shaker, v. 41, p. 32-55.

Harris, J. F., Taylor G. L., Walper, J. L., 1960, Relations of deformational fractures of sedimentary rocks to regional and local structures: AAPG Bulletin, v. 44, p. 1853-1873.

Hass, W. H., Huddle, J. W., 1965, Late Devonian and Early Mississippian age of the Woodford Shale in Oklahoma as determined by conodonts: U.S. Geological Survey Professional Paper, 525-D, p. 125-132.

Hatcher, D. R., 1995, Strucutural Geology: Principles, Concepts and Problems: Prentice Halls Inc., 2. Edition, 525p.

Hanks, C., Lithologic and structural controls on natural fracture distribution and behavior within the Lisburne Group, northeastern Brooks Range and North Slope subsurface, Alaska, v. 81, p. 1700-1718.

Hancock, P. L., 1984, Brittle microtectonics: principles and practice: Journal of Structural Geology, v.7, Nos.3/4, p.437-457.

Hester, T.C., Schmoker, J.W., and Sahl, H.L., 1990, Log-derived regional source- rock characteristics of the Woodford Shale, Anadarko basin, Oklahoma: U.S. Geological Survey Bulletin 1866-D, 38 p.

Heidbach, 2007, World Stress Map: Episodes, v.30, no.3, p.197.

Hobbs, C. W., 1967, The Formation of Tension Joints in Sedimentary Rocks: an Explanation, Geological Magazine, v.104, p.550-556.

Hodgson, R. A., 1961, Classification of fractures on joint surfaces: American Journal Science, v. 259, p. 493-502.

Laderia, F. L., Price, N. J., 1981, Relationship between fracture spacing and bed thickness: Journal of Structure Geology, v. 3, n. 2, p. 183-198.

Lambert, M., 1993, Internal stratigraphy and organic facies of the Devonian-Mississippian Chattanooga (Woodford) Shale in Oklahoma and Kansas: AAGP Bulletin, v. 37, p. 163-176.

Lee, W., 1956, Stratigraphy and structural development of Salina Basin area: Kansas Geological Survey Bulletin, v. 121, 167p.

Mashak, S., Mitra, G., 1988, Basic Methods of Structural Geology: Prentice Hall Inc., 446p.

Muller, B., Heidbach, O., Tingay, M., 2006, The World Stress Map – A freely Accessible Tool for Geohazard Assessment: Heildelberg Academy of Sciences and Humanities Geophysical Institute, Karlsruhe University.

Miller, R., Young, R., 2007, Characterization of the Woodford Shale in Outcrop and Subsurface in Pontotoc and Coal Counties, Oklahoma: Search and Discovery Article, #50052.

Narr, W., Suppe, J., 1991, Joint spacing in sedimentary rocks: Journal of Structural Geology, v. 13, n. 9, p.1037-1048.

Nelson, R. A., 1985, Geologic analysis of naturally fractured reservoirs: Petroleum Geology and Engineering, Gulf Publishing Co., 320p.

Nelson, R., 2001**,** Geologic Analysis of Naturally Fractured Reservoirs: Gulf Professional Publishing Company; 2. Edition, 320 p.

Ortega, O., 2006, A scale-independent approach to fracture intensity and average spacing measurement: AAPG Bulletin, v. 90, i.2, p. 193-200.

Over, D., Barrick, J., 1990, The Devonian/Carboniferous boundary in the Woodford Shale, Lawrence uplift, Southcentral Oklahoma: Oklahoma Geological Survey Guidebook 27, p. 63-73.

Price, N. J., 1966, Fault and Joint development in brittle and semi-brittle rock: Pergammon Press, London, 176p.

Pollard, D. D., Aydin, A., 1988, Progress in understanding jointing over the past century: Geological Society of America Bulletin, v. 100, p. 1181-1204.

Pybas, K., Cemen, I., Al-Shaieb, Z., 1995, The Collings Ranch Conglomerate of the Oklahoma Arbuckles: Its origin and Tectonic significance: Oklahoma Geological Survey Circular 97, p. 132-143.

Ramez, M., Mosalamy, F., 1969, Deformed nature of various size fractions in some clastic sands: Journal of Sedimentary Petrology, v. 39, p. 1882.

Randel, C., 2008, Structure and chronology of the Washita Valley Fault, Southern Oklahoma Aulacogen: Shale Shaker, v.39, p. 2-13.

Rohrbaugh, M., Dunne, W. M., Mauldon, M., 2002, Estimating fracture trace intensity, density and mean length using circular scan lines and windows: AAPG Bulletin, v.86, no.12, p. 2089-2104.

Roznovsky, T. A., Aydin, A., 2001, Concentration of shearing deformation related to changes in strike of monoclinal fold axes: the Waterpocket monocline, Utah: Journal of Structural Geology, v. 23, p. 1567-1579.

Saxon, C. P., 1994, Surface to subsurface structural analysis, northwest Arbuckle Mountains, southern Oklahoma: Baylor University, MSc. Thesis, 191p.

Saxon, C. P., 1998, Surface Structural style of the Wichita and Arbuckle Orogenies, Southern Oklahoma: The University of Oklahoma, PhD. Thesis, 248p.

Schatzki, N. S., 1946, The Great Donets Basin and the Wichita system--comparative tectonics of ancient platforms: SSSR Akad. Nauk. Isv., Geology Series No. 1, p. 5-62.

Stearns, D.W., 1964, Macrofracture patterns on Teton Anticline, Nortwest Montana, *American Geophysical Union Transactions,* 45, 107-108.

Stearns, D., W. Friedman, M., 1972, Reservoirs in Fractured Rocks: AAPG Memoir, v.16, p. 82-100.

Sullivan, K. L., 1985, Organic facies variation of the Woodford Shale in western Oklahoma: Shale Shaker, v. 35, p. 76-89.

Suneson, H., 1997, The geology of the Eastern Arbuckle Mountains in Pontotoc and Johnston Counties, Oklahoma: Oklahoma Geological Survey, 4-49, 22p.

Suneson, H., 1996, The geology of the Ardmore Basin in the Lake Murray State Park Area, Oklahoma: Field Trip, Oklahoma Geological Survey, 32p.

Tanner, J. H., 1967, Wrench fault movement along the Washita Valley fault, Arbuckle Mountain area, Oklahoma: AAPG Bulletin, v. 51, p. 126-134.

Twiss, R. J., Moores, M. E., 1992, Structural Geology: W. H. Freeman and Company Publishing, 532 p.

Underwood, C. A., Cooke, M. L., Simo, J. A., Muldoon, M. A., 2003, Stratigraphic controls fracture patterns in Silurian dolomite, northeastern Wisconsin: AAPG Bulletin, v. 87, no. 1,p. 121-142.

Van Der Pluijm, B.A.; Marshak, S., 2004, Brittle Deformation, *in* Wiegman, L.A.W. (ed.): Earth Structure, 2nd Edition. W.W. Norton & Company, p. 114-138.

Walper, J., 1977, Paleozoic tectonics of the Southern Margin in North America: Gulf Coast Association of Geological Societies, v. 27, p.230-241.

Wickham, J., 1978, The Southern Oklahoma Aulacogen: School of Geology & Geophysics, University of Oklahoma, 41p.

Wiltschko, D., Corbett, K. P., Friedman, M., Hung, J., 1991, Predicting fracture connectivity and intensity within the Austin Chalk from outcrop fracture maps and scanline data: Gulf Coast Association of Geological Societies, v. 61, p. 702-718.

APPENDIX A

FRACTURE MEASUREMENTS FROM SELECTED OUTCROPS

LAKE CLASSEN SPILLWAY OUTCROP

Dip Angle	Dip Direction	Dip Angle	Dip Direction	Dip Angle	Dip Direction
54	S41E	79	N27W	25	N69W
45	N30W	20	S45E	7	N14W
57	N41W	64	N29W	14	N61W
46	S34E	84	N33W	60	N29W
39	S31E	74	N25W	38	S29E
54	N31W	27	S58E	32	S34E
34	S20E	21	S28E	70	N28W
43	N28W	10	N80W	71	N34W
34	S35E	12	S57E	86	N21W
51	N26W	13	N86W	33	S32E
33	S41E	84	S21E	29	S40E
74	N28W	78	S18E	31	S42E
57	S49E	14	S24W	86	S24E
76	N32W	73	N29W	84	N32W
64	N33W	71	N35W	66	N33W
89	N34W	81	N22W	76	N21W
36	S19E	86	N33W	29	S41E
4	S20E	68	N26W	33	S34E
12	S16E	26	S40E	69	N32W
11	S11W	17	S37E	77	N47W
14	N41W	24	S26E	16	S36E

I-35 NORTH LIMB OUTCROP

N18E	19SE	N22E	70NW	N9E	84NW
N19E	12SE	N26E	82NW	N52E	38NW
N24E	75NW	N16W	19NE	N23E	74NW
N18E	58NW	N16E	82NW	N21W	12NE
N31E	49NW	N7W	8NE	N35W	17NE
N19E	71NW	N26E	41NW	N28E	87NW
N5W	21NE	N20E	66NW	N31E	51NW
N20E	63NW	N19W	24NE	N41E	61NW
N12W	21NE	N39E	16NW	N74W	5NE
N9E	84NW	N37E	71NW	N32E	81NW
N52E	38NW	N15W	12NE	N14W	19NE
N23E	74NW	N23E	66NW	N26E	71NW
N21W	12NE	N34E	71NW	N32E	66NW
N35W	17NE	N18W	26NE	N22E	83SE
N28E	87NW	N13W	23NE	N15W	9NE
N31E	51NW	N25E	49NW	N59E	29NW
N41E	61NW	N21E	84NW	N26W	23NE
N74W	5NE	N14W	17NE	N39E	80SE
N32E	81NW	N36E	54NW	N14E	60NW
N14W	19NE	N14E	59NW	N21W	14NE
N26E	71NW	N42E	58NW	N18E	52NW
N32E	66NW	N31E	57NW	N21E	78SE
N22E	83SE	N11W	21NE	N34E	69NW
N15W	9NE	N36E	63NW	N17E	78NW
N59E	29NW	N41W	21NE	N8W	17NE
N26W	23NE	N22E	87NW	N35E	31NW
N39E	80SE	N59E	52NW	N13W	21NE
N14E	60NW	N29E	85NW	N29E	65NW
N21W	14NE	N34W	15NE	N18W	18NE
N18E	52NW	N21E	79NW	N19E	76NW

N12W	17NE	N32E	41NW		
N17E	78NW	N4W	20NE	N15E	74NW
N8W	17NE	N41E	46NW	N12W	21NE
N35E	31NW	N24E	41NW	N31E	84NW
N13W	21NE	N29E	74NW	N14E	19SE
N29E	65NW	N30E	72NW	N34W	15NE
N18W	18NE	N6W	17NE	N46E	44NW
N19E	76NW	N9W	27NE	N18E	19SE
N9W	23NE	N22E	84NW	N19E	12SE
N32E	41NW	N36E	33NW	N24E	75NW
N15E	74NW	N24E	46NW	N18E	58NW
N12W	21NE	N34W	15NE	N31E	49NW
N31E	84NW	N46E	44NW	N19E	71NW
N14E	19SE	N31E	67NW	N25E	49NW
N22E	70NW	N12W	17NE	N21E	84NW
N26E	82NW	N4W	20NE	N14W	17NE
N16W	19NE	N41E	46NW	N36E	54NW
N16E	82NW	N24E	41NW	N14E	59NW
N7W	8NE	N29E	74NW	N42E	58NW
N26E	41NW	N30E	72NW	N31E	57NW
N20E	66NW	N6W	17NE	N11W	21NE
N19W	24NE	N9W	27NE	N36E	63NW
N39E	16NW	N22E	84NW	N41W	21NE
N37E	71NW	N36E	33NW	N22E	87NW
N15W	12NE	N24E	46NW	N59E	52NW
N23E	66NW	N5W	21NE	N29E	85NW
N34E	71NW	N18W	26NE	N34W	15NE
N21E	78SE	N13W	23NE	N21E	79NW
N34E	69NW	N31E	67NW	N9W	23NE

I-35 SOUTH LIMB OUTCROP

N39E		N70E	55SE	N40E	60NW
N45E	88SE	N66E	52SE	N37E	64NW
N41E	74NW	N70E	46SE	N30E	60NW
N40E		N60E	55SE	N38E	60NW
N37E	87SE	N75E	57SE	N01W	44NE
N54E	63NW	N62E	51SE	N02W	74NE
N61E	60NW	N80E	60SE	N05W	70NE
N66E	54NW	N78W	55SE	N05E	74NW
N62E	60NW	N25E	80E	N03W	64NE
N61E	63NW	N28E	78SE	N06E	81SE
N65E	61NW	N30E	75SE	N10W	64NE
N61E	71NW	N35E	70SE	N08W	77NE
N62E	61NW	N21E	75SE	N77E	24NW
N59E	64NW	N20E	68SE	N65E	30NW
N54E	59NW	N30E	70SE	N63E	32NW
N61E	66NW	N25E	65SE	N68E	33NW
N60E	61NW	N18E	60SE	N70E	30NW
N67E	55NW	N15E	60SE	N78E	25NW
N61E	59NW	N01E	90S	N05E	50E
N60E	65NW	N10E	80SE	NS	45E
N57E	66NW	N05E	78S	N10W	50NE
N16W	55NE	N10E	75S	N08W	52NE
N19W	60NE	N09E	70S	N30W	50NE
N11W	52NE	N05W	65N	N11W	56NE
N21W	59NE	N03W	60N	N30W	25NE
N39E		N08W	65N	N24W	33NE
N59E	59NW	N10W	70N	N60E	62SE
N53E	54NW	N11W	75N	N44E	66NW
N51E	64NW	N60E	70NW	N43E	66NW

N44E	66NW	N84E	24NW	N42W	32NE
N46E	54NW	N78E	21NW	N50W	35NE
N54E	64NW	N80E	32NW	N50W	45NE
N56E	62NW	N81E	30NW	N47W	33NE
N25E	88SE	N86E	25NW	N50W	34NE
N32E	87SE	N50E	76NW	N22E	82SE
N30E	88SE	N50E	70NW	N29E	89SE
N29E	86SE	N38E	40	N22E	80SE
N29E	89SE	N36E	87NW	N24E	80SE
N32E	86SE	N45W	35NE	N52W	36NE
N22E	80SE	N63W	46NE	N61W	36NE
N30E	88SE	N47W	35NE	N50W	45NE
N25E	89SE	N50W	39NE		

MC ALLISTER SHALE PIT OUTCROP

N46E	N44E	N51E	N53E	N78E	N64E
N38E	N45E	N63E	N65E	N82E	N66E
N36E	N41E	N52E	N61E	N81E	N63E
N21E	N54E	N54E	N67E	N45E	N60E
N23E	N64E	N69E	N55E	N41E	N63E
N31E	N71E	N39E	N54E	N35E	N65E
N29E	N69E	N34E	N64E	N28E	N25E
N32E	N72E	N43E	N44E	N33E	N29E
N44E	N68E	N54E	N41E	N64E	N30E
N30E	N63E	N84E	N24E	N38E	N26E
N34E	N73E	N72E	N26E	N48E	N82E
N51E	N72E	N41E	N84E	N36E	N62E
N42E	N68E	N34E	N79E	N88E	N79E
N34E	N75E	N32E	N81E	N44E	N24E
N38E	N66E	N28E	N55E	N48E	N41E
N42E	N74E	N34E	N59E	N49E	N43E
N44E	N76E	N31E	N57E	N25E	N39E
N37E	N44E	N27E	N64E	N26E	N42E
N36E	N25E	N25E	N61E	N27E	N25E
N38E	N22E	N35E	N38E	N24E	N76E
N24E	N21E	N83E	N37E	N18E	N74E
N30E	N26E	N79E	N39E	N21E	N76E
N45E	N33E	N71E	N55E	N54E	N73E
N36E	N29E	N843	N39E	N68E	N36E
N43E	N24E	N71E	N59E	N30E	N25E
N47E	N19E	N74E	N61E	N35E	N18E
N40E	N26E	N46E	N40E	N36E	N79E
N29E	N28E	N44E	N12E	N54E	N84E
N46E	N77E	N36E	N66E	N64E	N82E
N56E	N44E	N82E	N64E	N71E	N72E

N65E	N82E	N77E	N18E	N72E	N76E
N7E	N34E	N58E	N22E	N77E	N76E
N9E	N52E	N63E	N26E	N74E	N75E
N51E	N57E	N69E	N27E	N76E	N38E
N56E	N67E	N61E	N25E	N73E	N40E
N61E	N83E	N74E	N73E	N77E	N42E
N57E	N87E	N86E	N69E	N79E	N46E
N51E	N71E	N29E	N76E	N72E	N39E
N21E	N77E	N35E	N74E	N63E	N30E
N65E	N74E	N34E	N68E	N73E	N37E
N72E	N75E	N33E	N75E	N75E	N35E
N56E	N72E	N28E	N74E	N68E	N29E
N43E	N77E	N34E	N76E	N74E	N31E
N47E	N76E	N29E	N45E	N76E	N82E
N56E	N73E	N85E	N46E	N77E	N84E
N46E	N74E	N84E	N23E	N73E	N81E
N78E	N76E	N83E	N28E	N25E	N34E
N83E	N65E	N76E	N79E	N73E	N44E
N78E	N67E	N78E	N29E	N75E	N43E
N40E	N82E	N72E	N36E	N67E	N46E
N74E	N75E	N26E	N34E	N69E	N75E
N75E	N83E	N41E	N37E	N70E	N76E
N78E	N82E	N32E	N25E	N76E	N76E
N75E	N72E	N38E	N29E	N80E	N74E
N77E	N68E	N41E			

SCRATCH HILL/EAST ATOKA ROAD CUT OUTCROP

N74E	N50W
N78E	N52W
N82E	N64W
N79E	N55W
N70E	N59W
N73E	N56W
N71E	N48W
N85E	N49W
N79E	N60W
N80E	N68W
N76E	N25W
N79E	N60W
N73E	N61W
N65E	N58W
N79E	N57W
N24E	N65W
N36E	N68W
N39E	N60W
N40E	N79W
N29E	N81W
N33E	N74W
N35E	N45W
N41E	N84W
N36E	N85W
N37E	N73W
N38E	N83W
N45E	N80W
N20E	N69W
N34E	N69W
N42E	N66W
N34E	N72W

N42E	N74W
N32E	N21E
N24E	N35E
N32E	N44E

WAPANUCKA SHALE PIT

N85E	N19E
N81W	N16E
N84W	N12E
N83W	N21E
E-W	N14E
N82E	N16E
N76E	N10E
N70E	N4E
N83E	N12E
N89W	N11E
N82E	N19E
N85W	N18E
N88E	N17E
N89W	

CLARITA SHALE PIT

N85W	N22E
N86W	N27E
N86W	N31E
N87E	N35E
N87W	N25E
N87W	N3E
N88W	N26E
N89W	N27E
N87W	N24E
E-W	N26E
N89W	N24E
N84W	N21E
N19	N27E
N21E	N23
N22E	

VITA

Onur Ataman

Candidate for the Degree of

Master of Science

Thesis: NATURAL FRACTURE SYSTEMS IN THE WOODFORD SHALE, ARBUCKLE MOUNTAINS, OKLAHOMA

Major Field: Geology

Biographical:

Personal Data:

Born January 22, 1983 in Adana, Turkey
Parents: Aysel and Mehmet Ataman,
Married to Ipek Ataman

Education:

O.C. Bilfen High School, Adana, Turkey, 2000
Geological Engineering, B.S., Cukurova University, Turkey August, 2006.
Geology Department, M.S., Oklahoma State University, Stillwater, 2007.

Experience:

Research Assistant, Oklahoma State University – School of Geology
Geological Engineer Intern, Cukurova University, Turkey
Geology Student Assistant, Center of Environmental Research, Turkey

Professional Memberships:

American Association of Petroleum Geologists (AAPG)
Society of Exploration Geophysicists (SEG)
American Geophysical Union (AGU)
Cukurova University Alumni Society

Name: Onur Ataman Date of Degree: December, 2008

Institution: Oklahoma State University Location: Stillwater, Oklahoma

Title of Study: NATURAL FRACTURE SYSTEMS IN THE WOODFORD SHALE, ARBUCKLE MOUNTAINS, OKLAHOMA

Pages in Study: 168 Candidate for the Degree of Master of Science

Major Field: Geology

Scope and Method of Study:

The focus of this study is the characterization of natural fracture systems in the Devonian/Lower Mississippian Woodford shale in the southern Oklahoma to understand nature of fracturing better. Geologic controls (such as; structural position, mechanical stratigraphy and petrography) that are affected on fractures and fracture behaviors under controlled stress by doing experiments are examined.

Findings and Conclusions:

A decrease in average fracture density between organic rich shale and cherty/silica rich shale has been systematically observed. There is a systematic decrease in fracture density moving from cherty and silica rich shale to organic rich shale. Minimum values are observed on organic rich beds and fractures often terminate within the organic rich beds. The general systematic fracture developments on seven outcrops are directly related to local structures and regional stresses.

ADVISER'S APPROVAL: Dr. Ibrahim Cemen

Fracture Orientations of the Woodford Shale, Arbuckle Anticline

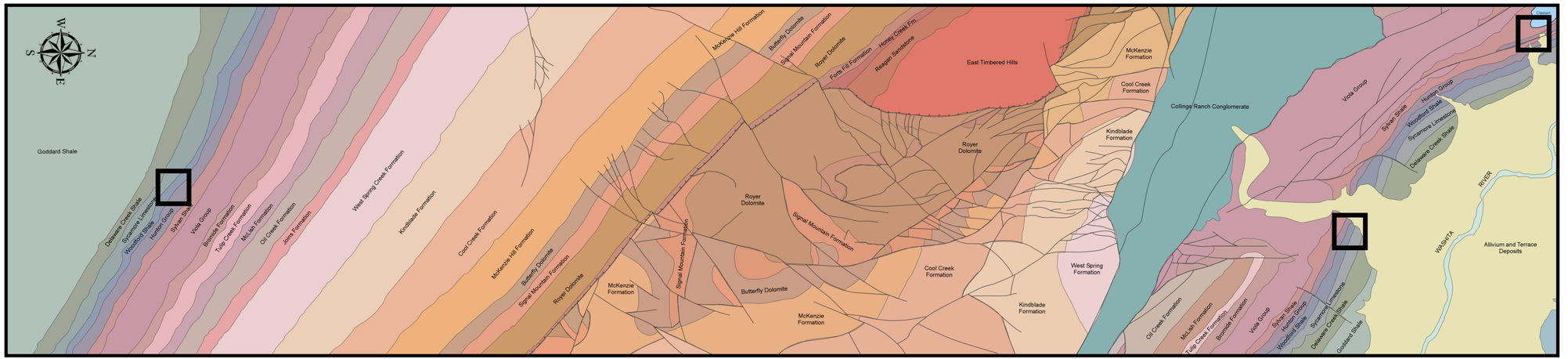

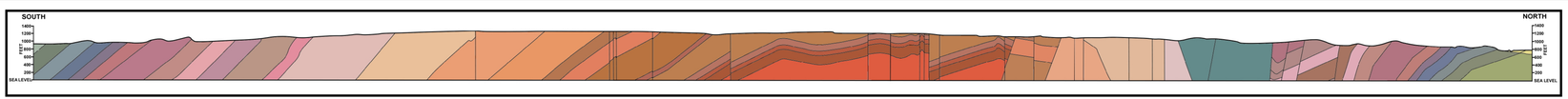

Lake Classen Spillway Outcrop

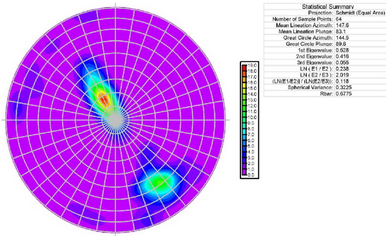

I-35 South Limb Outcrop

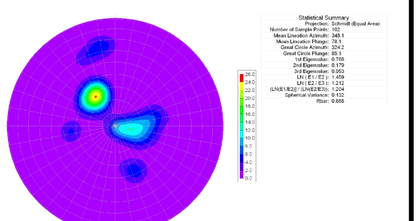

I-35 North Limb Outcrop

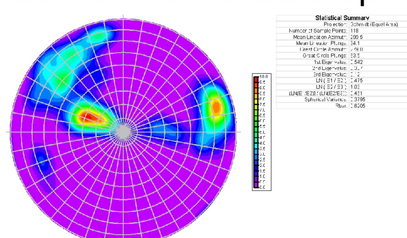

Fracture Orientations of the Woodford Shale, McAlister Shale Pit Outcrop

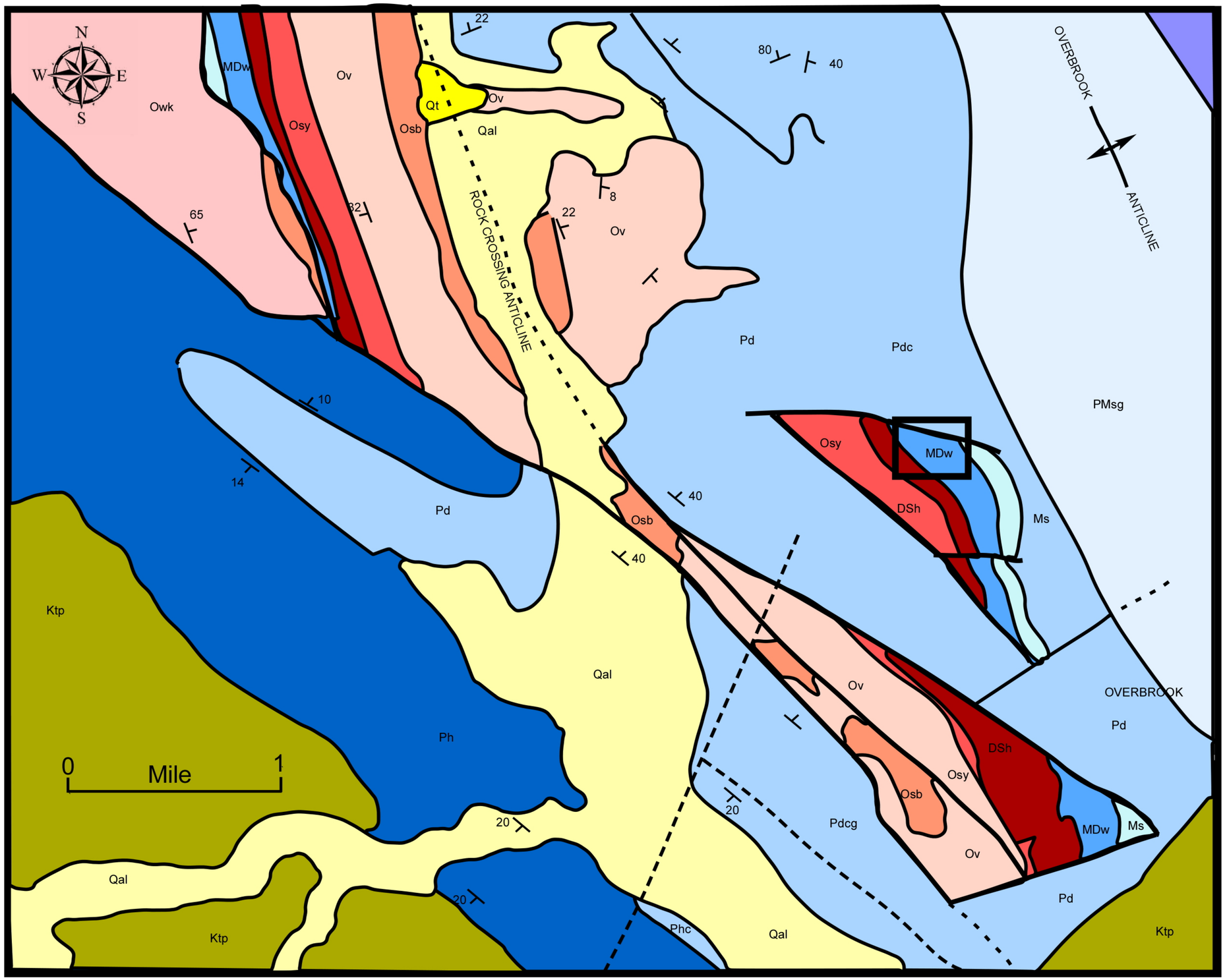

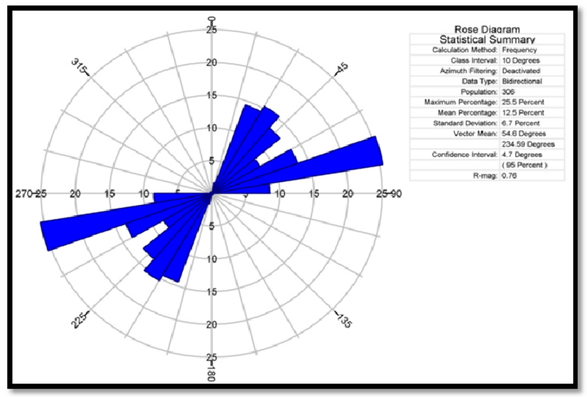

- Terrace
- Alluvium
- Paluxy Sand
- Hoxbar Group
- Deese Group
- Springer and Goddard Fm.
- Sycamore Limestone
- Woodford Shale
- Hunton Group
- Sylvan Shale
- Viola Limestone
- Bromide Formation
- West Spring Creek and Kindblade Fm.

FRACTURE ORIENTATIONS FROM OUACHITA MOUNTAINS

WAPANUCKA SHALE PIT

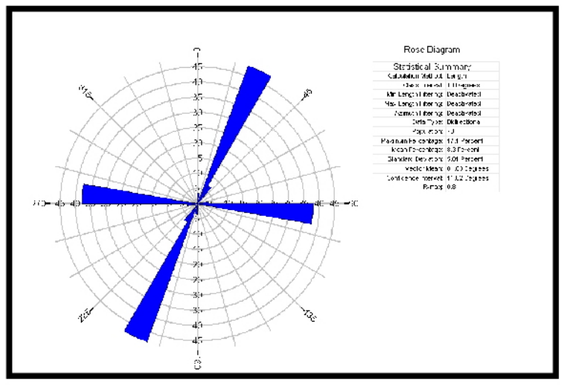

SCRATCH HILL/ EAST ATOKA ROAD

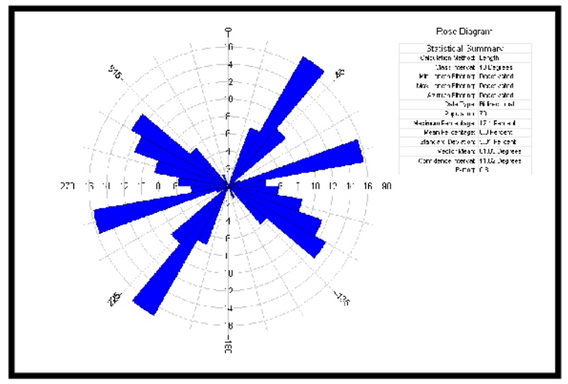

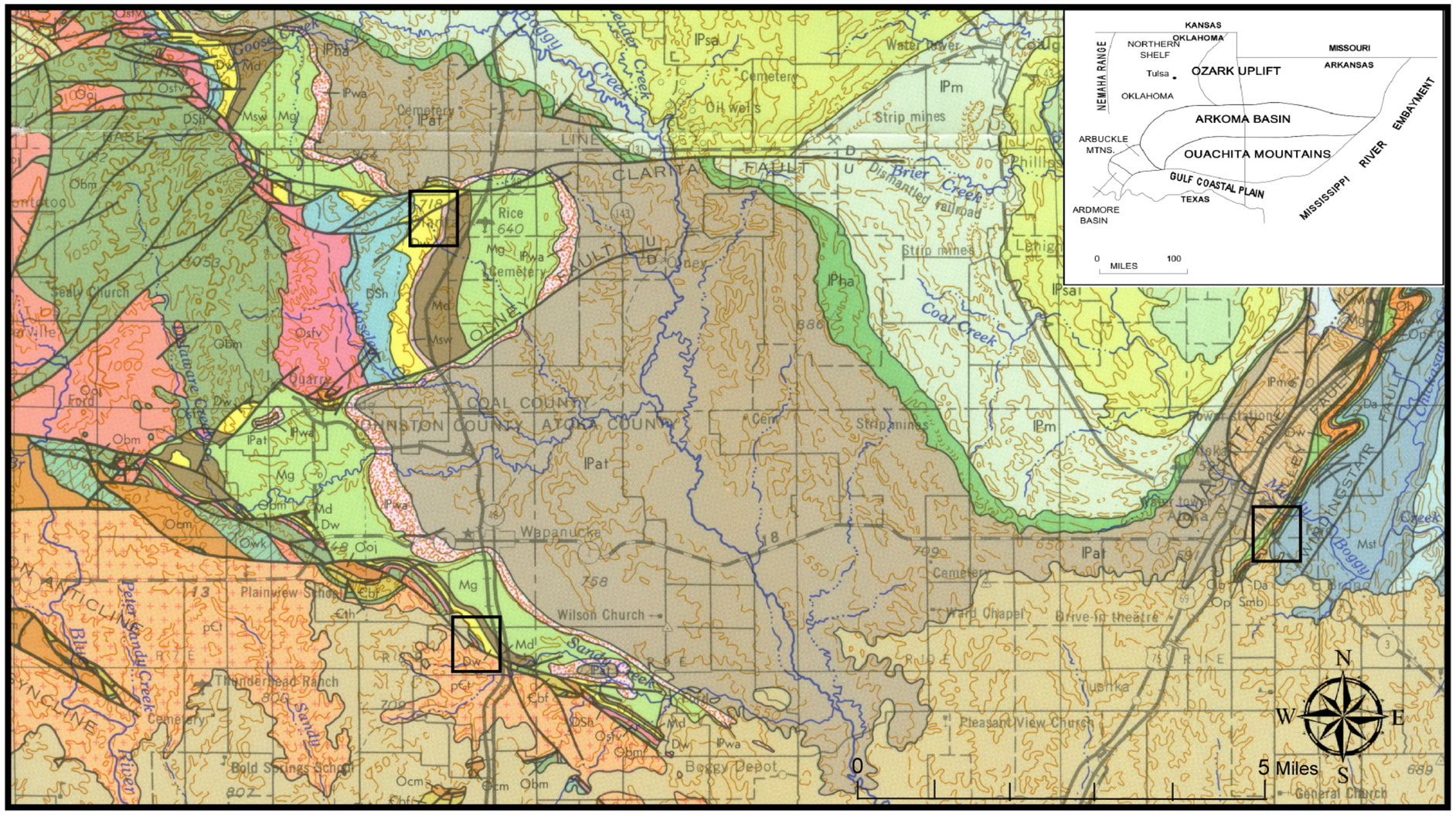

CLARITA SHALE PIT

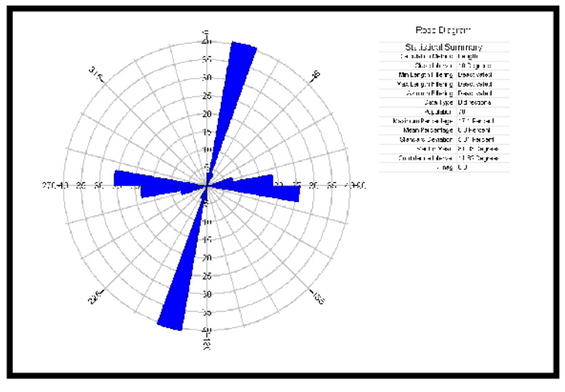

I35S Stratigraphy - Fracture Orientation Correlation

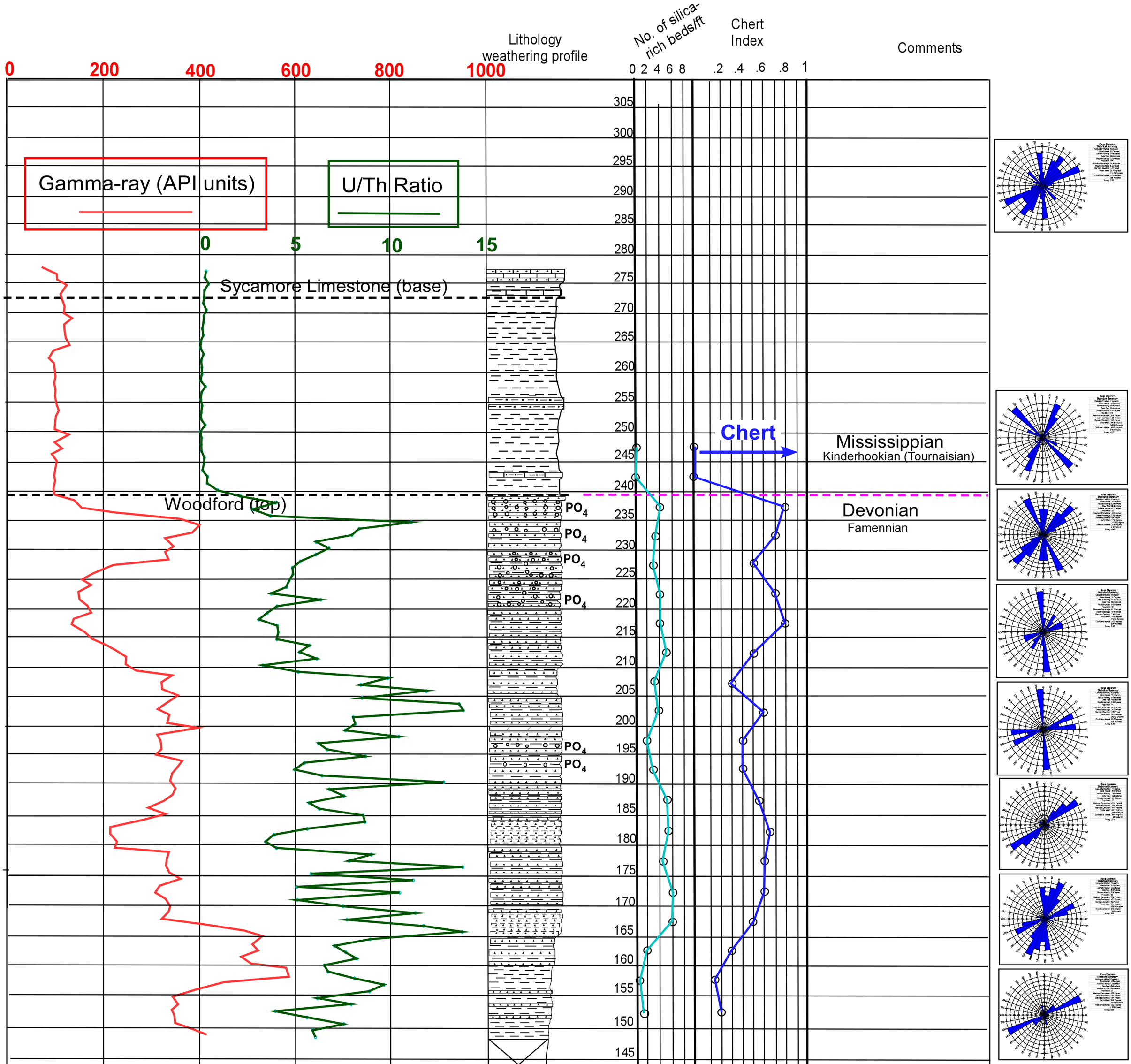

McAlister Shale Pit Stratigraphy - Fracture Orientation Correlation

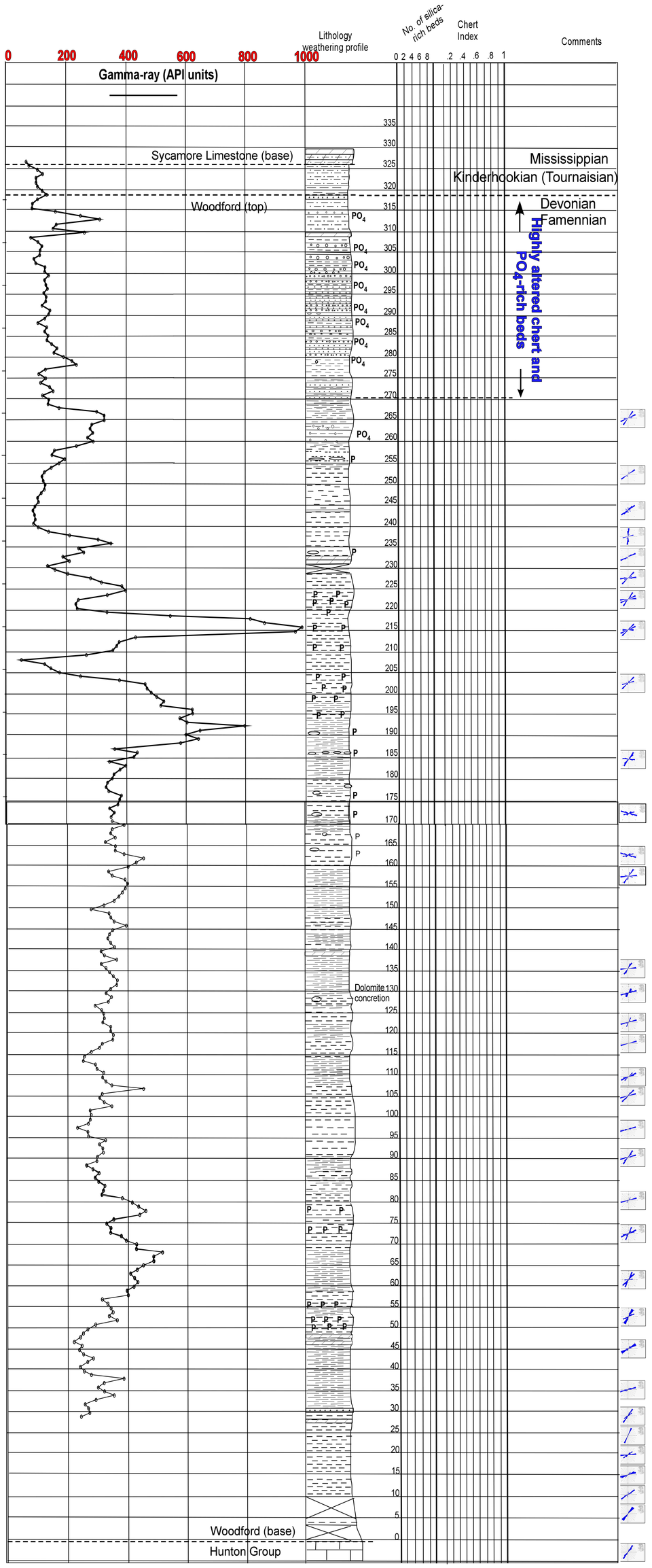

Stratch Hill / East Atoka Road Stratigraphy - Fracture Orientation Correlation

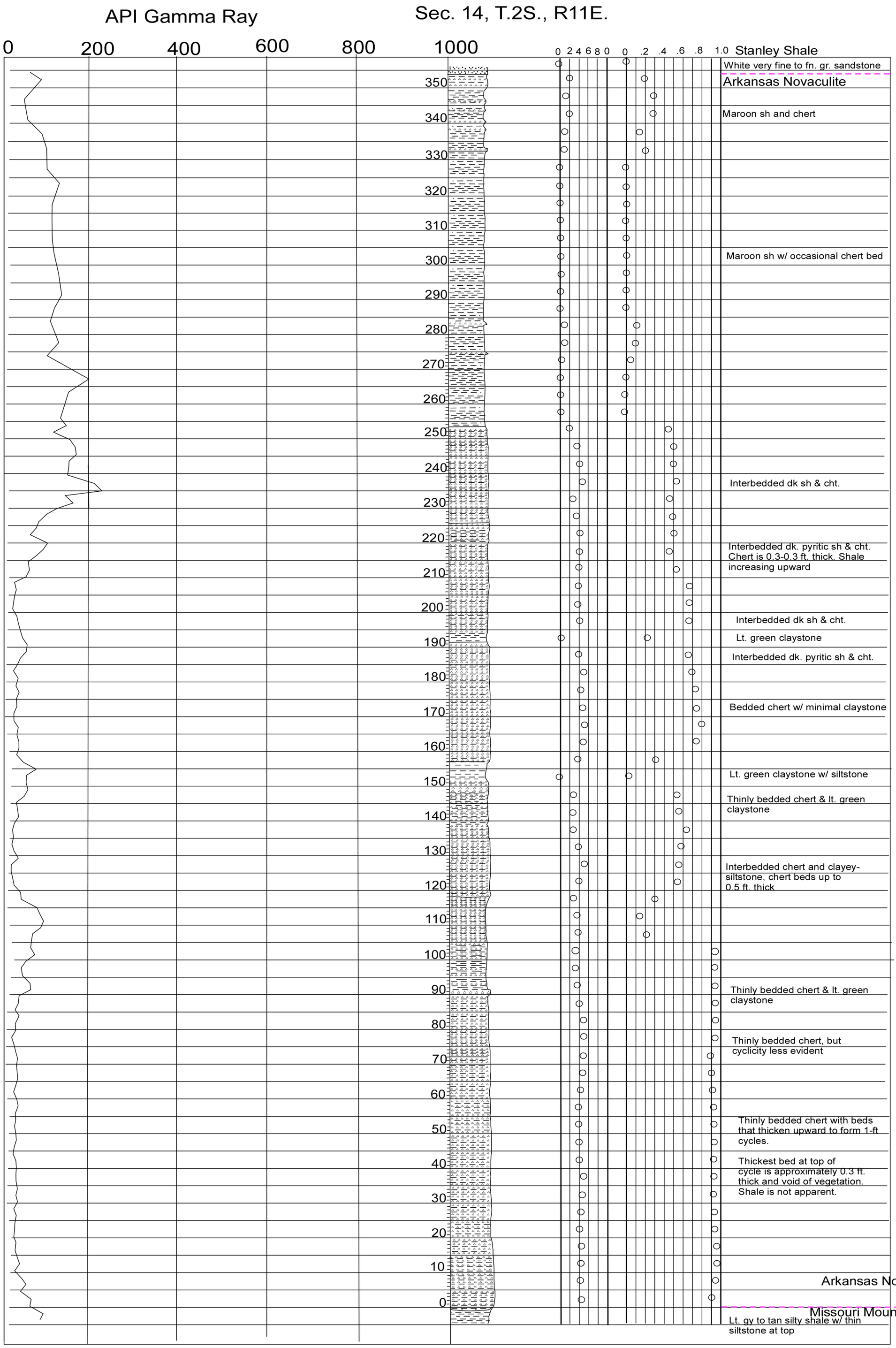

Wapanucka Shale Pit Stratigraphy - Fracture Orientation Correlation

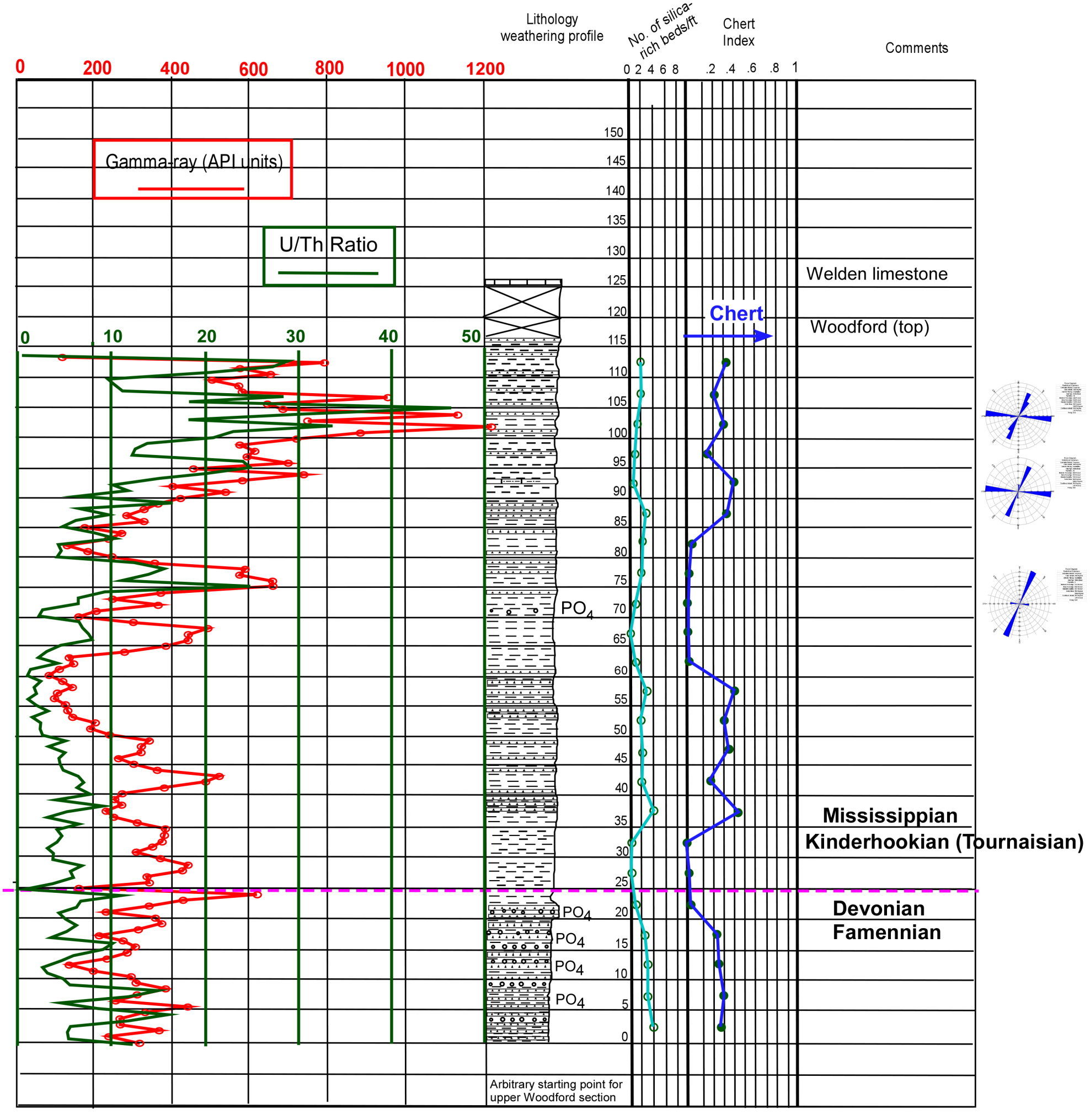

Fracture Orientations of the Woodford Shale, Arbuckle Anticline

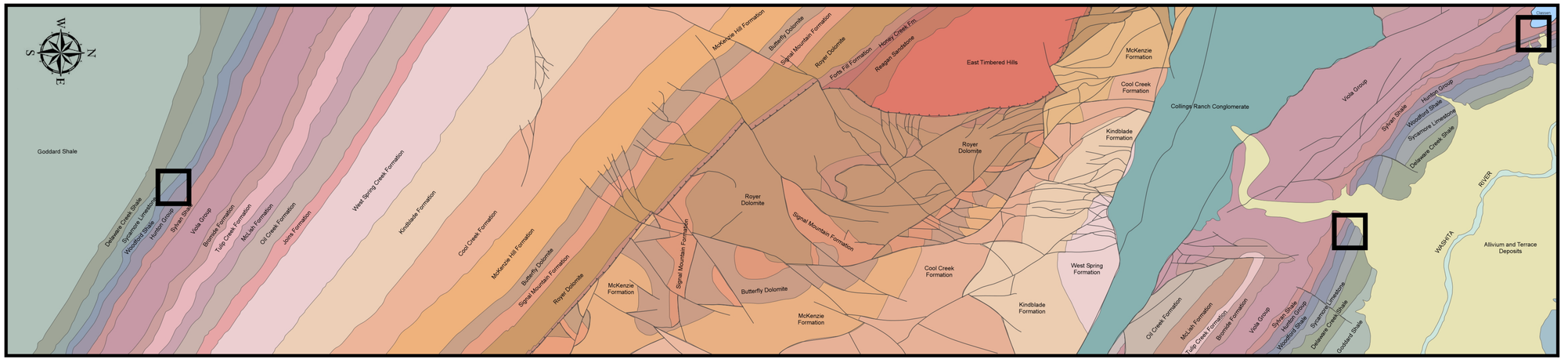

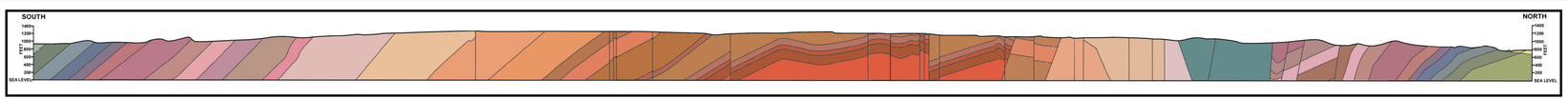

Lake Classen Spillway Outcrop

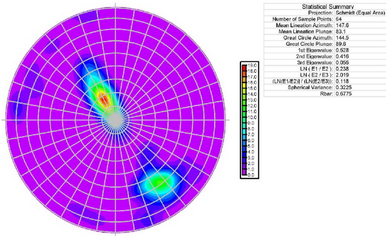

I-35 South Limb Outcrop

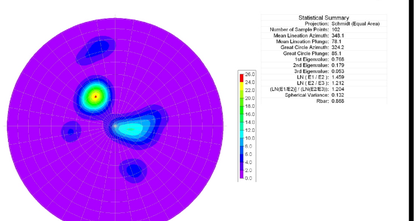

I-35 North Limb Outcrop

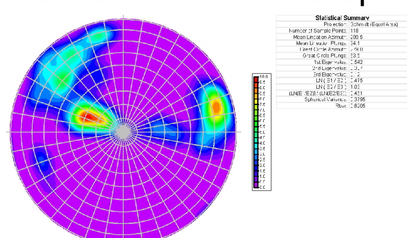

Fracture Orientations of the Woodford Shale, McAlister Shale Pit Outcrop

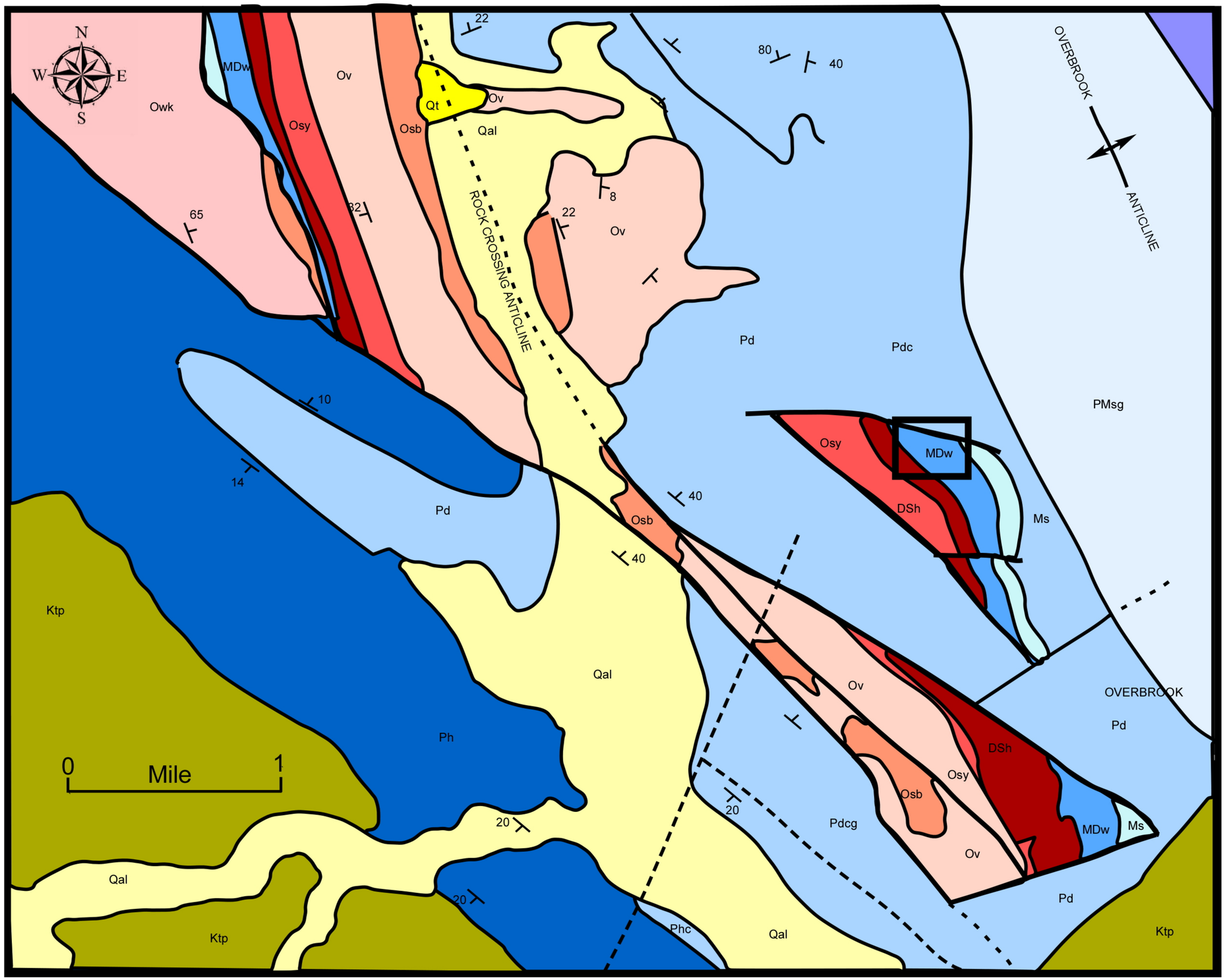

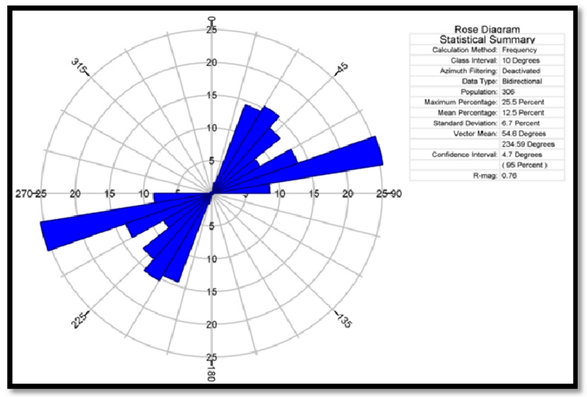

- Terrace
- Alluvium
- Paluxy Sand
- Hoxbar Group
- Deese Group
- Springer and Goddard Fm.
- Sycamore Limestone
- Woodford Shale
- Hunton Group
- Sylvan Shale
- Viola Limestone
- Bromide Formation
- West Spring Creek and Kindblade Fm.

FRACTURE ORIENTATIONS FROM OUACHITA MOUNTAINS

WAPANUCKA SHALE PIT

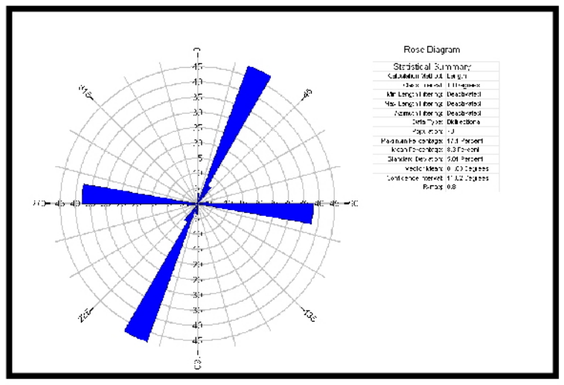

SCRATCH HILL/ EAST ATOKA ROAD

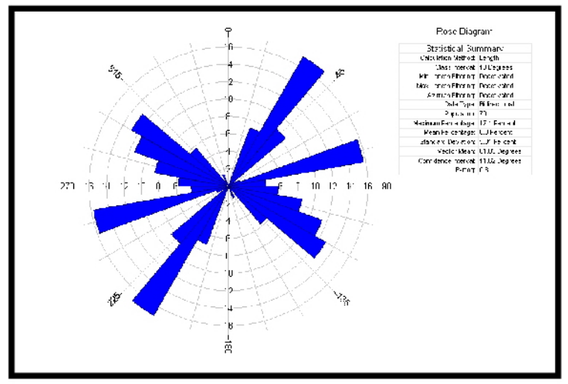

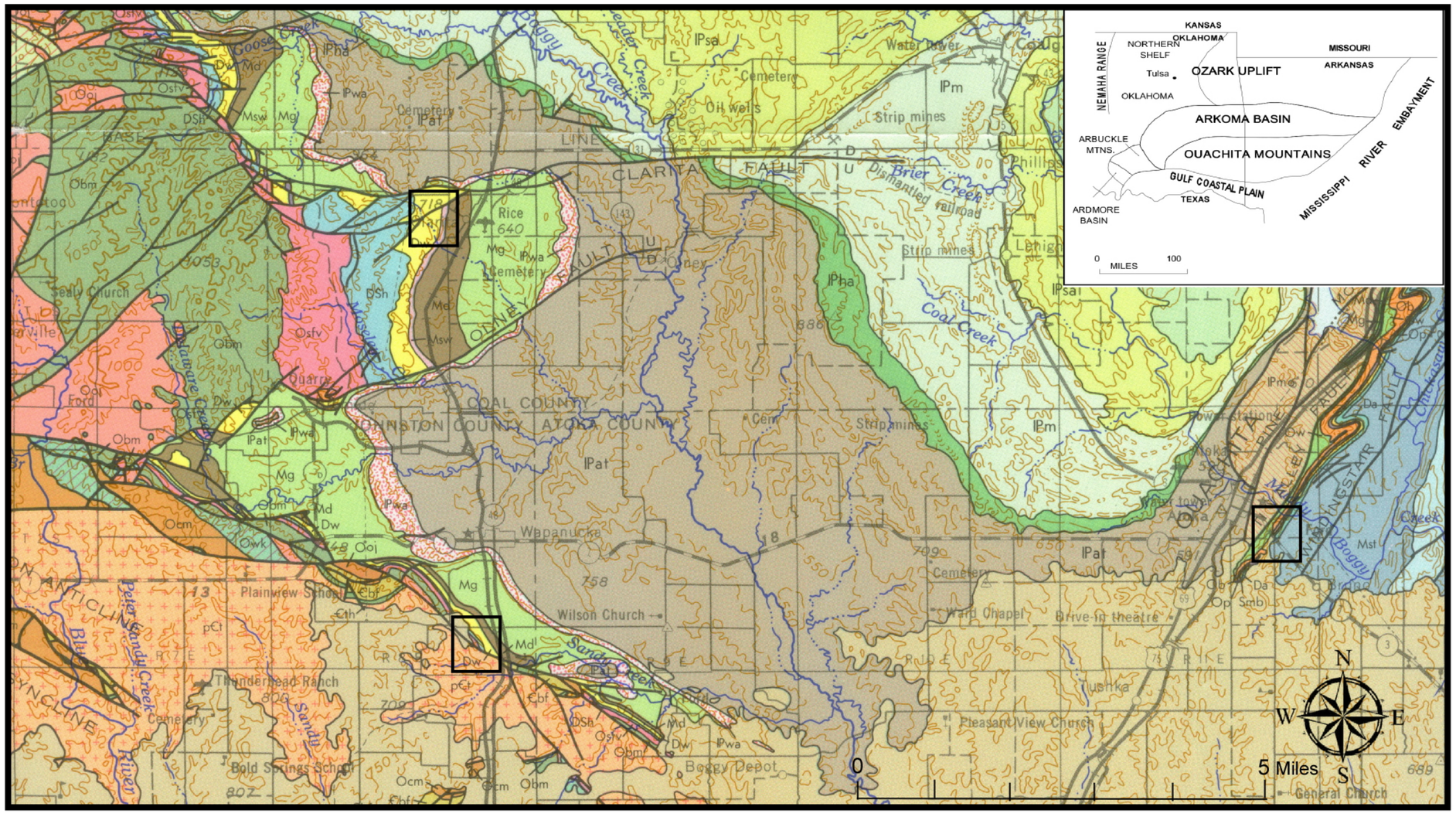

CLARITA SHALE PIT

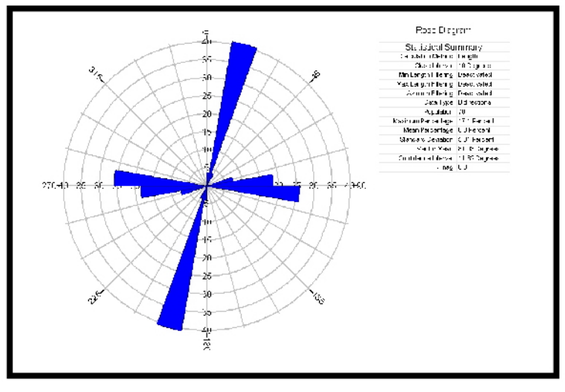

I35S Stratigraphy - Fracture Orientation Correlation

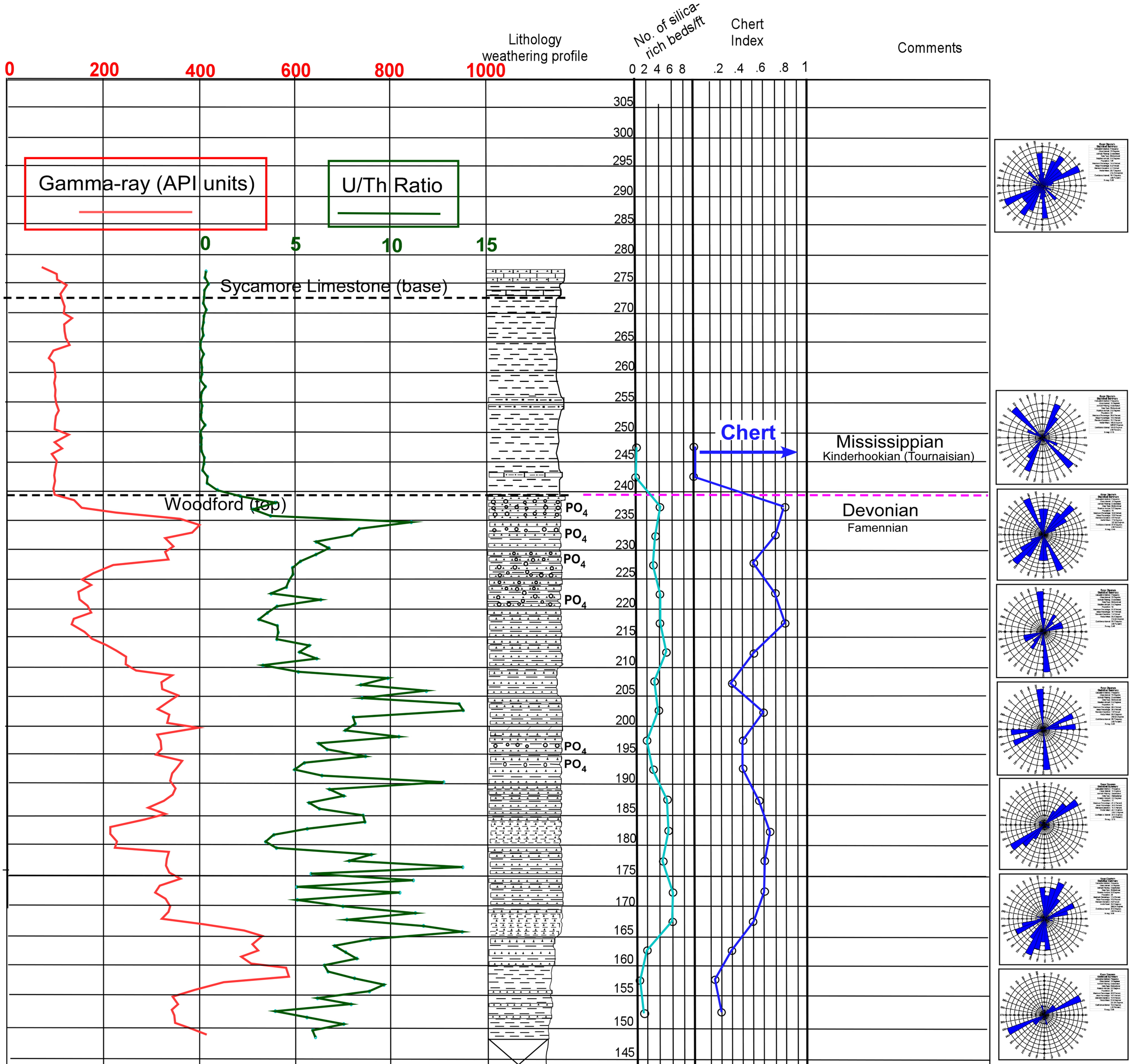

McAlister Shale Pit Stratigraphy - Fracture Orientation Correlation

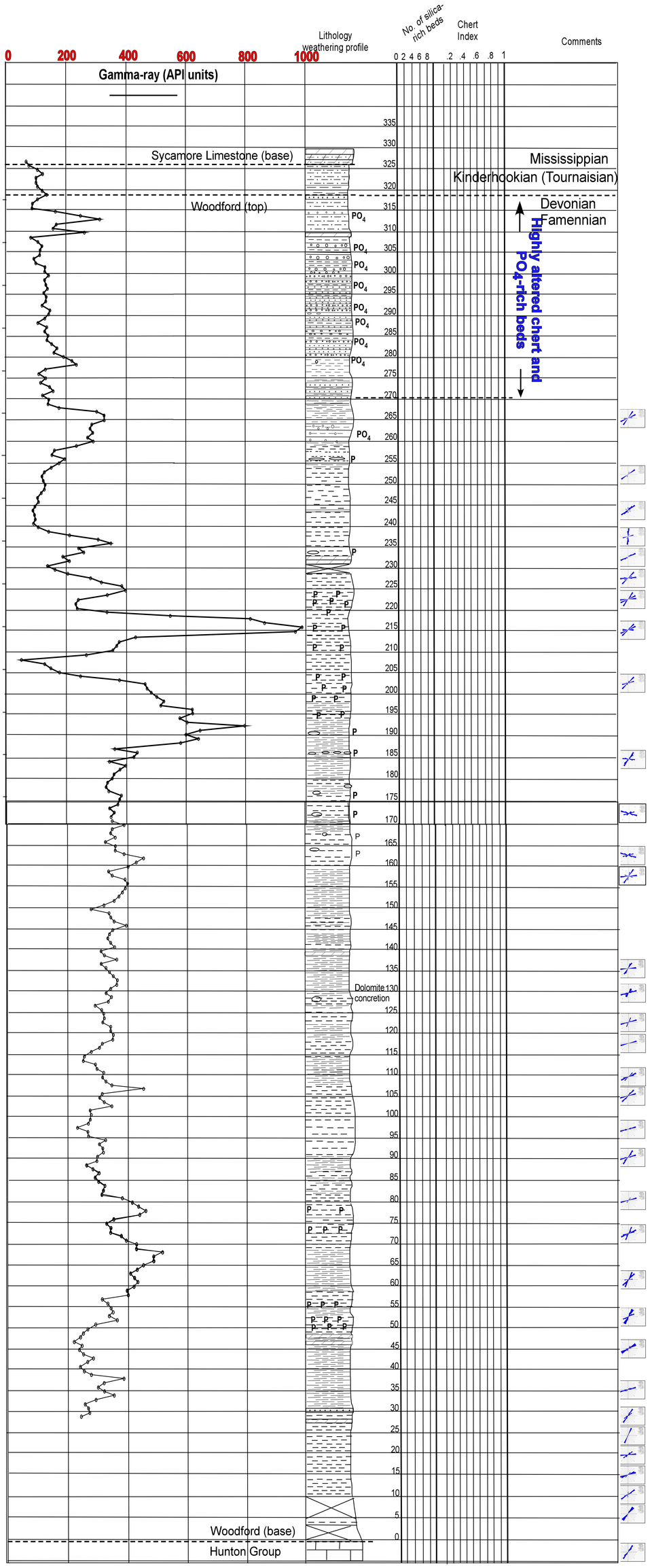

Stratch Hill / East Atoka Road Stratigraphy - Fracture Orientation Correlation

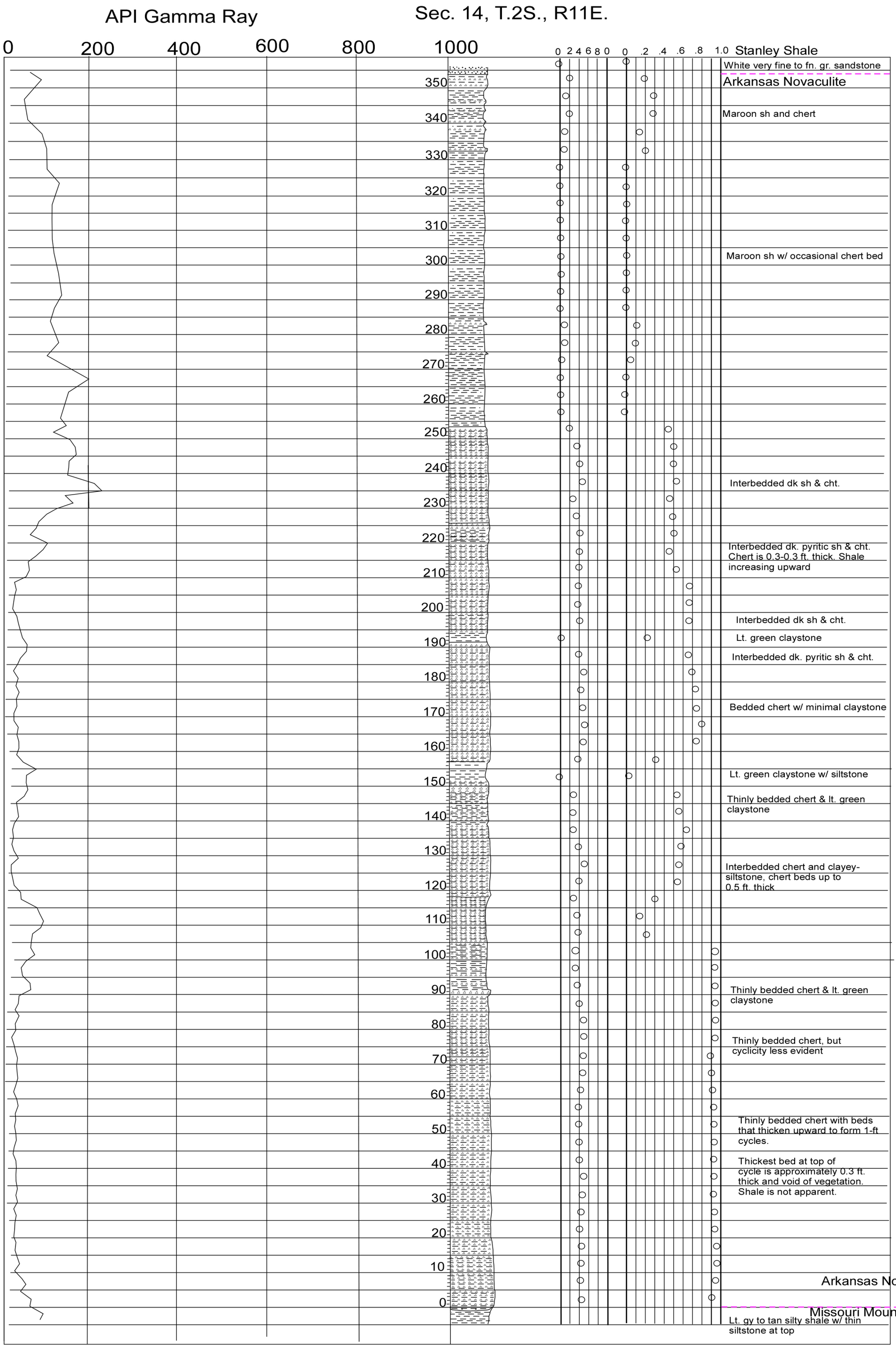

Wapanucka Shale Pit Stratigraphy - Fracture Orientation Correlation